AFML-TR-65-226

# SURFACE AND INTERFACIAL EFFECTS IN RELATION TO BRITTLENESS IN REFRACTORY METALS

*A. FOURDEUX*
*F. RUEDA*
*E. VOTAVA*
*A. WRONSKI*

# FOREWORD

This report was prepared by Union Carbide European Research Associates, s.a., Brussels 18, Belgium, under USAF Contract AF61(052)-774. The work was conducted under Project No. 7351,"Metallic Materials," Task No. 735101, "Refractory Metals". This project was administered under the direction of the Air Force Materials Laboratory, Research and Technology Division with Lt. Larry D. Blackburn serving as project monitor.

This report describes the results of research conducted during the period 1 March 1964 through 31 March 1965.

Manuscript released by authors December 1965 for publication as an AFML Technical Report.

This technical report has been reviewed and is approved.

I. PERLMUTTER
Chief, Physical Metallurgy Branch
Metals and Ceramics Division
AF Materials Laboratory

## ABSTRACT

An experimental program was conducted to compare the mechanical properties of high purity and impure niobium and the mechanical properties of high purity tungsten, both in polycrystalline and single crystal forms.

Slip in high purity niobium takes place on the {110} planes in the <111> directions and yielding is governed by the conservative motion of jogs in screw dislocations, rather than by the unlocking of dislocations from the interstitial impurity cloud. Between the upper and lower yield points there is a sudden generation of a large number of dislocations by double cross-slip mechanism. High purity niobium has greater ductility, higher uniform elongation, increased work hardening, but lower strength than impure Columbium. Further, it has a yield point in the temperature range 20°C to 800°C.

Appreciable ductility can be achieved at room temperature in commercially pure tungsten, but the mechanical properties are strongly orientation dependent. The ductile-to-brittle transition temperature is about 100°C higher in sintered material than in melted material which is of coarser gran size and probably higher purity. Very high purity polycrystalline tungsten was found to show some ductility down to -196°C in the recrystallized condition. However, the fracture process is controlled to a considerable extent by grain boundaries in the temperature range +200°C to -196°C.

TABLE OF CONTENTS

SUMMARY.

In view of the limited duration of the present contract effort was concentrated on a comparison of the mechanical properties of high-purity niobium and impure niobium and on the mechanical properties of high-purity tungsten, both in polycrystalline form and as single crystals. The work is reported under seven different headings, each section dealing with one particular aspect of the program and written up so as to form a self-contained chapter.

The first section contains a literature survey on the low-temperature deformation of monocrystalline and polycrystalline tungsten and monocrystalline niobium and on the effects of the surface on the mechanical properties of tungsten. Since it revealed the existence of considerable published information on the last point, no work was undertaken in that area.

The work reported in the second section was found necessary to round off a previous investigation on the mechanical properties of high-purity niobium single crystals ; it was possible to show that slip in high-purity niobium takes place on {110} planes in ⟨111⟩ directions and that yielding is governed by the conservative motion of jogs in screw dislocations rather than by the unlocking of dislocations from the interstitial impurity cloud. Between the upper and the lower yield points there is sudden generation of a large number of dislocations by a double cross-slip mechanism.

The next section reports an investigation of the effect of purity on the mechanical properties of niobium. Samples, either simply recrystallized in an electron-beam zone refiner or purified by nineteen passes of electron-beam zone melting, were cold swaged to 90% reduction and annealed isochronally. It was found that the purified niobium has greater ductility,

greater uniform elongation, increased work hardening, but lower strength. Further it has a yield point in the temperature range 20°C to 800°C. Increased strength was found for both kinds of niobium between 400°C and 600°C and is attributed to the influence of carbon in the samples.

Investigation of the yielding and plastic deformation of high-purity tungsten single crystals at room temperature, described in the next section, confirmed that appreciable ductility can be achieved at room temperature, but showed that the mechanical properties depend strongly on orientation. However, no detailed explanation of the mechanism of deformation was possible since the slip lines were hardly visible even after large strain increments.

Section V deals with the ductile-to-brittle transformation of polycrystalline tungsten of different degrees of commercial purity. It was found that the ductile-to-brittle transition temperature is about 100°C higher in sintered material than in material that has been melted and is of coarser grain size and probably of higher purity. Whereas the brittle fracture stress of recrystallized swaged single crystals increases with decreasing temperature, the sintered material did not behave reproducibly ; this is attributed to the presence of small gas bubbles or voids, which were observed in sintered tungsten but were absent in the melted material.

The ductile-to-brittle transition behavior of high-purity polycrystalline tungsten is reported in Section VI. Single crystals were purified by electron-beam zone melting, swaged, and then recrystallized in an ultra-high vacuum of at least $10^{-8}$ Torr. This material was found to show some ductility down to -196°C ; this proves unequivocally that brittleness is not

an inherent property of polycrystalline tungsten. However, in the range of temperatures investigated, + 200°C to - 196°C, the fracture process is still controlled to a considerable extent by the grain boundaries. The temperature dependence of the yield stress makes it evident that the increase of the yield stress with decreasing temperature is not due to a large Peierls-Nabarro force.

Examination of high-purity niobium single crystals by transmission electron microscopy, reported in the last Section, revealed the occasional presence of domain walls and of stacking-fault-like structures. It is assumed that both are due to accidental oxygen contamination, but further diffraction work is necessary to clarify this point. Deformation experiments inside the electron microscope proved that in tungsten dislocation movement is restricted essentially to single slip planes, whereas in niobium extensive cross-slip occurs.

This observation is most important in relation to the observed differences in the mechanical properties of monocrystalline and polycrystalline niobium and tungsten, as reported in sections II to VI. Since slip is transmitted over the entire length of the crystal by cross-slip, all possible slip planes can be activated and exhausted, so that there is more ductility than in the absence of cross-slip, in which case only a restricted number of slip planes becomes operative. In addition stress concentrations around precipitates, voids, and grain boundaries will be reduced considerably by cross-slip, thereby diminishing the possibility for crack formation. In the absence of cross-slip stress concentrations will unavoidably occur and precipitates, voids, and grain boundaries will play an essential rôle

in the formation of cracks, as reported in sections V and VI for the case of tungsten. In high-purity tungsten, that is in the absence of precipitates and voids, the grain boundaries still control the fracture process to a considerable extent, although some ductility appears as a consequence of the absence of grain-boundary films.

Thus the essential difference between niobium and tungsten is the difference in the deformation mechanism and this difference probably holds also for the two other refractory metals, tantalum on one hand and molybdenum on the other.

## SECTION I.

# A Literature Survey on the Low-Temperature Deformation of Monocrystalline and Polycrystalline Tungsten and Monocrystalline Niobium, and on the Effects of the Surface on the Mechanical Properties of Niobium and Tungsten.

by

A. Wronski

Introduction.

Tungsten is considered one of the most brittle metals and, so far, only single crystals have been found to possess appreciable ductility below room temperature. The development of the electron-beam zone-refining technique (Calverley et al., 1957) and the need for structural materials for high temperatures have led to several recent studies of the tensile properties of tungsten single crystals (for a review see Atkinson et al., 1961). Up to 5% elongation in uniaxial tension at room temperature has been reported for polycrystalline tungsten (details unavailable, see Maloof, 1963) and low temperature studies have been concerned mainly with fracture (Wronski and Fourdeux, 1964) or twinning and deformation in compression (Sheely et al., 1961). The single crystal studies have shown, as up to 4% deformation is possible at 20°K (Schadler, 1960b), that tungsten is no more "intrinsically brittle" than any other metal. Fabrication of polycrystalline material from monocrystalline tungsten, however, leads generally to an increase in the ductile-brittle transition temperature of about 300°C. At room temperature the best elongation reported for such material, in wire form, was about 0.5% (Orehotsky and Steinitz, 1962). It is held by some that the embrittlement is due to contamination during the mechanical and thermal treatments and thus it is important to reduce such contamination to the now practically obtainable minimum, i.e. by electropolishing followed by annealing in hydrocarbon-free vacua below $10^{-8}$ Torr. Mihailov et al. (1960) have demonstrated that commercial tungsten wire annealed in a 'cold' vacuum of $\sim 10^{-6}$ Torr at high temperatures retains its bend ductility. Koo, (1963c), however, has shown that the high ductility of single crystals grown by a strain-annealing technique is not due to purification and

further suggests that the high ductility of single crystals grown by electron-beam zone melting is also mainly caused by the absence of grain boundaries. Deformation properties of tungsten are also particularly sensitive to the state of its surface and this problem will be considered in Section D.

Before reviewing the literature it is thought best to explain the symbols, definitions, and conventions used in this report. Let us consider an idealised case of a small, unnotched tensile specimen of good uniform surface finish, tested in the ductile range of the material at a uniform slow strain rate in uniaxial tension using a hard-beam testing machine. As the specimen is loaded it behaves elastically until $\sigma_E$, the "true" elastic limit (Brown and Ekvall, 1962) is reached (Fig. 1), which is normally not detectable in a load-elongation curve. At a relatively larger value of stress, $\sigma_A$, the anelastic limit is reached and this, in general, is the normally detectable apparent proportional limit. Upper yield point at stress $\sigma_U$, yield drop, and lower yield point at stress $\sigma_Y$ can then result, which are sometimes followed by the Lüders strain.

In some instances there is appreciable plastic deformation before the upper yield point is reached - this is termed pre-yield microstrain. Having yielded the material work-hardens. Fracture may occur after a further small strain whilst the material is work-hardening, usually by cleavage at the stress $\sigma_F$, or only after the ultimate tensile stress, UTS, has been reached and necking has taken place (dashed line in Fig. 1). If there is no detectable plastic strain, then and only then, is the material considered brittle. The total plastic strain, $\epsilon_t$, and the uniform plastic strain, $\epsilon_p$, are also indicated in Fig. 1.

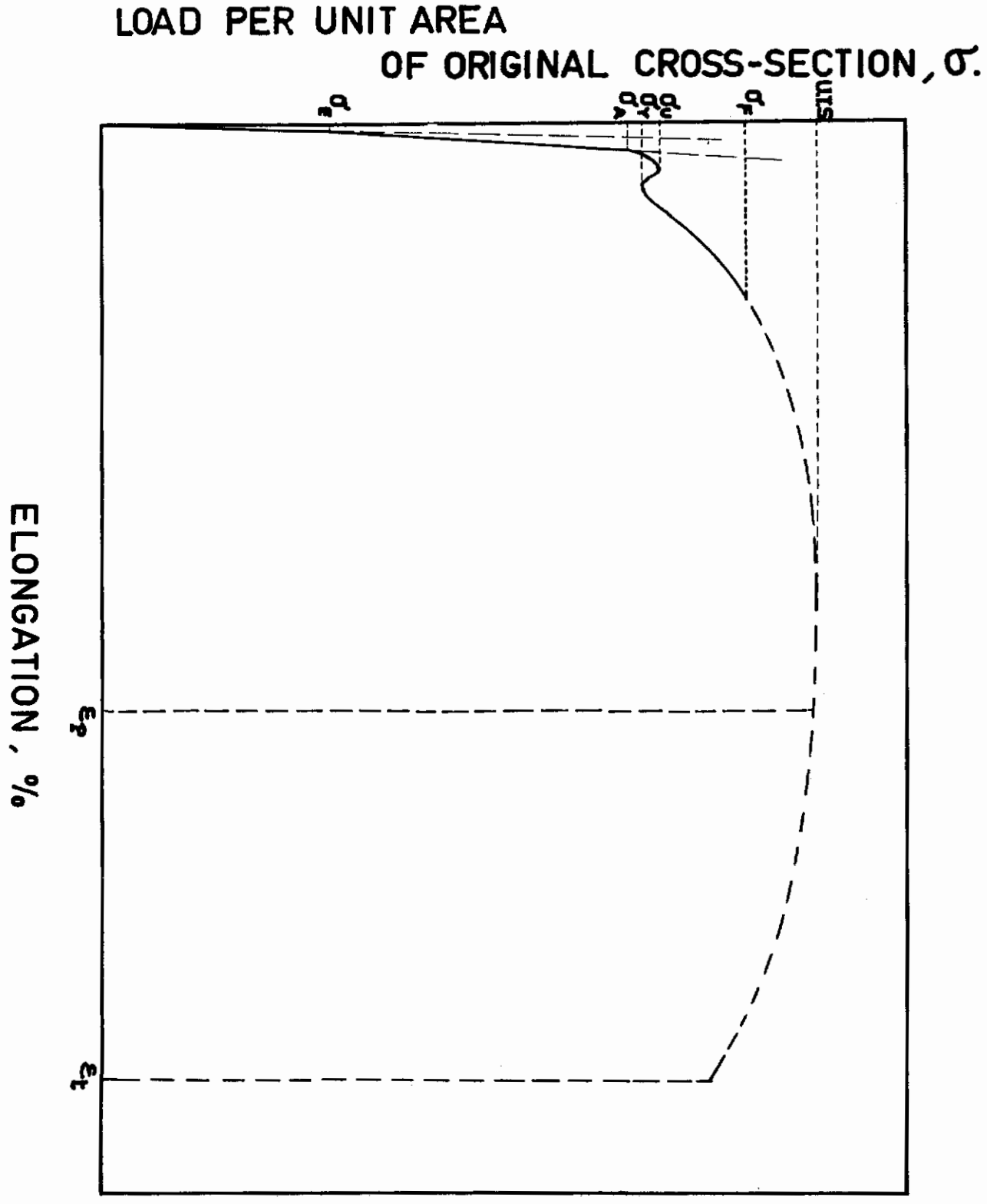


FIG. 1.

A schematic load-elongation curve of a body-centred cubic transition metal strained in its ductile range.

A. The low temperature deformation of monocrystalline tungsten.

Much of the work on the mechanical properties of monocrystalline tungsten has been done on Air Force contracts and detailed reports are available (e. g. Ferris, Rose and Wulff, 1961 ; Schadler and Low, 1962 and Atkinson et al. , 1960 ; Sell et al. , 1961, 1962). Schadler (1960b) has determined the modes and the crystallography of plastic deformation at 298°, 77° and 20°K. He found that at 77° and 20°K plastic deformation occurs by slip on systems of the type (011) [111] and by twinning on (112)-type planes and that at 298°K slip only takes place in [111] directions on either (011)- or (112)-type planes. (Nevertheless, it is customary to resolve stress for room temperature tests on (011) [111]-type systems). Wolff (1962), however, observed mechanical twins in crystals of a variety of axial orientations deformed at room temperature in tension or bending. The twinning plane was always of type {112} and twinning occurred after considerable prior slip. In discussing her results Wolff points out that the stress level of Schadler's crystals tested at 77°K was approximately equal to the stresses found in her investigation at room temperature and takes up the suggestion that there might be a critical shear stress for twinning as well as for slip. This she calculates to be ~ 45 kg $mm^{-2}$. (Twinning at room temperature was also observed by Fourdeux and Wronski - unpublished results - of this laboratory for an electroshaped Linde ⟨111⟩ crystal, Fig. 2). Koo (1963a) found an unusual dependence of twinning on test temperature for "five-pass" single crystals : twinning takes place only in the temperature range 95°-178°K but neither at room temperature nor at 77°K. Koo's results do not appear to correlate with Wolff's hypothesis.

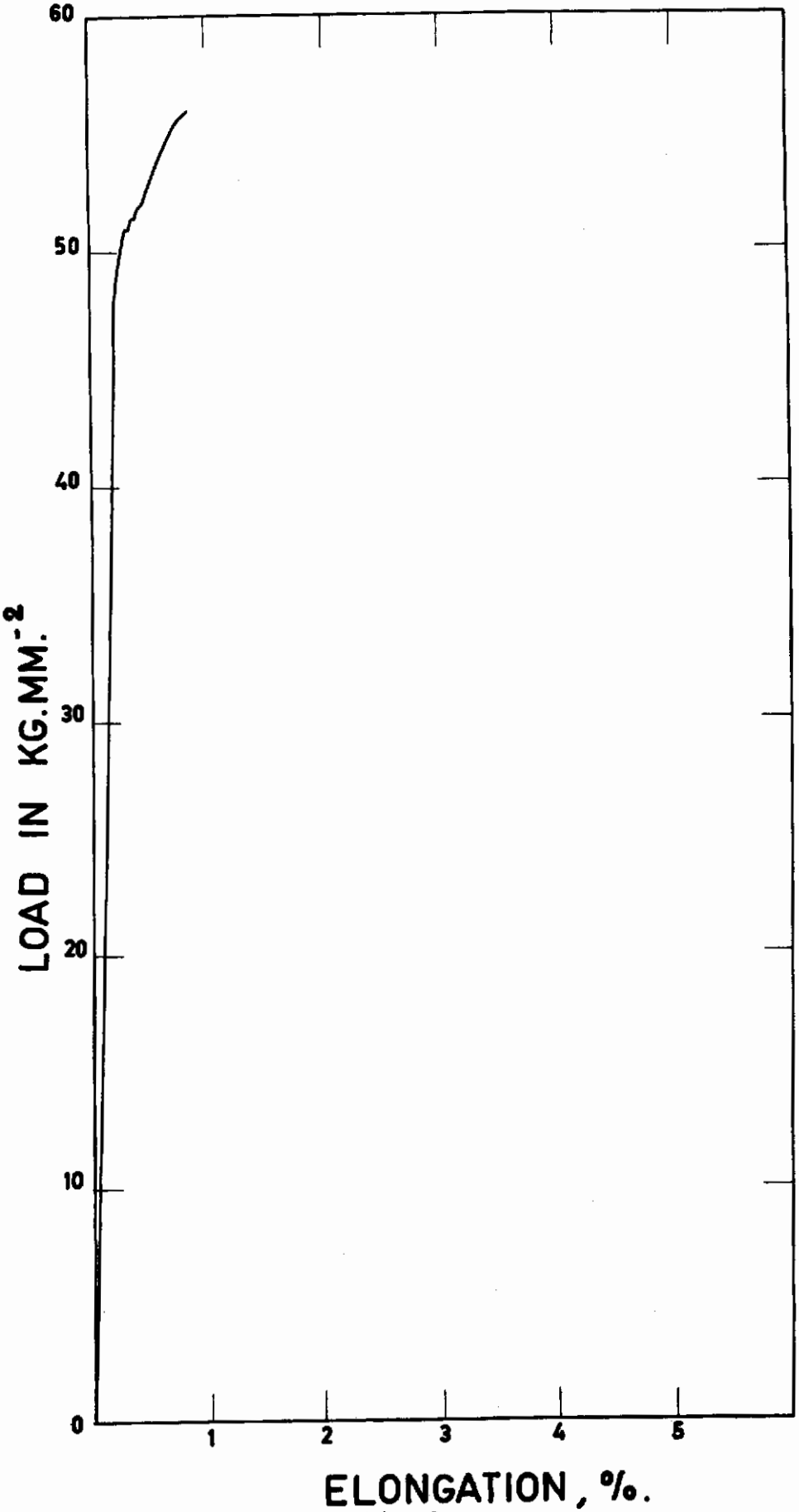


Load-elongation curve for a Linde electroshaped ⟨111⟩ single crystal strained at room temperature at a rate of 0.5% $min^{-1}$.

Fig 2

The mechanical properties of tungsten single crystals, strain-annealed (S. A.) and electron-beam zone-refined (Z. R.) have been studied by numerous workers and some of the results are summarized in Table 1. Critical resolved shear stresses, $\tau_C$, or yield stresses, $\sigma_Y$, are given as in the original publications. The question of the relative importance of lack of grain boundaries and increased purity in promoting ductility has not been satisfactorily resolved: Lawley (1963) notes that Pugh showed conclusively that the high ductility of electron-beam refined single crystals is directly related to the reduction in impurity content, but concludes that it is apparent that the presence of high-angle grain boundaries is more detrimental to low-temperature ductility than is the presence of impurity elements. It has already been noted that Koo (1963c) stresses more strongly the importance of the absence of grain boundaries in promoting the ductility of monocrystalline tungsten. It is agreed, however, (e.g. Koo, 1963a) that increasing the number of zone-melting passes decreases $\tau_C$, increases the ductility and possibly facilitates deformation twinning. This is generally attributed to "increase in the overall purity" as chemical analyses (Koo, 1963a) and dosing experiments (Allen, Maykuth and Jaffee, 1961-2; Stephens, 1963b) have not revealed the rôle of specific impurities at low concentrations. Koo (1963a) further concludes that the large amount of strengthening by trace impurities cannot be explained by current theories of strengthening based on elastic interaction of interstitial solute atoms with dislocations. The dramatic effect of aging (Schadler and Low, 1962) at 600°C on the shape of the stress-strain curve of [100] single crystals has been reported, but again, the impurity or impurities responsible were not identified. A feature of these experiments were load drops of up to a third of $\sigma_A$, obtained on the Instron machine of which

the loading arrangement had been modified to dispense with the bayonet coupling between the load cell and the pull rods, thereby eliminating a substantial part of the machine's softeness.

Internal friction peaks (Sell et al., 1962) have been found at 300° and 475°C, and the latter is tentatively attributed to carbon. Stephens (1963b) found that oxygen additions had only a slight effect on the ductile-brittle transition temperature and Allen et al. (1961-2), who investigated the mechanical properties at room temperature and 400°C, report similarly small effects of nitrogen and carbon as well as of oxygen.

Table 1

| Reference | Orientation | Temperature °K | Strain rate % $min^{-1}$ | $\sigma_A$ $kg.\,mm^{-2}$ | $\sigma_Y$ $kg.\,mm^{-2}$ | $\tau_C$ $kg.\,mm^{-2}$ | Strain % t=tensile s=shear | Mode of deformation | Resistivity ratio 298° / 42°K |
|---|---|---|---|---|---|---|---|---|---|
| Maloof (1963) S.A. | [011] | 295<br>295 | | 24 | | 19 | 12t<br>12s | slip | |
| Koo (1963) S.A. | [421] | 295 | 2 | | 84 | | 13t | slip | |
| Schadler (1960b) Z.R. | various | 295 | 2 | | | | 15t | (011)[11$\bar{1}$] or (112)[11$\bar{1}$] slip | 5400 |
| | | 77 | 2 | | | 27 | 2-4t | (011)[11$\bar{1}$] slip | |
| | | 20 | 2 | | | | 2-4t | (112) twinning | |
| Schadler (1964) Z.R. | [001] | 300 | 0.04 | 8 | | | | | |
| | [001] | 300 | 43 | 26 | | | | slip | |
| | [001] | 77 | 0.4 | 52 | | | | | |
| | [001] | 77 | 4 | 63 | | | | | |
| | [491] | 300 | 0.4 | 19 | | | | | |
| | [491] | 300 | 43 | 37 | | | | slip | |
| | [491] | 77 | 0.4 | 88 | | | | | |
| | [491] | 77 | 4 | 120 | | | | | |
| Allen, Maykuth and Jaffee (1961-2) Z.R. | [215] | 298 | 2 | | | 14 | 0.6t | slip | |
| | [215] | 673 | 2 | | | 3.5 | 80t | | |
| Wolff (1962) Z.R. | [111] | 298 | 2 | 77 | | | 14t | slip and twinning | |
| | [$\bar{0}$01] | 298 | 2 | 49 | | | 12t | | |
| Koo (1963a) Z.R. | | 143 | 2 | | | 41 | 4t | | |
| | | 128 | 2 | | | 41 | 5t | | 41000 |
| | | 113 | 2 | | | 45 | 1t | | |
| | | 77 | 2 | | | 55 | 2t | | |
| Rose, Ferriss and Wulff (1962) Z.R. | [110] | 373 | 2 | 52 | | | | | |
| | [110] | 300 | 2 | 65 | 87 | | | slip | |
| | [110] | 195 | 2 | 84 | 113 | | | | |
| | [110] | 77 | 2 | 155 | | | | | |
| | [100] | 373 | 2 | 17 | | | | | |
| | [100] | 300 | 2 | 22 | | | | | |
| | [100] | 195 | 2 | 36 | | | | slip | |
| | [100] | 77 | 2 | 75 | | | | | |
| | [111] | 373 | 2 | 35 | | | | | |
| | [111] | 300 | 2 | 46 | | | | slip | |
| | [111] | 77 | 2 | 133 | | | | | |

| | | | | | | | | | |
|---|---|---|---|---|---|---|---|---|---|
| | [110] | 300 | 0.2 | 25 | 81 | | | slip | |
| | [110] | 300 | 25 | 89 | 95 | | | | |
| | [110] | 300 | 250 | 106 | 102 | | | | |
| | [100] | 300 | 0.2 | 17 | | | | | |
| | [100] | 300 | 25 | 46 | | | | slip | |
| | [100] | 300 | 250 | 93 | | | | | |
| | [111] | 300 | 0.2 | 36 | | | | | |
| | [111] | 300 | 25 | 63 | | | | slip | |
| | [111] | 300 | 250 | 74-109 | | | | | |

Table 1.
A summary of published results on the deformation characteristics of tungsten single crystals at low temperatures

B. The low temperature deformation of polycrystalline tungsten.

No detailed quantitative data for the tensile properties of polycrystalline tungsten in the ductile-brittle transition region have been reported, probably because of the exceptional susceptibility to "accidental" brittle fracture of tungsten in the polycrystalline state (Koo, 1963b). Wronski and Fourdeux (1964) have reported that the brittle fracture stress of electroshaped (Fourdeux and Wronski, 1963a) specimens of recrystallized swaged tungsten single crystals increases with decreasing test temperature, whereas in commercially pure material no variation is observed (Bechtold and Shewmon, 1954). The yield stress measured in compression (Sheely et al., 1961) also increases as the temperature is lowered. Twinning takes place at 77°K on deforming polycrystalline tungsten in tension or compression.

Electron-beam zone refined crystals have been both swaged and rolled, but usually at temperatures not below 400°C (Schadler, 1960a ; Allen, Maykuth and Jaffee, 1961-2 ; Sell et al., 1962). In the work of Sell et al. no difference in purity was detected between the monocrystalline and polycrystalline material, although it has been suggested that contamination takes place during the mechanical and thermal treatments necessary to produce recrystallization. Ductile-brittle transitions in sintered, arc-cast and worked, recrystallized single crystals (Atkinson et al., 1961) have been found to occur at very similar temperatures, about 200°C, indicating that purification as a result of arc casting or zone refining has only a small effect on ductility.

Most of the work on the effect of impurities on the recrystallization and ductile-brittle transition temperatures of tungsten has been done with fine wires. With more massive samples also there are indications that trace metallic impurities (eg. Al) have a more potent effect than the interstitial

impurities on the recrystallization temperature (Allen et al., 1961-2) and (e.g. Ni, Atkinson et al., 1960) on the ductile-brittle transition temperature. Koo (1963b) found that it is not the grain size but the annealing temperature which determines principally the ductile-brittle transition temperature. As, in general, for the other body-centred cubic transition metals different grain sizes are achieved by annealing specimens at various temperatures, Koo questions the implicit assumption that the distribution of impurities which might occur simultaneously with the production of various grain sizes has only a negligible effect on the mechanical properties. Also recently Sell et al. (1962) found that the strengths of monocrystalline and polycrystalline materials of similar purity were comparable, though the ductility of the former was far larger. In Koo's work, however, the vacuum was no better than $10^{-5}$ Torr and metallographic examination of the fractured specimens suggested that the loss of ductility with increasing annealing temperature was presumably due to precipitation or melting of impurities along grain boundaries. Fracture of specimens annealed at temperatures of 2350°C and above was completely intergranular. Evidence that damage in, a coarse grained specimen originated at a grain boundary is also presented.

The mechanism of slip-induced cleavage in polycrystalline tungsten foils was studied recently by transmission electron microscopy (Wronski and Fourdeux, 1964). Dislocations were found to nucleate within the grains and move in both the {110} and the {112} planes. The dislocations did not generally "pile-up" against the grain boundaries but formed arrays of a different configuration. Microcracks were seen to be nucleated within these dense dislocation arrays in the {110} planes only. They propagated in

these planes to the grain boundaries and then continued in transcrystalline and/or intergranular fashion. These results contrast with those on monocrystalline material for which {100} is the generally observed cleavage plane.

For massive polycrystalline samples it is generally assumed that the brittle fractures are grain boundary and/or precipitate particle induced, but recently Gavrilyuk, Chaporova et al. (1962) reported the absence of foreign phases on the boundaries of recrystallized tungsten. Wronski and Fourdeux (1964) have suggested that for melted material slip-induced {110} cleavage is a possible additional fracture process, the boundary acting initially only as a barrier for the slip dislocations. Zapffe and Landgraf (1949) have studied the fractography of recrystallized sintered tungsten and reported transgranular and intergranular fractures and small (on the microscopic scale) gas holes within the grains. On the electron-microscopic scale gas bubbles (or voids) have been found to be present (Wronski and Fourdeux, unpublished) in the grain boundaries and in the matrix of sintered tungsten and it is believed that there is a direct connection between the presence of the gas bubbles and low-stress failures in recrystallized sintered material. It should be noted that electromicrographs of annealed sintered tungsten already published (Weissmann et al., 1961, Thomas et al., 1962) exhibit the features which Wronski and Fourdeux attribute to gas bubbles.

C. The low temperature deformation of monocrystalline niobium.

Three-stage work hardening has recently been found to occur for certain orientations of niobium single crystals tested at room temperature (Mitchell et al., 1963 ; Votava, 1964). Votava in addition has started the study in some detail of the yielding process (to be reported more fully later) and Mitchell et al. studied the temperature and strain-rate dependence of the work-hardening properties. This work is concerned with purer materials than used previously (Maddin and Chen, 1954 ; Lindtveit et al., 1963) and thus only the two recent papers will be considered.

Mitchell et al. found that in stage I, which follows the onset of plastic flow after a short transition region (stage 0), the work-hardening rate $\theta_I$ is low, $\sim 10^{-4}$ G at room temperature (G being the shear modulus), in stage II $\theta_{II}$ it is $\sim$ G/600, and in stage III the work-hardening rate decreases continuously until fracture occurs. The main effects of increasing the number of zone passes (increasing the purity) were to decrease the initial flow stress and to increase $\theta_{II}$. The initial flow stress, $\tau_o$, increases rapidly with decreasing temperature, $\theta_I$ decreases with decreasing temperature, while $\theta_{II}$ is approximately constant above 295°K and appears to show a maximum at 273°K, before decreasing at lower temperatures. Below 228°K Mitchell et al. found three-stage hardening to disappear and at temperatures below 175°K necking to follow the onset of plastic flow almost immediately. At room temperature the extent of stage I decreases as the orientation approaches the [001] - [101] symmetry plane and for multiple slip orientations stage I is completely absent. Votava found that for the [111] orientation no reproducible behaviour was found and describes the phenomenon as repeated work-softening, possibly caused

by repeated interaction with stage I as a consequence of a reduction of slip systems and by small misorientations in the single crystals. Mitchell et al. report that the main effect of increasing the strain rate, $\dot{\epsilon}$, is to increase $\tau_o$ and decrease $\theta_I$ and $\theta_{II}$, although $\theta_{II}$ appears to exhibit a slight maximum. Their slip line observations indicate that edge dislocations can slip over large distances on (011) planes in stage I, while screw dislocations slip much smaller distances (observations consistent with the double cross-slip mechanism proposed for silicon iron, Low and Guard, 1959). The transition to stage II was found to be accompanied by the appearance of secondary slip bands.

Mitchell et al. sometimes observed yield points at room temperature in stage 0, mostly for less pure specimens. Votava, however, who used a new method of production of strain-free tensile specimens, reports that all the single crystals he investigated show pronounced yield points, the yield drop depending on the orientation and perfection of the crystal, the ⟨111⟩ orientation giving the smallest and the ⟨110⟩ orientation the largest drop. In addition, a tendency for large yield drops was observed along the line [011] - [$\bar{1}$12]. Since breaking up of dislocations networks and non-conservative motion of dislocations is excluded as a consequence of the large energies required, this behaviour was explained as being due to jogs, which cannot move conservatively because of zero resolved shear stress on the jog planes for the above orientations.

For the [123] orientation, studied in detail by Votava, ($\bar{1}$01) was identified as the primary and (110) as the cross-slip plane. He also found that as orientation changes from [011] to [$\bar{1}$23] easy glide develops and similarly two-stage hardening becomes three-stage hardening on changing from [001] to [$\bar{1}$23]; [$\bar{1}$23] is the centre of the easy-glide region and this range is extending

to the $[\bar{1}11]$-[011] line rather than to [001]. For crystals with ⟨110⟩-orientation "self-stabilization" of the four {110} ⟨111⟩ active slip planes due to the crystallographic relationships was found, whereas for crystals with ⟨100⟩-orientation selection of the four active slip planes in pairs was observed.

Niobium does not show the grain-size dependence of the yield stress typical of the body-centred cubic transition metals ; the mechanical properties of polycrystals therefore strongly resemble those of monocrystals and for those of comparable purity (obtained by "flash-annealing") results on strain-rate dependence (Fourdeux and Wronski, 1963b) and deformation mechanisms (Fourdeux, and Wronski, 1964) similar to those on single crystals have been reported.

D. The effects of the surface on the mechanical properties of niobium and tungsten.

The ductile-brittle transition in tungsten is particularly sensitive to the surface condition ; this is generally recognized as is the fact that surface removal by chemical or electrolytic methods lead to enhanced "ductility" (Swiss patent 271 659, 1948). Many investigators have now established (Sedlatschek and Thomas, 1957 ; Stephens, 1963a and 1963b ; Berghezan, 1961 ; Steigerwald and Guarnieri, 1962) that electropolishing results in samples with the highest ductility and lowest transition temperature. Stephens (1963a) has shown that electropolishing 0.13 mm produces an increase in bend ductility from 17° to 153° for rod tested at room temperature, whilst the removal of only half that thickness has little effect in increasing ductility. Measures of surface roughness (Steigerwald and Guarnieri, 1962) do not correlate with ductility and

Berghezan (1961) suggested that removal of carbide layer, produced during mechanical and thermal treatments undergone by the tungsten, was the effective mechanism of inducing ductility. Whilst carbide layers lead to embrittlement, it has been shown that this cannot be the only mechanism, as grinding instead of polishing off the surface layers does not reduce the brittleness (Stephens, 1963b ; Steigerwald and Guarnieri, 1962). It is generally believed that electropolishing removes cracks and other stress concentrations, whereas grinding is known to distort the newly formed surface layers. Stephens (1963b) goes further to suggest that the same mechanism operates when bend ductility is increased by surface oxidation, whereas Berghezan (1961) postulated that oxygen removes the carbon-contaminated surface layer. Mihailov et al. (1960) have shown that carbide, $W_2C$, is formed on the surface of tungsten wires annealed in a "normal" vacuum above 1200°C and that the original ductility can be returned to the wires by annealing in "cold" vacuum using a mercury diffusion pump or by electropolishing off the carbide layer.

The effect of surface gas contamination on the mechanical properties of polycrystalline niobium has been studied by Smallman et al. (1962-3). These authors have shown that embrittlement results after heating for short times at fairly low temperatures (e. g. 30 min. at 300°C) in air, oxygen or nitrogen. Such treatment gives rise to an impregnation of the surface layer of the bulk material with oxygen and/or nitrogen and these layers were found to crack at low stresses during mechanical testing. Smallman et al. conclude that these surface cracks are the direct cause of embrittlement, acting as sharp notches. Tungsten being more notch-sensitive, its surface produced by grinding probably contains enough small notches to embrittle the material without recourse to any additional treatment as gas contamination by e. g. hydrocarbon vapours.

REFERENCES

B.C. Allen, D.J. Maykuth and R.I. Jaffee, 1961-2, J.I.M., 90, 120.

R.H. Atkinson et al., 1960, WADD 60-37, Pt.I.

R.H. Atkinson, C.H. Keith and R.C. Koo, 1961, Refractory Metals and Alloys (Interscience), p. 319.

J.H. Bechtold and P.G. Shewmon, 1954, Trans. A.S.M. 46, 397.

A. Berghezan, 1961, Met. Soc. Meeting, A.I.M.E. (Detroit, Mich.).

N. Brown and R.A. Ekvall, Acta Met., 10, 1101.

A. Calverley, M. Davis and R.F. Lever 1957, J. Sc. Instr., 34, 142.

D.P. Ferris, R.M. Rose and J. Wulff, 1961, Final Report on DA-19-ORD-4543.

A. Fourdeux and A. Wronski, 1963a, Brit. J. Appl. Phys., 14, 218
1963b, Acta Met., 11, 1271
1964, J. Less-Common Metals, 6, 11.

M.I. Gavrilyuk, I.N. Chaporova et al., 1962, Fiz. Met. Metalloven., 13, 693.

R.C. Koo, 1963a, Acta Met., 11, 1083
1963b, Trans. A.I.M.E., 227, 280
1963c, (submitted for publication), see also Sell et al., 1962.

J.R. Low and R.W. Guard, 1959, Acta Met. 7, 111.

A. Lawley, 1963, Proc. Fourth Symp. on Electron Beam Technology (Alloyd Electronics) p. 133.

T. Lindtveit, I. Kvernes and P. Storvik, 1963, S.I. Rep. No. 404.

J.R. Low, 1956, I.U.T.A.M. Madrid Colloquium (Springer-Berlin), p. 60
1963, Fracture of Solids (Interscience), p. 208.

R. Maddin and N.K. Chem, 1953, J. Metals, 5, 1131.

S.R. Maloof, 1963, Proc. Fourth Symp. on Electron Beam Technology (Alloyd Electronics), p. 190.

I.F. Mihailov, U.S. Kogan, N.A. Kosik, 1960, Fiz. Metal. Metalloved, 9, 283.

T.E. Mitchell, R.A. Foxall and P.B. Hirsch, 1963, Phil. Mag., 8, 1895.

J. L. Orehotsky and R. Steinitz, 1962, Trans. AIME, 224, 556.

R. M. Rose, D. P. Ferris and J. Wulff, 1962, Trans. AIME, 224, 981.

H. W. Schadler, 1960a, Rpt. 60-RL-(2534M),
1960b, Trans. AIME, 218, 649
1964, Acta Met. (to be published).

H. W. Schadler and J. R. Low, 1962, Fnl. Rept. on Nonr-2614-(00).

H. G. Sell et al., 1961, WADD TR 60-37, Pt. II
1962, WADD TR 60-37, Pt. III.

K. Sedlatschek and D. A. Thomas, 1957, Powder Metallurgy Bul., 8, 35.

W. Sheely et al., 1961, ASD 61-3.

R. E. Smallman, J. Hernaez, and M. Adams, 1962-3, J. I. M., 91, 279.

E. A. Steigerwald and G. J. Guarnieri, 1962, Trans. ASM. 55, 307.

J. R. Stephens, 1963a, High Temperature Materials II (Interscience), p. 125
1963b, NASA TND-1581.

D. A. Thomas et al., 1962, WADD TR 61-181 (Pt. II), p. 107.

E. Votava, 1964, Phys. Stat. Sol., 5, 421.

S. Weissmann, Y. Nakayama and I. Imura, 1961, WADD TR 61-181 (Pt. I), p. 141.

U. E. Wolff, 1962, Trans. AIME, 224, 327.

A. Wronski and A. Fourdeux, 1964, J. Less-Common Met., 6, 413.

C. A. Zapffe and F. K. Landgraf, 1949, Trans. ASM, 41, 396.

## SECTION II.

## Investigation of Room Temperature Slip and Yielding on Zone-Melted Niobium Single Crystals.

by

E. Votava

Introduction.

There is no general agreement on slip in body-centered cubic metals. Maddin and Chen (1) assume that slip in niobium and molybdenum takes place on {110} and that the wavy slip lines characteristic for bcc metals are the result of composite slip on pairs of non-parallel {110}-planes.

Opinsky and Smoluchowski (2), experimenting with silicon-iron alloys, assume on the contrary that slip in bcc metals is orientation dependent and that that set of planes belonging to a ⟨111⟩-zone becomes always operative on which the resolved shear stress is a maximum.

An investigation of the orientation dependence of the mechanical properties of electron-beam zone melted high-purity niobium single crystals prepared in a strain-free way had been carried out previously (3) for purposes of interpretation and also to clarify the above discrepancy it was found necessary to study in more detail the room temperature slip, the operative glide planes and the mechanism of deformation of such crystals. The results obtained up to now are presented below.

Experimental Technique :

The niobium single crystals used for this work were prepared by a special technique described in (3). They were ball-ended, circular and strain-free. The crystals had an orientation near ⟨321⟩ and this orientation was chosen because it had been found (3) (4) that a pronounced "easy glide" region develops around it which makes slip line observations much more easy. The crystals were deformed at room temperature at successive points of the stress-strain curve ; a special gripping device, shown in Fig. 1 was used. This device made self-alignment of the crystal during deformation possible due to the hemispherical housing and collar, and further the crystal could be removed for microscopic inspection and X-ray analysis easily without introducing additional deformations.

The determination of the slip plane was carried out in the following way. As the slip lines were well visible even after small amounts of deformation, a Laue picture was taken of the crystal mounted horizontally in such a way that the incident X-ray beam, the crystal axis and the normal to the slip plane were all situated in one plane. Adjustment to these conditions was facilitated by painting one part of the crystal up to a prominent glide ellipse with red ink. A stereomicroscope and goniometer mounting of the crystal as well as fiducial markings on both ends of the crystal were also found most helpful. For further deformation studies the red ink could be removed easily by water followed by cleaning with alcohol. For the determination of the glide plane from the Laue picture the angle between the glide plane and the crystal axis was measured microscopically with the crystal mounted on a goniometer.

Experimental Results :

Niobium single crystal N° 270a(i) - orientation near ⟨321⟩.

The deformation of this crystal was stopped at three different points on the stress-strain curve and the orientation of the axis, the glide planes and the glide directions were determined. Fig. 2 shows the complete stress-strain curve and the points at which deformation had been stopped ; it consists of four different regions, the yield point region, the "easy glide" region, followed by work hardening, which later flattens out.

The results of our measurements are summarized in Fig. 3. At the lower yield point (point 1 of the stress-strain curve) the crystal axis has not moved appreciably and one observes the development of two different glide systems. The primary system is well developed with marked slip lines at fairly great distances with slip on {110}-planes. The secondary system is much fainter and all our measurements indicate also slip on {110}. Apparently cross slip on non-parallel {110}-planes has taken place. This aspect can be seen on Fig. 4, which is a micrograph of a part of the crystal surface at point 1.

Stretching the crystal further to point 2 of the stress-strain curve brings more primary slip into action and the distance between the slip lines decreases. The secondary system becomes evident as extensive cross slip. However, no additional glide planes were observed at point 2 as compared with point 1.

At point 3 of the stress-strain curve, at which appreciable work-hardening has already occurred, additional slip traces are observed, which are probably symmetrical to the first two {110}-planes. However, no exact determination of the new glide planes was possible at this stage due to the great disorder of the surface.

The glide direction was determined from the movement of the crystal axis and as can be deduced from Fig. 3 is ⟨111⟩ for the primary glide system. From surface observations, which will be reported later, the conclusion could be also drawn that the secondary glide system has also a ⟨111⟩-glide direction and that both systems have a common glide direction.

Niobium single crystal No 271 a(p) - orientation near ⟨321⟩.

During the various microscopic inspections of crystal N° 270 a (i) it was recognized that the slip lines were not developed homogeneously around the whole crystal but that there are places where no slip lines become visible at all and other places where cross slip occurred preferentially. The orientation dependence of the slip-line figures was therefore studied in more detail with another niobium crystal of nearly the same orientation and the results reported below were also verified for the niobium single crystal N° 270 a (i) at point 1 of the stress-strain curve.

Fig. 5 shows the stress-strain curve of crystal N° 271 a (p) with point 1, where the following slip-line observations were made. As this point is situated just beyond the upper yield point, the observations allow also some conclusions to be drawn on the mechanism of deformation around the yield point itself. Fig. 6a and 6b are micrographs of the surface of this crystal taken at different angles, which are indicated on Fig. 6c. A comparison of the micrographs with the angle relations shows clearly that cross slip takes place preferentially at and around the point of emergence of the ⟨111⟩-slip direction. At right angles to ⟨111⟩ in the direction ⟨211⟩, a region can be found where even with most careful microscopic methods no slip lines can be detected. Only primary slip is observed between these two extremes.

Fig. 7 shows the results of the determination of the slip planes and slip directions of this crystal, obtained by the combined microscopic and back-reflection X-ray techniques. Thus slip has taken place on pairs of non-parallel {110}-planes with a common ⟨111⟩-direction.

Discussion :

The present investigation confirms the results of Maddin and Chen (1) at least as regards the specific orientation near {321} investigated. According to Opinsky and Smoluchowski[2] slip should take place for this orientation on {321}. This, however, could not be confirmed. It is possible that at higher temperatures slip on this plane and other planes belonging to a ⟨111⟩-zone will take place ; some indications for such a behaviour has been found by Harris (4), although in this work no complete agreement with the viewpoint of Opinsky and Smoluchowski has been found either. However, as the present measurements were made within the "easy glide" area and this area extends fairly far within the stereographic triangle (3) (4) one can assume that the present finding holds for the whole area at least at room temperature. Further measurements will be necessary to support this assumption.

The mechanism of deformation as found in this work definitely confirms the sudden generation of a large number of dislocations between the upper and the lower yield points by a double cross-slip mechanism, first proposed by Koehler (6) and by Orowan (7) and discussed later by Low and Guard (8), Johnston and Gilman (9) and Conrad (10). This is demonstrated in Fig. 6a, 6b and 6c, at a state of deformation just after the upper yield point. This can be interpreted in the sense that the edge components of the mobile dislocations move over great distances on {110}-p anes in a ⟨111⟩-direction, thereby

extending the length of the screw components and increasing the probability for cross slip, a process which takes place frequently in niobium (11). Double cross slip is then a means of transmitting slip over the entire length of the crystal and of creating at the same time the large number of dislocations required to drop the stress from the upper to the lower yield point.

However, as cross slip occurs easily in niobium (11), double cross slip alone cannot explain the development of a yield point. For the stress to rise to the upper yield point an obstruction to plastic flow must be present until the sudden multiplication of the dislocations decreases the stress again. Considering the recent finding (3) that the yield point drop in niobium depends strongly on orientation it is more probable to assume that the obstruction to plastic flow is the result of a special dislocation configuration rather than one of the locking of the dislocations by interstitial atoms.

Dislocation configurations satisfying this condition have been proposed by Schoeck (12), namely jogs within the dislocation segment of the network which acts as Frank-Read source. Since in b c c metals the hexagonal network of dislocations formed by the reaction $a/2\,[111] + a/2\,[1\bar{1}\bar{1}] \longrightarrow a\,[100]$ is very stable, it is unlikely that it can be broken up. On the other hand the presence of jogs will restrict the movement of dislocations considerably since a screw dislocation with a jog can move easily only in the plane of the jog. Glide on any other plane is non-conservative and will require large energies due to the creation of vacancies and interstitial atoms.

Thus as the breaking-up of networks and the non-conservative motion of jogs are unfavourable, there remains, as already pointed out by Rose, Ferris and Wulff (13), the conservative motion of dislocation loops and jogs within

the network. This, however, will depend on the resolved shear stress on the plane of the jog and as this is in general smaller than the resolved shear stress on the primary slip plane an obstruction to plastic flow will result. As a consequence dislocation sources will develop badly at the beginning (pre-yield) until a critical stress brings the multiplication of the dislocations by double cross slip into action. The extreme case for maximum obstruction should therefore take place for ⟨110⟩-oriented crystals since the resolved shear stress on the jog plane is zero in this case. This has been demonstrated for tungsten by (13) and for niobium by (3). Similar results have been obtained for tantalum single crystals with the same orientation (14).

Acknowledgements :

The author gratefully acknowledges the assistance of E. Vanderschueren for the construction of the gripping device and the growing of the single crystals and of J. Dossin for the deformation and X-ray work.

REFERENCES


(1) : R. Maddin and N.K. Chen : J. Metals, 5, 1131 (1953).

(2) : A.J. Opinsky and R. Smoluchowski : J. appl. Phys. 22, 1380 (1951) ; ibid : 22, 1488 (1951).

(3) : E. Votava : Phys. stat. Sol. 5, 421 (1964) ; Plansee Proceedings, 1965.

(4) : T.E. Mitchell, R.A. Foxall and P.B. Hirsch : Phil. Mag. 8, 1895 (1963).

(5) : B. Harris : J. Inst. Met. 92, 89 (1964).

(6) : J.S. Koehler : Phys. Rev. 86, 52 (1952).

(7) : E. Orowan : "Dislocations in metals", 103 ; 1954, New York, AIME.

(8) : J.R. Low and R.W. Guard : Acta Met., 7, 171 (1959).

(9) : W.G. Johnston and J.J. Gilman : J. Appl. Phys. 31, 632 (1960).

(10) : H. Conrad : J. Iron Steel Inst. 198, 364 (1961).

(11) : A. Fourdeux and A. Berghezan : 6ème Colloque de Métallurgie, Saclay, p. 91 (1962).

(12) : G. Schoeck : Acta Met., 9 382 (1961).

(13) : D.P. Ferriss, R.M. Rose and J. Wulff : Trans. Metall. Soc. AIME 224, 982 (1962).

(14) : E. Votava : private communication.

Legends to Figures :

Fig. 1 : The gripping device for the single crystals : (1) holder with hemispherical housing, (2) hemispherical collar, (3) single crystals, (4) spring to hold the collar.

Fig. 2 : Stress-strain curve of niobium single crystal No 270a(i) deformed at room temperature. At point 1, 2 and 3 the crystal was demounted for microscopic inspection and X-ray analysis.

Fig. 3 : Glide elements and glide directions in crystal No. 270a (i).

Fig. 4 : Aspect of a part of the surface of crystal No. 270a (i) deformed till the lower yield point (point 1 in Fig. 2). The two non-parallel {110}-slip system are clearly visible.

Fig. 5 : Stress-strain curve of niobium single crystal No. 271 a(p) deformed at room temperature.

Fig. 6 : a) and b) : Aspect of the different parts of the surface of crystal No. 271a (p) after deformation till point 1 (see Fig. 5). The angle relations of the different micrographs are given in Fig. 6c.

Fig. 7 : Glide elements and glide directions in crystal No. 27A a(p).

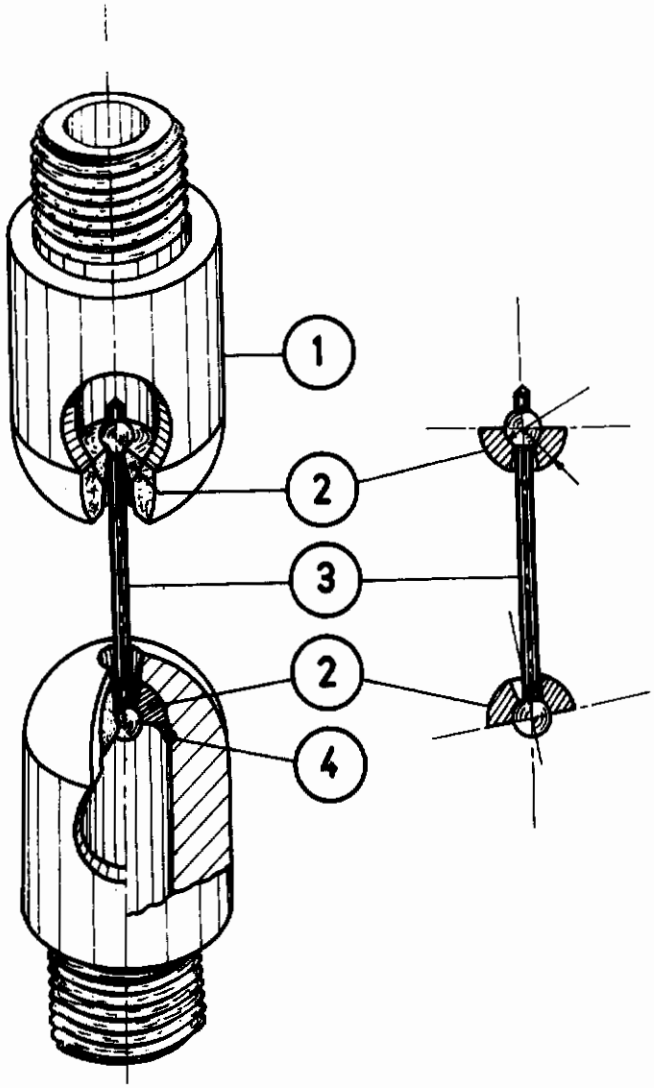


Fig. 1

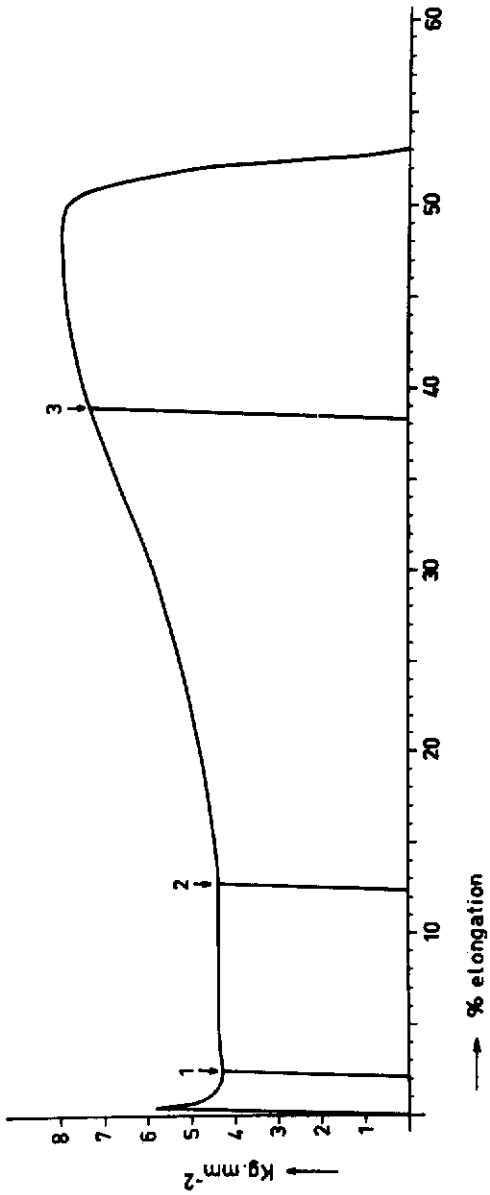


Fig. 2

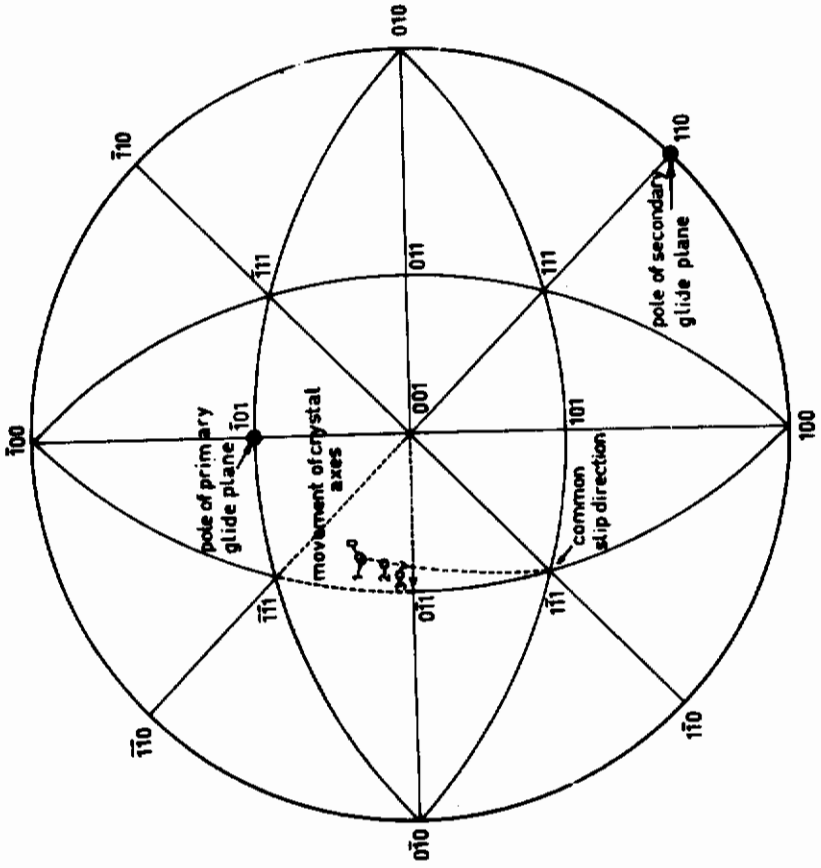


Fig. 3


Fig. 4

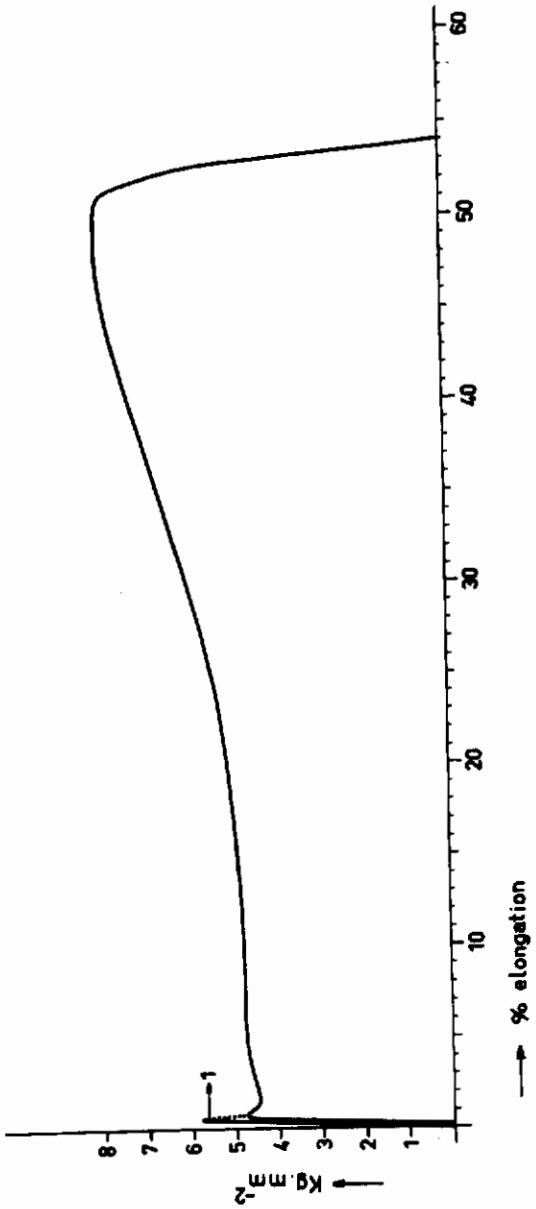


Fig.5

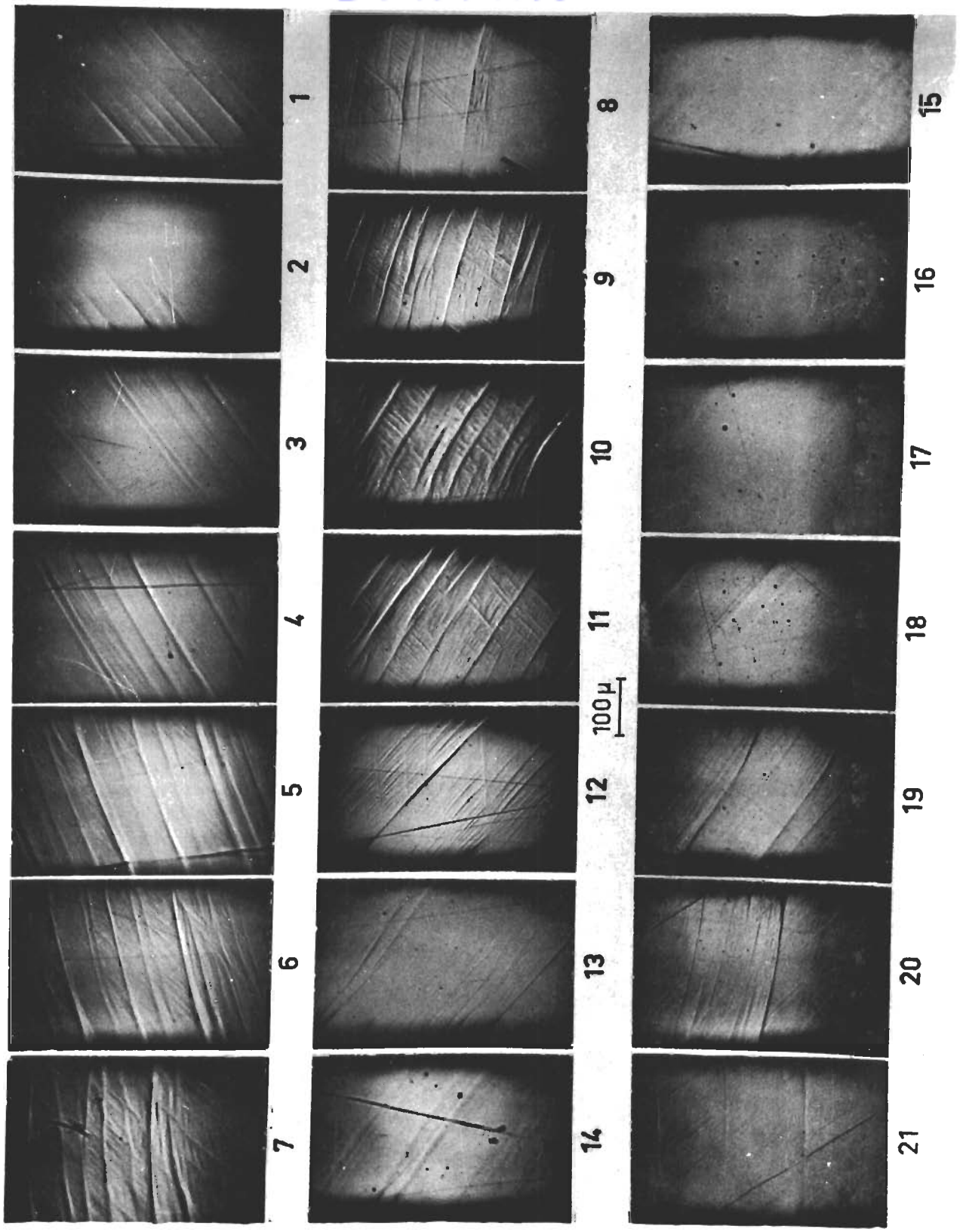


Fig. 6a

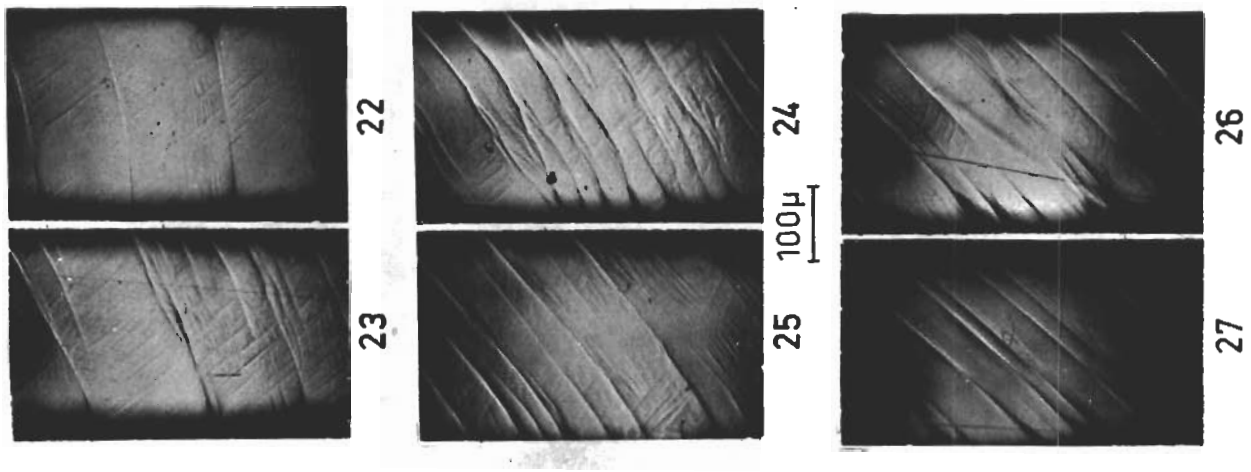


Fig. 6b

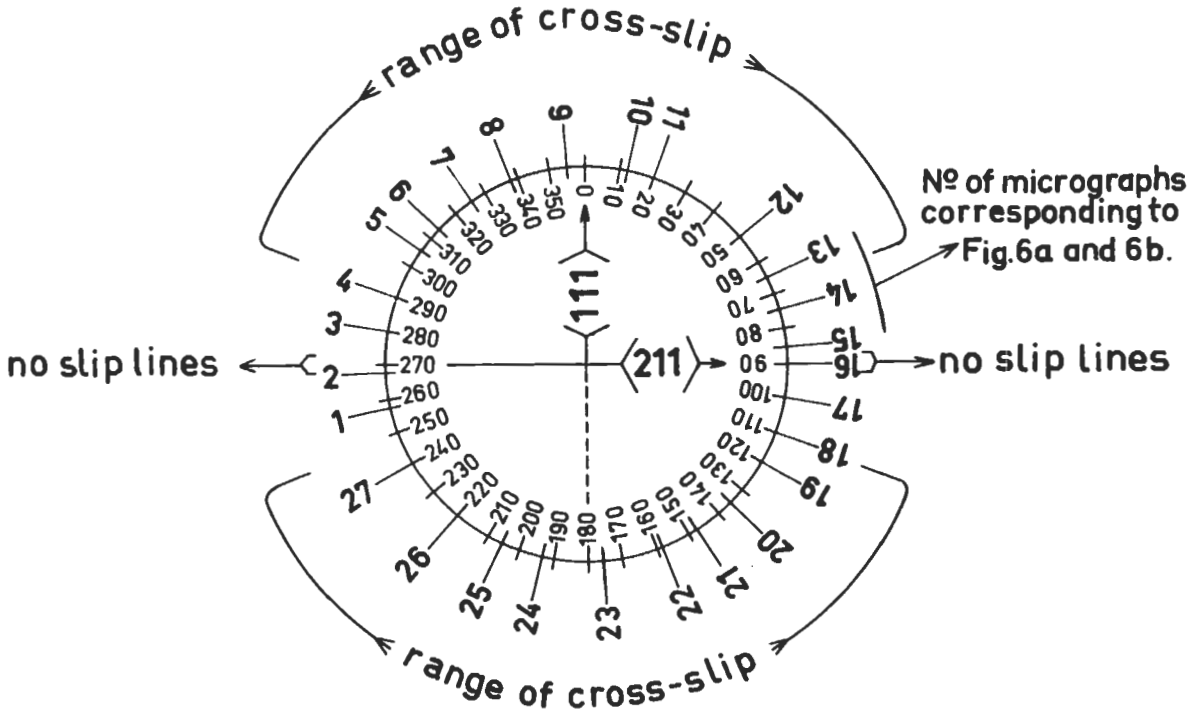


Fig. 6c

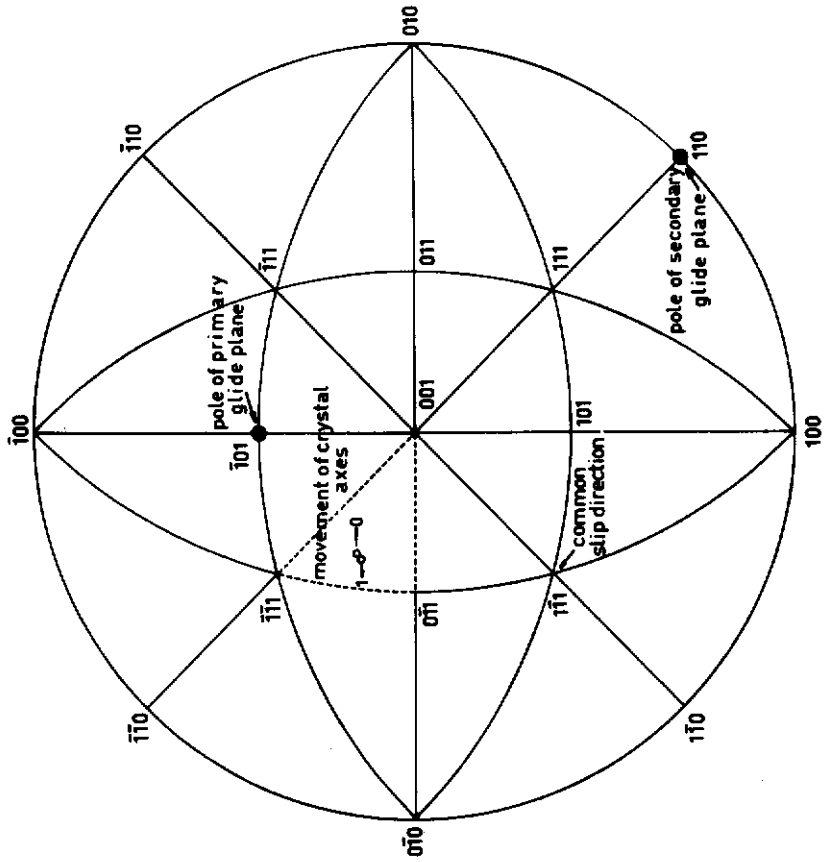


Fig.7

## SECTION III.

## Effect of Purity on the Mechanical Properties of Niobium.

by

E. Votava

## Introduction.

Niobium possesses a number of interesting properties such as high melting point, low vapour pressure, moderate density, good fabricability, low ductile-to-brittle transition temperature and low thermal neutron absorption cross section. All this makes this metal interesting both for high temperature applications and for nuclear reactors.

In order to explore efficiently the use of this metal for such applications one needs to understand better the mechanical properties and also the underlying mechanisms determining these properties. Work in this direction has started only in the last few years, both on polycrystalline material (1) (2) (3) (4) (5) (6) and on single crystals (7) (8) (9) (10) (11). The present work has been initiated with the aim of evaluating the effect of zone-melting on the mechanical properties of niobium on isochronal annealing after cold swaging.

Experimental Techniques :

Niobium of Murex origin was used. For testing the mechanical properties of the impure nionium 1 cm thick bars were zone recrystallized several times in an electron-beam zone refiner at approximately 2000°C in a vacuum of about $5 \times 10^{-6}$ Torr and later cold swaged to 90% reduction in cross section. To test the properties of the high-purity niobium, bars of the same origin and from the same batch were electron-beam zone melted 19 times and then also cold swaged to 90% reduction in cross section. After zone melting the niobium bars were single crystals. The distribution of the remaining interstitial impurities along the bars can be regarded as sufficiently homogeneous since purification by electron-beam zone melting proceeds mostly by vacuum distillation (8) (12). An improved gun design with a niobium filament (13) was used for all electron-beam operations in order to avoid metallic contamination from the cathode.

After cold swaging samples of 3.5 cm length were cut from the bars and annealed isochronically for 2 hours every 100°C between 300°C and 1000°C. Due to shortage of material only two samples were chosen for each temperature with the exception for 20°C. Annealing was carried out by sliding a preheated furnace over a 35mm outer diameter quartz tube, which was pumped continuously by a 100 l/sec mercury diffusion pump with a metallic liquid-air baffle, thus avoiding carbon contamination during the heat treatment. The vacuum as read on a gauge was mostly $5 \times 10^{-7}$ Torr during the heat treatment. Cooling was effected by withdrawing the furnace.

The tensile tests were made at room temperature using an Instron tensile tester and a specially developed pressure gripping device. For all samples tested a crosshead speed of 0.05 cm. $min^{-1}$ was chosen, corresponding to an average strain rate of $5.5 \times 10^{-4} sec^{-1}$.

The interstitial impurity contents of niobium before and after zone recrystallization and after zone melting are listed in table I. For the two latter cases the contents of H, N and O have been measured by two different laboratories and it can be seen that there are significant differences especially as regards the nitrogen content. However, in spite of the considerable scatter in the values given in table I, the tendency for solid-state purification during zone recrystallization is evident as well as the purification effect after zone melting.

Results and Discussion :

Fig. 1 and Fig. 2 show the change in the mechanical properties (ultimate tensile strength = UTS, elastic limit = EL, total elongation = $E_t$, uniform elongation = $E_U$) on isochronal annealing of the recrystallized impure niobium and of zone-melted niobium after 90% reduction in cross section. Obviously the most important difference is the higher UTS, the higher elastic limit and the lower ductility as expressed by total and by uniform elongation for the impure niobium and this for the whole range of 20°C to 1000°C. This behavior is quite understandable in view of the difference in interstitial content. Mincher and Sheely (6) have studied the influence of interstitial impurities on the mechanical properties of niobium and have found a similar behavior, although the interstitial content of the electron-beam melted niobium and the difference between the interstitial contents of the two kinds of niobium used by them was considerably higher than is the case for our samples. Consequently

their UTS values are still higher than ours, although they were not measured after isochronal annealing but directly as a function of the temperature itself. This becomes evident by comparing the room temperature values of their measurements with ours, as done in table II, which clearly demonstrates the great influence of interstitial impurities on the mechanical properties of niobium and shows also that with decreasing impurity content the ductility increases and the UTS decreases considerably.

The question arises which of the properties is influenced most by zone purification. To answer this the different properties shown in Fig. 1 and Fig. 2 were compared using the values at 20°C as a 100% basis. Fig. 3, Fig. 4, Fig. 5, and Fig. 6 show this comparison. Obviously the greatest change occurs for the uniform elongation, (see Fig. 6), the curve for which is considerably smoother after purification. The reason for this behavior is found when comparing the aspect of the stress-strain curves before and after purification, given in Fig. 7 and Fig. 8. Practically no work hardening is observed for the impure zone-recrystallized niobium after cold swaging and necking takes place fairly early. With progressive annealing temperature, but only from 600°C on, more and more work hardening is introduced as the result of recrystallization setting in. On the other hand, some work hardening is already present in electron beam zone melted niobium after cold swaging, which improves further from between 500°C and 600°C on, but not so drastically as for unpurified niobium. Hence in view of the creation of work hardening after zone purification a similar behaviour to that in high purity single crystals is found, as shown by (7) and (8).

A further very interesting aspect of the stress-strain curves of Fig. 8 is the appearance of a yield point for zone melted and cold swaged niobium, which persists after isochronal annealing between 20°C and 700°C ; even at 800°C a small plateau still remains. The disappearance of the yield point at higher annealing temperatures is obviously connected with recrystallization setting in. On the other hand, as Fig. 7 shows, this phenomenon is absent for niobium which has not been zone melted, apart from a small bump at 20°C.

It is difficult to understand the creation of this yield point in the light of current yield point theories, especially since it is found for the purer material and after severe deformation, where normally a yield point should already have been eliminated, as has been demonstrated for the case of uniaxial tension by (3). The absence of a yield point for niobium which has not been zone melted can be a masking effect due to the absence of work hardening as a consequence of lower purity and the small bump at 20°C (see Fig. 7) supports well this hypothesis. However, assuming also that for such niobium a screened yield point is present, the severe deformation after cold swaging will certainly have created a great number of mobile dislocations, so that the model of Hahn (14) and Johnston (15) for yielding is not applicable in this case. Thus as uniaxial tension destroys the yield point (3) and cold swaging creates a yield point, one is led to the assumption that the mode of deformation produced by cold swaging creates a special structure, which on further testing in uniaxial tension resists the initial movement of dislocations. It is well known that swaging produces a fibrous structure with the bundle of crystals of similar orientation more or less parallel to the swaging direction.

It is possible that such a structure can restrict dislocation movement at the beginning, as probably a large number of the dislocations are oriented parallel to the applied force when tested in uniaxial tension.

Another characteristic feature of the tensile properties is an increase of the UTS between 400°C and 600°C for both kinds of niobium investigated as can be seen from Fig. 7 and 8. Since primary recrystallization starts after 600°C, as evidenced by a continuous decrease of the UTS, one might expect that in this temperature range restauration phenomena such as polygonization and anihilation of the dislocations take place. However, restauration alone cannot explain this increase in the UTS, since one would expect rather a decrease due to the change to a more perfect state after severe cold swaging. The only remaining possibility, therefore, is impurity interaction with the dislocations, which became active in this temperature range and hinder to a certain extent plastic deformation at room temperature. Mincher and Sheely (6) also observed such an increase round 500°C and attributed it to a strain-aging effect of nitrogen and carbon. As, however, in our case the nitrogen content does not differ very much between the two kinds of niobium (see table I) and is much smaller than that of Mincher and Sheely's samples, the only element responsible for this could in our case be carbon.

Acknowledgements :

Experimental assistance of E. Vanderschueren and J. Dossin is appreciated.

Table I.

| | | H ppm | N ppm | O ppm | C ppm |
|---|---|---|---|---|---|
| Niobium (Murex) as received | | 11-23 | 27-66 | 35-51 | ~ 100 |
| Niobium (Murex) after zone-recrystallization | analysed by Heraeus-Hanau Germany | ~ 1 | 13-22 | 10-24 | not analysed |
| | analysed by Union Carbide Parma Research Center, Ohio, USA | 0.4 | < 1 | 12 | 1 |
| Niobium (Murex) after 19 zone passes | analysed by Heraeus-Hanau Germany | ~0.6 | 5-9 | 5-13 | not analysed |
| | analysed by Union Carbide Parma Research Center, Ohio, USA | 0.7 | < 1 | 3.8 | < 1 |

Table II

Comparison of room temperature tensile properties of niobium of different purity.

| | UTS kg. mm$^{-2}$ | total elon-gation % | Impurity content in p.p.m. | | | |
|---|---|---|---|---|---|---|
| | | | H | N | O | C |
| Arc melted and cold swaged 81% ($A_2$) (Mincher and Sheely) | 64.1 | 15 | <10 | 200 | 400 | 300 |
| Arc melted, cold swaged 81% and recrystallized 3h at 1065°C ($A_2$) (Mincher and Sheely) | 37 | 42 | | | | |
| Arc melted and cold swaged 80% ($A_3$) (Mincher and Sheely) | 57.75 | 17 | <10 | 100 | 400 | 270 |
| Arc melted, cold swaged 80% and recrystallized 3h at 1065°C ($A_3$) (Mincher and Sheely) | 35.2 | 49 | | | | |
| Electron-beam melted and cold swaged 95% (Mincher and Sheely) | 42.46 | 20 | 8 | 90 | 100 | 210 |
| Electron-beam melted, cold swaged 95% and recrystallized 2h at 1093°C (Mincher and Sheely) | ≈23 | 60 | | | | |
| Niobium Murex, electron-beam zone recrystallized and cold swaged 90% (present work) | ≈22 | ≈30 | ~1 (0.4) | 13-22 (<1) | 10-24 (12) | (1) |
| Niobium Murex, electron-beam zone recrystallized , cold swaged 90% and recrystallized 2 h at 1000°C (present work) | 17.1 | ≈60 | | | | |
| Electron-beam zone melted and cold swaged 90% (present work) | ≈16 | 48 | ~0.6 (0.7) | 5-9 (<1) | 5-13 (3.8) | (<1) |
| Electron-beam zone melted, cold swaged 90% and recrystallized 2h at 1000°C (present work). | ≈15.5 | ≈60.5 | | | | |

REFERENCES

(1) : G.R. Tottle : J. Inst. Met. 85, 375 (1956-57).

(2) : E.T. Wessel : Trans. AIME, 209, 930 (1957).

(3) : B.F. Dyson, R.B. Jones and W.J. Mc G. Tegart : J. Inst. Met. 87, 340 (1958-59).

(4) : E.T. Wessel and D.D. Lawthers : Technology of Columbium (Niobium), p. 66 (1958) ; John Wiley & Sons, Inc., New York.

(5) : B.L. Mordike : J. Inst. Metals, 88, 272 (1959).

(6) : A.L. Mincher and W.F. Sheely : Trans. AIME, 221, 19 (1961).

(7) : T.E. Mitchell, R.A. Foxall and P.B. Hirsch : Phil. Mag. 8, 1895 (1963).

(8) : E. Votava : Phys. Stat. sol. 5, 421 (1964).

(9) : B. Harris : J. Inst. Met. 92, 89 (1963-64).

(10) : B. Harris : J. Less-Common Metals, 7, 185 (1964).

(11) : E. Votava : 3. Scientific Report - U.S. Air Force Contract AF61(052)-774, (1965).

(12) : B.L. Mordike : Z. Metallkde. 55, 304 (1964).

(13) : E. Vanderschueren and E. Votava : Rev. Scient. Inst. 33, 389 (1962).

(14) : G.T. Hahn : Acta Met. 10, 727 (1962).

(15) : W.G. Johnston : J. Appl. Phys. 33, 2716 (1962).

Legends to Figures :

Fig. 1 : Change of the mechanical properties (UTS = ultimate tensile strength, EL = elastic limit, $E_t$ = total elongation, $E_U$ = uniform elongation) of impure niobium after swaging 90% in cross section on isochronal annealing.

Fig. 2 : Change of the mechanical properties of electron beam zone refined niobium after swaging 90% in cross section on isochronal annealing.

Fig. 3 : Comparison of the change of the UTS for purified and unpurified niobium. Values at 20°C used as a 100% basis.

Fig. 4 : Comparison of the change of the elastic limit EL for purified and unpurified niobium.

Fig. 5 : Comparison of the change of total elongation $E_t$ for purified and unpurified niobium.

Fig. 6 : Comparison of the change of the uniform elongation $E_U$ for purified and unpurified niobium.

Fig. 7 : Typical stress-strain curves of impure niobium after swaging 90% in cross section on isochronal annealing.

Fig. 8 : Typical stress-strain curves of electron beam zone melted niobium after swaging 90% in cross section on isochronal annealing.

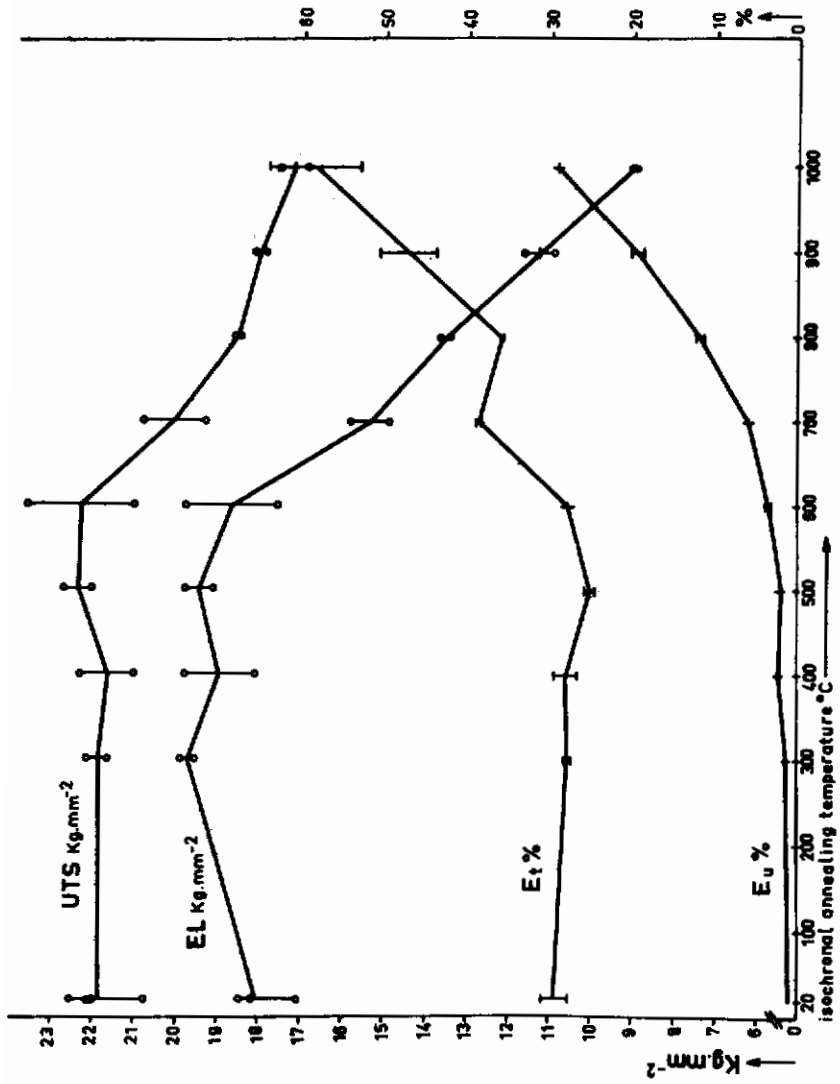


Fig.1

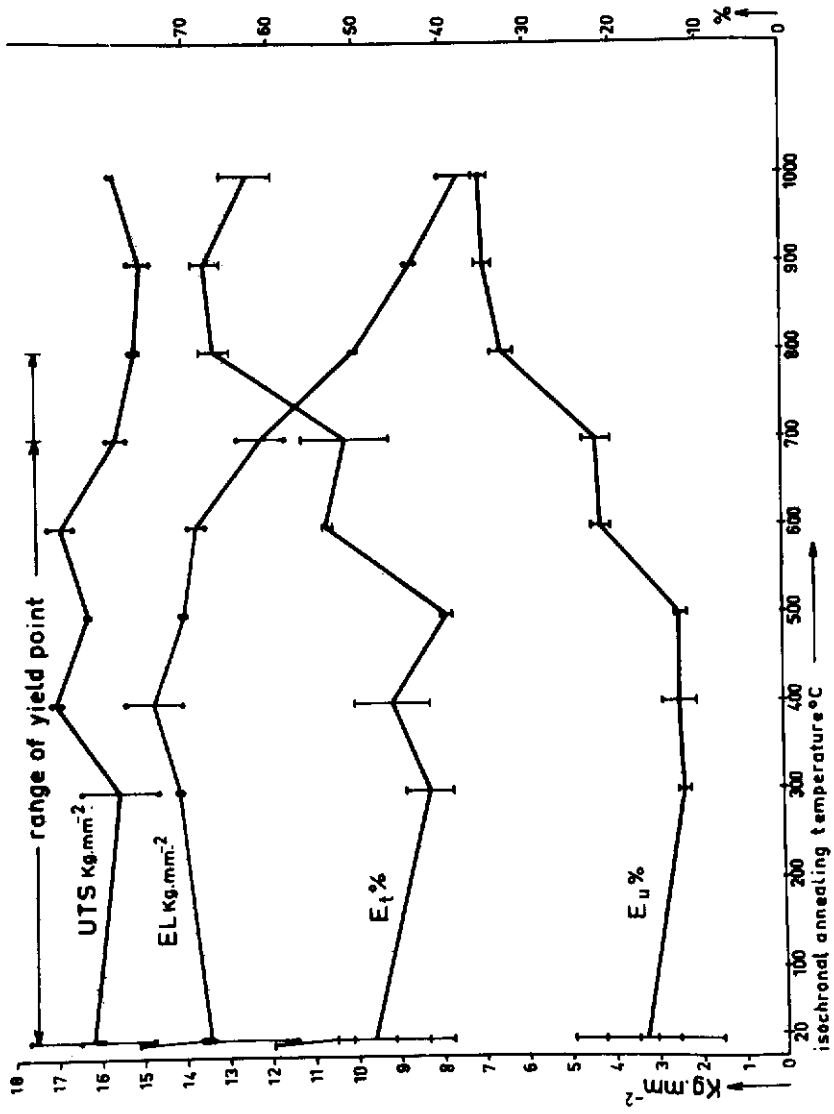


Fig.2

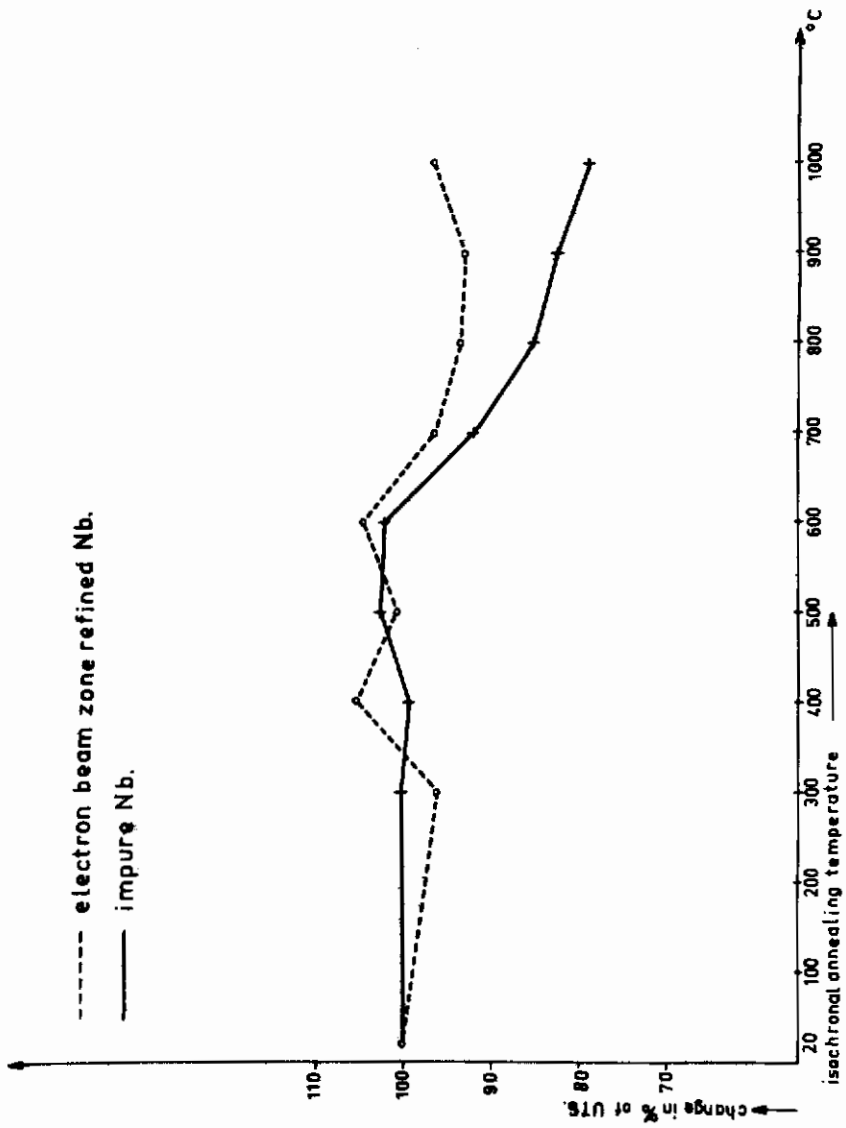


Fig.3

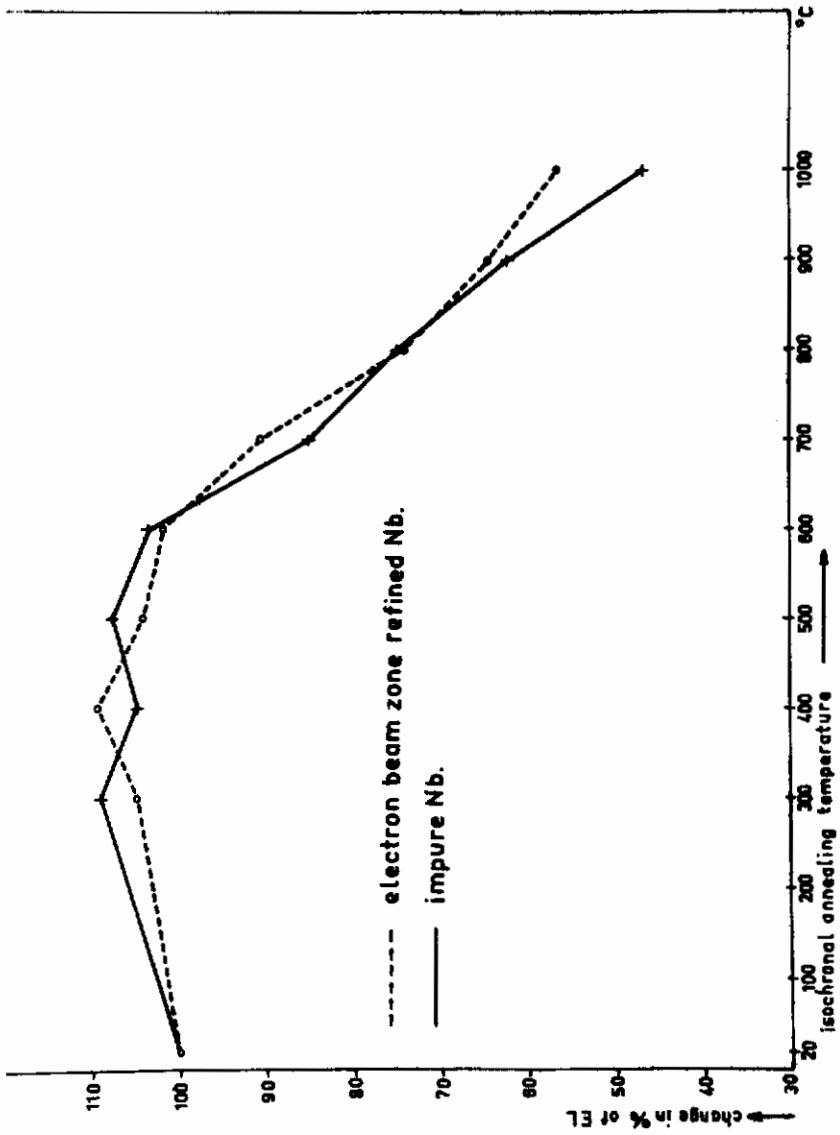


Fig.4

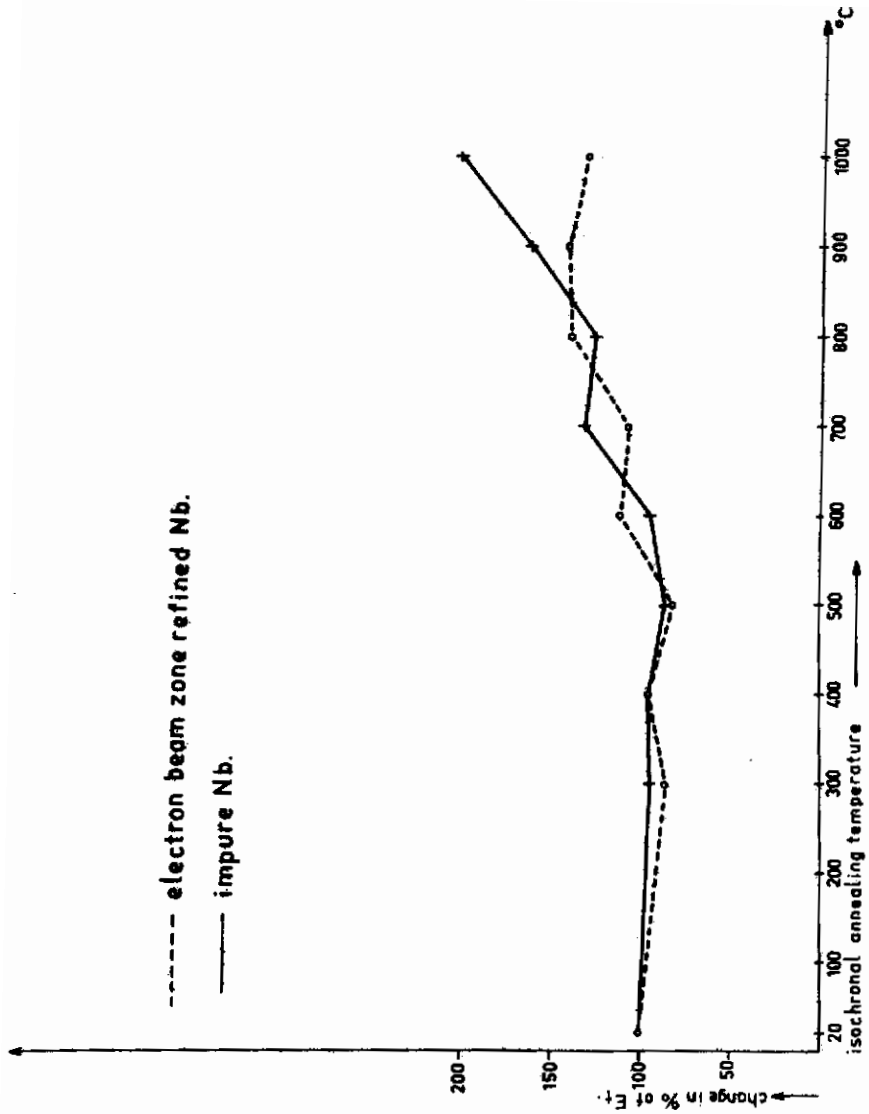


Fig.5

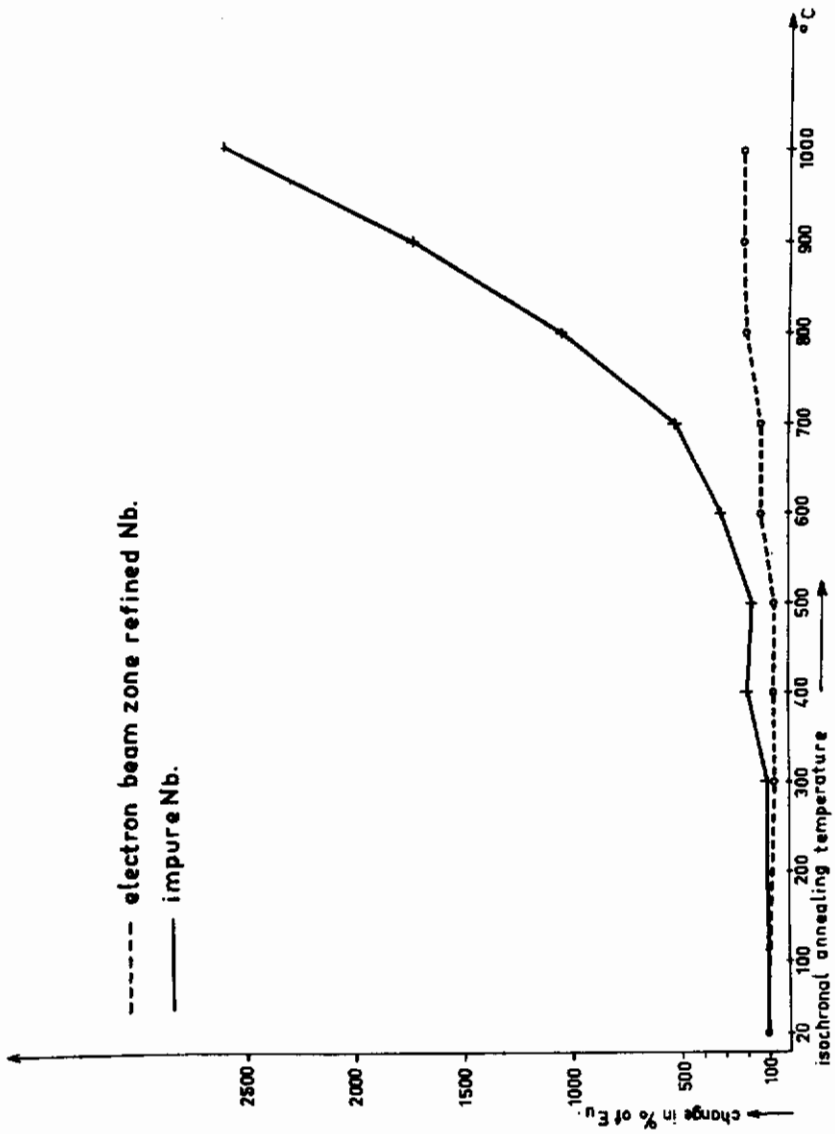


Fig.6

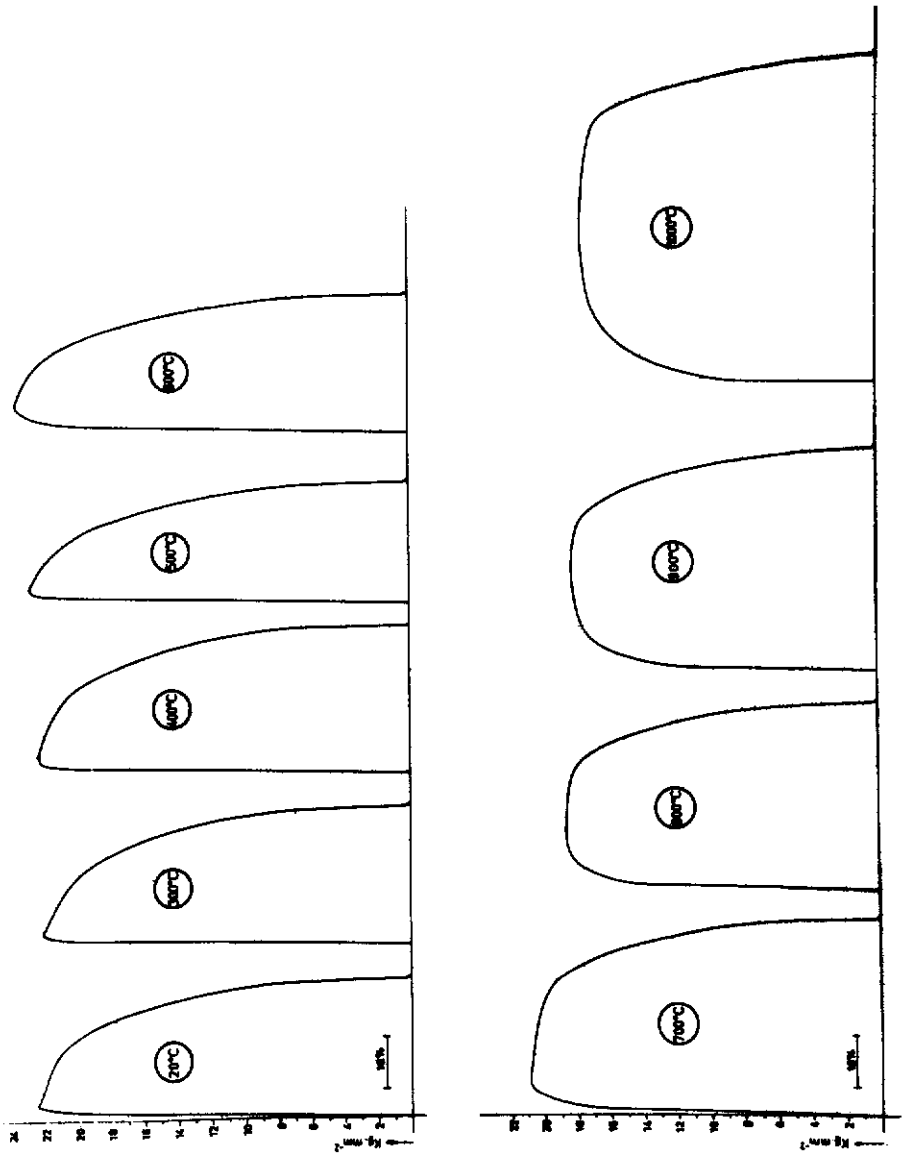

Fig.7

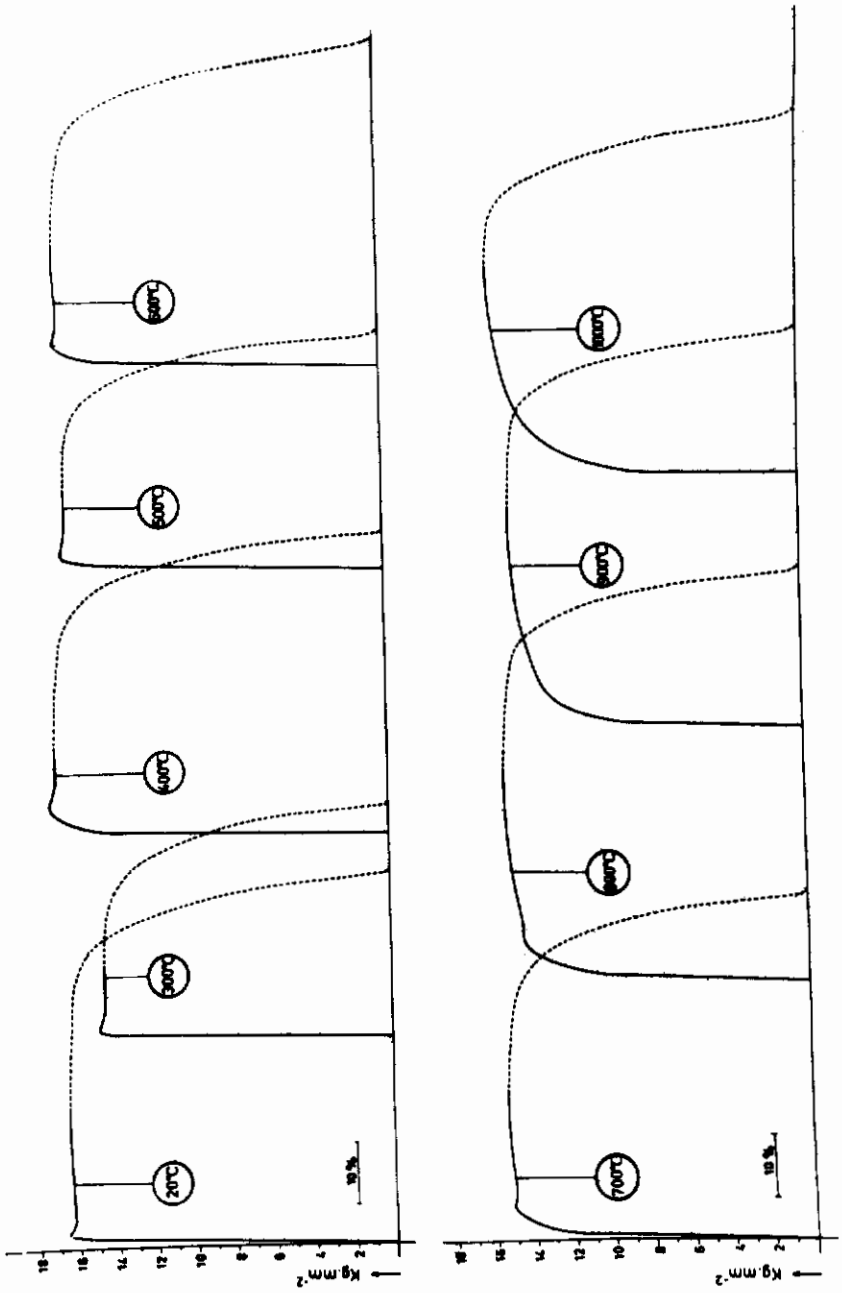


Fig.8

## SECTION IV.

## Yielding and Plastic Flow in High-Purity Tungsten Single Crystals.

by

E. Votava.

The mechanical properties of high-purity tungsten single crystals have been measured first by Rose et al. (1) and spectacular results have been obtained. It has been shown recently (2) for the case of niobium that great care has to be taken in the preparation of single-crystal tensile specimens in order not to influence the stress-strain curves as a result of predeformation. This is especially important for yield point investigations. For this reason a new method has been developed (2) which eliminates shaping either by centerless grinding or by spark erosion ; by this technique ball-ended single crystals are obtained. As this method has been proved to be applicable to all four refractory metals, Nb, Ta, Mo and W, an attempt has been made to verify the results of Rose et al. for the case of tungsten single crystals, since their measurements have been made with shoulder-type single crystal tensile specimens obtained by centerless grinding and subsequent electrolytic polishing.

Fig. 1 shows the mechanical properties at room temperature of such strain-free and high-purity tungsten single crystals as functions of the orientation. Comparison with the results of Rose et al., reproduced in Fig. 2, shows that the results are similar for the three corner orientations ⟨100⟩, ⟨110⟩ and ⟨111⟩ except that the stress is slightly smaller at all strain levels in the present investigation. This may be due to a small difference in purity. It is most interesting that as in the case of Rose et al. only the ⟨110⟩ - orientation has a yield point, indicating clearly that for the case of tungsten single crystals a shaping technique involving careful centerless grinding with subsequent electrolytic polishing does not influence the general aspect of the stress-strain curve. As mentioned before this is not the case for niobium (2) or tantalum single crystals (3). Molybdenum single crystals seem to behave like tungsten crystals (3).

Comparing the results of Fig. 1 with those of niobium single crystals (2) a marked difference is found. For example the ⟨100⟩- orientation in niobium has a two-stage work hardening, the ⟨110⟩-orientation a rather steep one-stage work hardening and for the ⟨111⟩- orientation no reproducible stress-strain curve could be found ; this orientation shows the effect of "repeated work softening". Further, the ⟨321⟩- orientation develops a pronounced easy-glide region with subsequent work hardening. These features are all absent for tungsten single crystals of the same orientation. There is only one similarity in that in both metals the ⟨110⟩- orientation develops a prominent yield point. Similar explanations have been advanced for the orientation dependence of the yield point of the two metals (1), (2), (4), based on the conservative motion of jogs within dislocations.

In order to clarify these differences between the two metals an attempt has been made to determine the active slip planes. Rather surprisingly, however, the slip traces were hardly visible even after large strain increments so that no conclusive results could be obtained.

Further work is therefore necessary to arrive at a complete understanding of the mechanical properties of tungsten single crystals.

Acknowledgements :

Experimental assistance of J.H. Dossin and E. Vanderschueren is appreciated.

References :

(1) : R.M. Rose, D.P. Ferriss and J. Wulff : Trans. Metall. Soc. AIME, 224, 981 (1962).

(2) : E. Votava : Phys. Stat. Sol. 5, 421 (1964) ; Plansee Proceedings, 473 (1964).

(3) : E. Votava : unpublished results.

(4) : E. Votava : present report, section II.

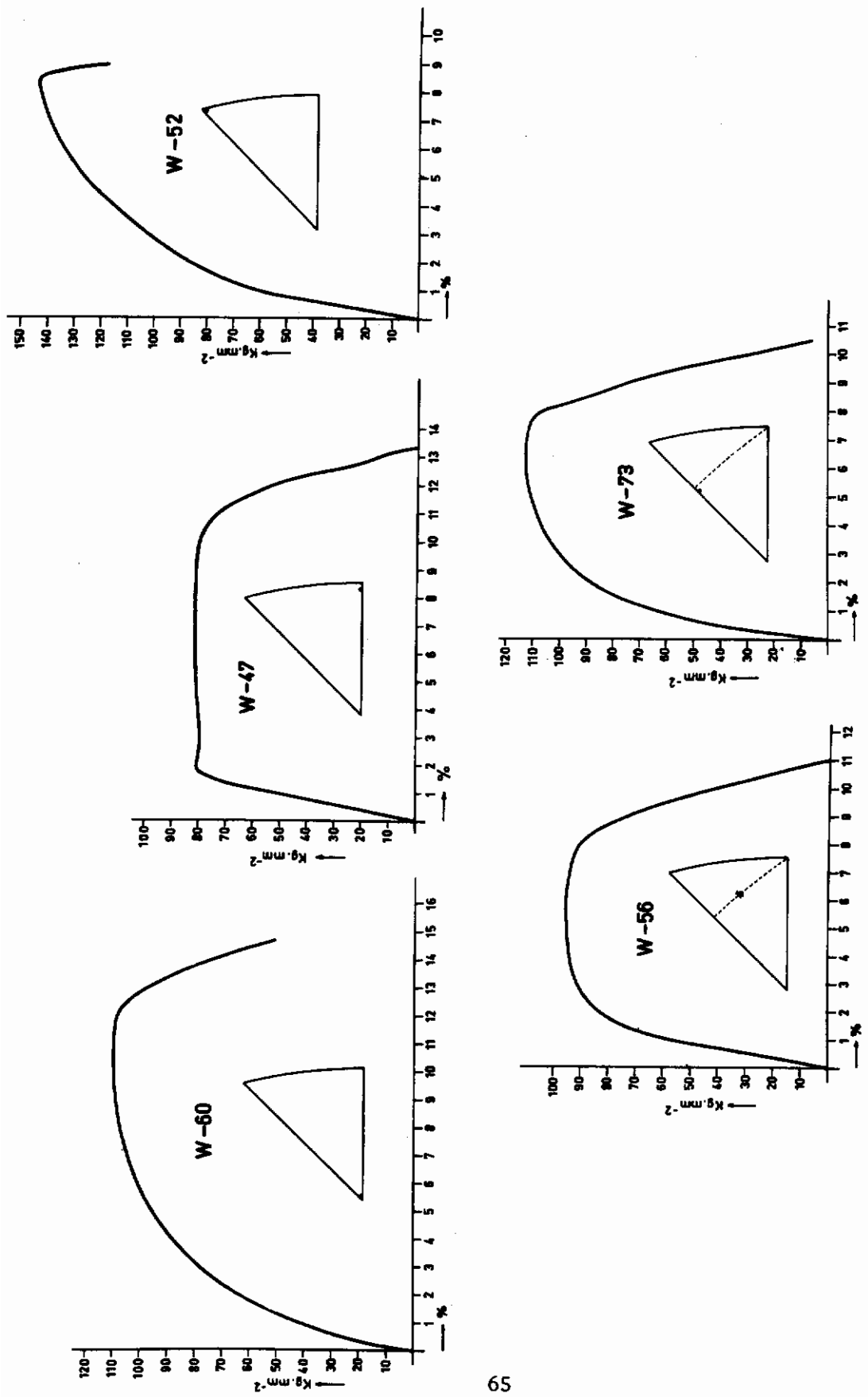


Fig. 1 - The orientation dependence of high-purity tungsten single crystals at room temperature.

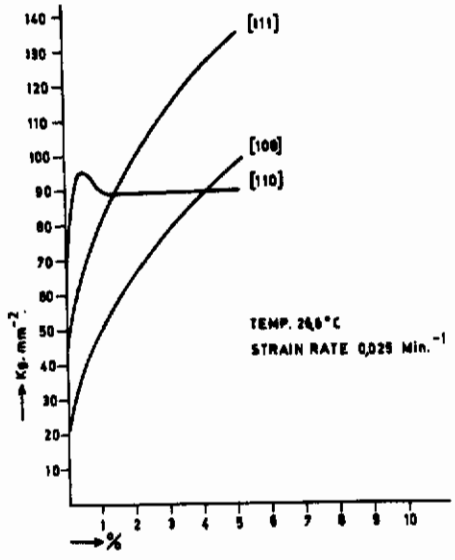


Fig.2.

## SECTION V.

# The Ductile-to-Brittle Transition in Polycrystalline Tungsten.

by

A. Wronski, and A. Fourdeux.

## THE DUCTILE-BRITTLE TRANSITION IN POLYCRYSTALLINE TUNGSTEN.

It has been reported in our earlier communication[1] that the brittle fracture stress of recrystallized swaged tungsten single crystals increases with decreasing test temperature, whereas in commercially pure material no variation is observed.[2] The yield stress measured in compression[3] does increase as the temperature is lowered below the ductile-brittle transition range and as there is evidence that for certain types of steel[4] and molybdenum [5] the yield stress in compression is equal to the brittle fracture stress in tension, it was decided to reinvestigate the problem for tungsten. No detailed quantitative data have been reported previously for the transition region, probably because of the exceptional susceptibility to "accidental" brittle fracture of tungsten in the polycrystalline state[6]. For iron and steel, Allen[7] has stated that "almost every possible type of relation between the yield point variation and the fracture stress variation was found" and considers it advisable to regard yield and fracture as potentially independent processes.

Three commercially available tungsten 5 mm diameter sintered rods obtained from Murex (b), Plansee (c) and Sylvania (d), together with a ⟨111⟩ Linde swaged (at ~ 1000°C in hydrogen by Murex) single crystal (a) were chosen for the investigation. Tensile test specimens with 20 mm gauge length and ~ 2.5 mm in diameter were electroshaped [8] and recrystallization was carried out in a hydrogen furnace for 1-3 hours at 1550°-1730°C. The resultant variations in grain size ; (a) 43-63μ, (b) 24-40μ, (c) 27-32μ and (d) 20-56μ did not appear to influence appreciably the yield stress at a given

temperature. Tensile testing after electropolishing was performed on an Instron machine at a strain rate of 0.5% $min^{-1}$ in the temperature range -24°-205°C. For above-ambient tests the specimens were immersed in an oil thermostat and lower temperatures were obtained by using constant temperature mixtures. No attempt to determine the impurity contents was made as different laboratories when analysing Linde material for interstitial contents obtained results that differed by up to two orders of magnitude [1]. Some specimens from the commercial materials exhibited yield points and some not, as all the Linde specimens, for these the stress at the apparent proportional limit was taken to be the yield stress. Measured values of the latter were always larger than the former, when both could be determined, and this accounts for most of the experimental scatter evident in Fig. 1. A large number of specimens broke in or near the "shoulders" at various stress values when tested in the brittle region. All these results are neglected (except the five shaded symbols of Fig. 1(c)). This frequent experimental difficulty prevented the detailed study of the transition region for (b) and (c), but the few valid results are presented for the sake of comparison. All the specimens obtained from the Linde crystal were used up to determine the deformation behaviour down to -24°C and as the brittle fracture of similar crystals has already been studied[1], it is considered that the increase of the brittle fracture stress with decreasing temperature, after the inflection[1,9] in the curve, is established for this material. Representative load-elongation curves for all the materials are shown in Fig. 2.

The increase of the yield stress with decreasing temperature is less rapid for (a) than for the commercial materials, which suggests that it is purer [10] and seems to rule out a large Peierls-Nabarro force as the

responsible mechanism for this behaviour [10, 11, 12]. As the dislocation velocity is influenced by purity [13], the results are consistent with the view [14, 15] that the temperature dependence of the yield stress is due to an increase in the dynamic resistance to dislocation motion as the temperature is lowered. Defining the transition temperature as the highest at which there is no detectable plastic deformation, it is seen to be about room temperature for (a), ~ 100°C lower than for (b), (c) and (d), which is another indication of the higher purity of (a).

Turning now to the brittle side of the transition, we see that in general the behaviour is complex and not surprisingly resembles that of iron and steel [7] and is consistent with the phenomenological analysis of Bechtold et al [16]. It should be pointed out, however, that the stresses for low strength fractures are still above the elastic limit [11] of tungsten estimated by us to be < 20 kg. $mm^{-2}$, but may be below the unelastic limit [17].

All the brittle fracture surfaces appeared to be made up of cleavage facets but microscopic examination revealed that the fracture paths were both transgranular and intergranular. Detailed analyses of fracture surfaces [18], microcracks [9] and grain hardnesses [19] were not attempted, but on so examining representative samples, no relation with fracture stress was found ; microcracks were few if any and there was no variation of microhardness as a grain boundary was traversed. No evidence of grain boundary films [6] was found either. (Recently Gavrilyuk et al [20], who worked with arc-cast tungsten, concluded that there was no formation of oxide or other phases at the grain boundaries and attributed brittleness to "intercrystalline internal adsorption of admixtures".).

A more detailed microfractographic study[1] was made for room temperature tests only, as the fracture surfaces must be fresh and clean for this technique to give valid results. In our previous communication [1] a microfractograph of the Linde material is presented. Results obtained with all the sintered materials are similar and the main differences between them and (a) are the more frequent cleavage in the latter and a greater density of the larger cavities (Fig. 3) in the former. The electron micrographs were similar to the one showing intergranular fracture of iron containing 0.02% oxygen, for which the surface features were attributed to small non-metallic inclusions[21]. Then, however, from microhardness measurements, there was evidence of grain boundary segregation of impurities (and no evidence of structural difference in the grain boundary regions from transmission electron microscopic studies). Striations, attributed to intergranular gas adsorption by Plateau et al[22], were also observed in tungsten, but more frequently in (a) than in (b), (c) and (d). Attempts were made at extraction (of any particles on the fracture surfaces) using techniques which are known to apply to oxides[23] and carbides[24], and also by making collodion replicas. All these attempts were unsuccessful. Thus the cavities were tentatively identified as due to gas bubbles [25,26,27], and confirmation was sought using the transmission electron microscopy technique. Examination of slices prepared from (b), (c) and (d) rods and (c) foils yielded ample evidence (e.g. Fig. 4) of gas bubbles or voids and no such diffraction images were ever formed on examining (a) rod and foil. Bubbles were both in the grain boundaries and in the matrix, then usually along former positions of fibre boundaries. Electronmicrographs of annealed sintered tungsten already published in the literature [1, 28, 29] are seen also to exhibit the features which we attribute to gas bubbles. (A study of this phenomenon is in progress ; similar observations on tungsten wires have also been made in this laboratory[30]).

The connection between low stress failures, sintered material and bubbles (or voids) appears to be established for tungsten (mechanical properties of molybdenum are similar[5] and bubbles or voids have been found in sintered but not cast foils) ; the question as to the reason for the relatively few large cavities present in (a) remains unanswered. The observations account for the weakening of grain boundaries when no precipitate is present, and show an additional factor which affects stress concentration and crack nucleation and propagation. It appears that low stress failures in relatively pure sintered tungsten are associated with local yielding and fracture in regions of stress concentration [31]. Even at above-ambient temperatures the grain boundaries are particularly rigid in tungsten. Berghezan and Fourdeux[32] stress the importance of this rigidity as niobium work-hardens and a mechanism of adsorption has been proposed by Berghezan[33] to account for the brittleness of high-purity iron of Talbot-Besnard[34]. For tungsten it is suggested that the grain boundaries may control the fracture process[1,5,18] in the absence of additional factors as precipitates, films and gas bubbles. The interpretation of the results is tentative in so far as direct proof of the existence of the gas is not available.

REFERENCES


1. A. Wronski and A. Fourdeux, J. Less-Common Metals, 6 (1964), 413.
2. J.H. Bechtold and P.G. Shewmon, Trans. A.S.M. 46 (1954) 397.
3. W. Sheely et al., A.S.D. 61-3 (1961).
4. J.R. Low, I.U.T.A.M. Madrid Colloquium (Springer-Berlin), p. 60 (1956).
5. A. Wronski, J. Inst. Metals, 92 (1963-64), 376.
6. R.C. Koo, Trans. A.I.M.E., 227 (1963), 280.
7. N.P. Allen, Iron and Its Dilute Solid Solutions (Interscience) p. 274 (1963).
8. A. Fourdeux and A. Wronski, Brit. J. Appl. Phys. 14 (1963) 218.
9. G.T. Hahn, B.L. Averbach, W.S. Owen and M. Cohen, Fracture (Wiley), p. 91 (1959).
10. D.F. Stein, J.R. Low and A.U. Seybolt, Acta Met., 11 (1963) 1253.
11. N. Brown and R.A. Ekvall, Acta Met., 10 (1962) 1101.
12. A. Fourdeux and A. Wronski, J. Less-Common Metals, 6 (1964), 11.
13. W.G. Johnston and J.J. Gilman, J. Appl. Phys. 30 (1959) 129.
14. D.F. Stein and J.R. Low, J. Appl. Phys., 31 (1960) 362.
15. H.W. Schadler, Acta Met (to be published).
16. J.H. Bechtold, E.T. Wessel and L.L. France, Refractory Metals and Alloys (Interscience) p. 25 (1961).
17. A. Wronski and A. Fourdeux, Phil. Mag. (to be published).
18. A. Gilbert, C.B. Reid and G.T. Hahn, J. Inst. Metals, 92 (1963-64)351.
19. J.H. Westbrook and D.L. Wood, Nature, 192 (1961) 1280.
20. M.I. Gavrilyuk, I.N. Chaporova, N.P. Vasilyeva and T.A. Sultanyan, Fiz. Met. Metalloven, 13 (1962) 693.
21. J.R. Low, Fracture of Solids (Interscience), p. 208 (1963).
22. J. Plateau, G. Henry and C. Crussard, I.S.I. Sp. Rpt. No. 64, p. 57 (1959).

23. R. P. Morgan et al., WADD TR 60-144 (1960).

24. A. Fourdeux, unpublished results (1963).

25. R.S. Barnes and D. J. Mazey, Phil. Mag., 5 (1960) 1274.

26. H. Mykura, Phil. Mag., 4 (1959) 907.

27. C.A. Zapffe and F.K. Landgraf, Trans. A.S.M., 41 (1949) 396.

28. S. Weissmann, Y. Nakayama and T. Imura, WADD TR 61-181 (Part I), p. 141 (1961).

29. D.A. Thomas et al, WADD TR 61-181 (Part II), p. 107 (1962).

30. A. Fourdeux and A. Berghezan, unpublished results (1962).

31. A.H. Cottrell, Proc. Roy. Soc. 276 A (1963) 1.

32. A. Berghezan and A. Fourdeux, ASD-TDR-63-324, p. 437 (1963).

33. A. Berghezan , 6ème Colloque de Métallurgie (CEN, Saclay), p. 136 (1962).

34. S. Talbot-Besnard, 6ème Colloque de Métallurgie (CEN, Saclay), p. 129 (1962).

Legends to Figures :

Fig. 1 : The effect of test temperature on the yield and brittle fracture stresses of (a) melted and (b), (c) and (d) sintered polycrystalline tungsten.

Fig. 2 : Representative load-elongation curves in the transition region for polycrystalline tungsten.

Fig. 3 : Microfractograph of sintered (b) polycrystalline tungsten. Note the cleavage fracture of grain $\alpha$, the totally intergranular fracture of $\beta$, $\gamma$, $\delta$ and $\varepsilon$ and the large voids.

Fig. 4 : Electronmicrograph of a slice of (b) polycrystalline tungsten. Note the grain boundary AB and the gas bubbles or voids, which are not present in (a).

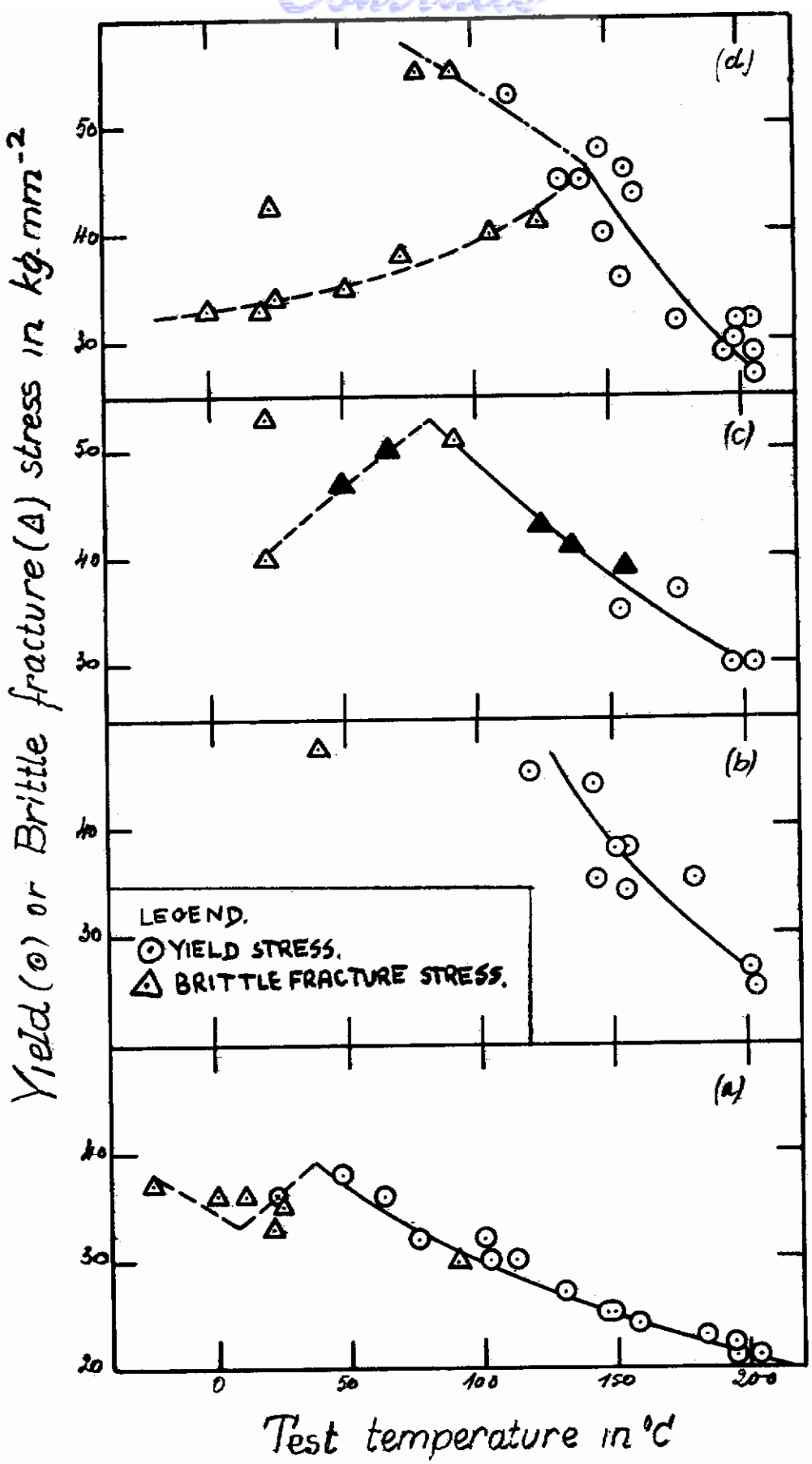


Fig. 1

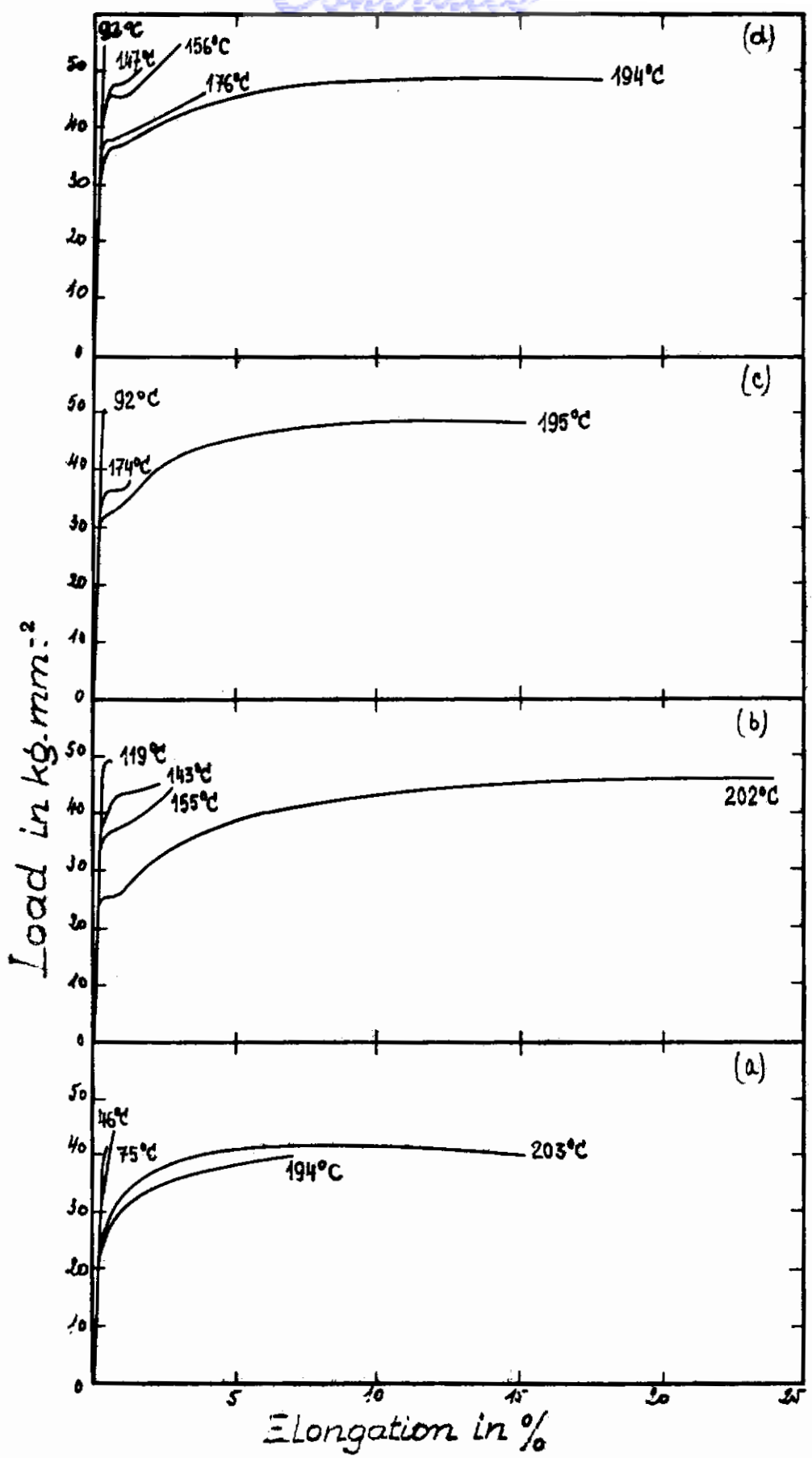


Fig. 2.

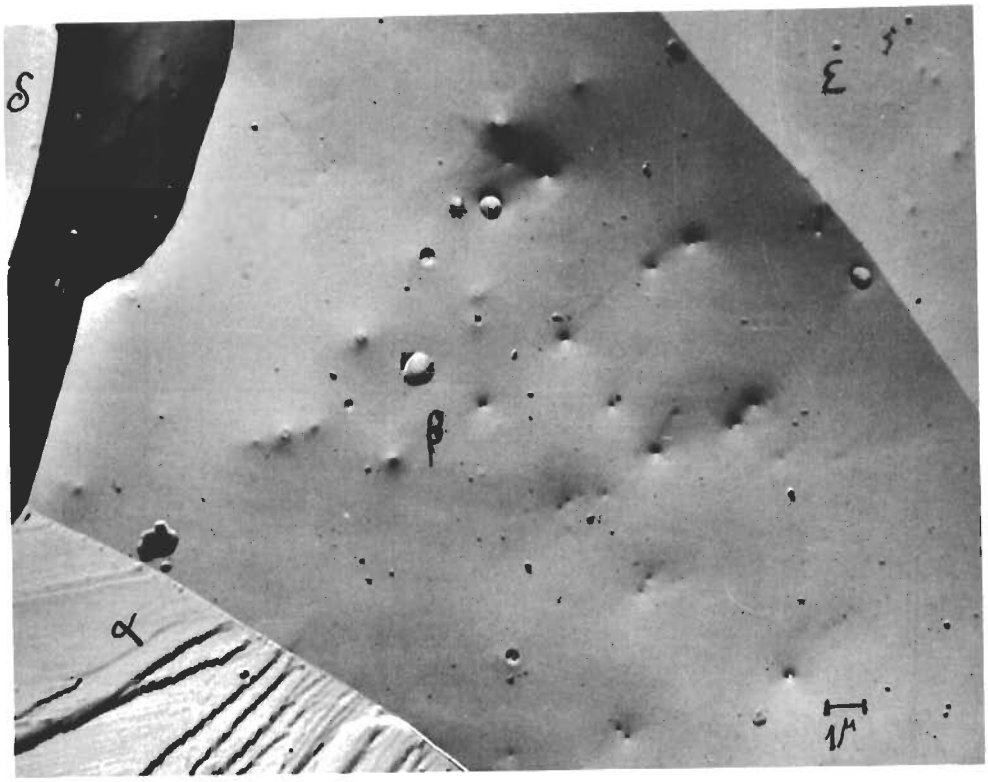


Fig.3.


Fig.4.

## SECTION VI.

## The Ductile-To-Brittle Transition in High Purity Polycrystalline Tungsten.

by

F. Rueda and E. Votava.

Introduction.

The ductile-to-brittle transition is found mainly in b.c.c. metals and is, especially for the case of tungsten, a serious limitation for its use as a structural material. Tungsten has appreciable ductility at room temperature if present either as a single crystal or heavily cold worked. However, it loses this ductility and becomes extremely brittle if recrystallized. Thus the essential problem of the room-temperature brittleness of tungsten is the rôle of the grain boundaries. In particular the presence of precipitates in the grain boundaries was thought to be the reason that fracture in tungsten is initiated at the grain boundaries. As such an embrittlement can be the result of contamination during the mechanical and thermal treatments, it is important to keep such contamination to the absolute minimum attainable.

The present investigation was therefore undertaken with the aim of evaluating the mechanical properties of high-purity polycrystalline tungsten prepared from high-purity single crystals and recrystallized under such conditions that contamination is avoided practically completely.

Experimental Techniques.

a) Ultra-high vacuum electron-beam annealing furnace.

A special electron-beam furnace was constructed for the recrystallization of the worked tungsten single crystals. The design of the furnace follows in principle that described by Chandrasekhar and P.A. Flinn (1). However, small modifications had to be made to adapt this principle to our purpose. The furnace is shown in Fig. 1, which is self explanatory. With a high-voltage power supply of 1.8 kW a maximum temperature of approximately 3200°C was obtained. Three samples could be annealed in this furnace simultaneously.

The temperature determination was done by optical pyrometry within $\pm$ 5°C. No gradient was observed along the gage length of the samples at 1700°C.

The furnace was incorporated into a S-shaped stainless steel tube of 150 mm inner diameter, which was surrounded along its whole length by a resistance furnace for outgassing at a maximum temperature of 450°C. This S-tube was connected to a mercury-in-steel diffusion pump with a metallic liquid nitrogen baffle (construction : E. Leybold/Germany) with a baffled pumping speed of approximately 275 l/sec. In addition, a liquid-nitrogen cooled stainless steel jacket, seen in Fig. 1, was built round the furnace. This considerably improved the vacuum, and prevented at the same time undue heating of the S-tube and the consequent degassing during the operation of the furnace. The joints used in this installation were either Granville-Phillips flat copper or gold wire gaskets, with the exception of two Viton gaskets incorporated into the baffled mercury diffusion pump. With this installation a vacuum of better than $10^{-9}$ Torr was obtained in a reproducible way after 15 hours of baking. At an operating temperature of 1700°C a vacuum of $5 \times 10^{-8}$ Torr could be kept over a sufficiently long time. The complete installation is shown in Fig. 2.

Provision was also made to connect a cryogenic pumping station to the S-tube. This equipment was built by the Linde Division of Union Carbide Corporation and is based essentially on the high adsorbing power of molecular sieves (zeolites) at the temperature of liquid nitrogen for the roughing pump and at liquid helium temperature for the main pump. This system has a remarkably high pumping speed : test reports quote 4000 l/sec for oxygen and nitrogen, 500 l/sec for hydrogen, and 100-200 l/sec for helium. Fig. 3 shows this equipment connected to the S-tube with the furnace. With this equipment a

vacuum of $\sim 5 \times 10^{-9}$ Torr was obtained after 15 hours of baking.

b) The preparation of the high-purity polycrystalline tungsten samples.

Tungsten rods which have been zone-melted in an electron bombardment apparatus are single crystals. In order to transform this high-purity material into a polycrystalline structure without impairing its purity a suitable method had to be found. As at 400°C no appreciable oxidation of tungsten takes place, rolling of 2 mm thick tungsten single crystals was first tried sucessfully. Closer investigation of the conditons of rolling, described in detail in appendix I, showed that such crystals can be rolled even at room temperature if they have a ⟨110⟩ orientation and are rolled in this direction on a {100} plane. In addition the rolling speed has to be reduced considerably, down to 1 mm/sec. Recrystallization experiments on such rolled single crystals showed , however, that they hardly recrystallize but retain their monocrystallinity. As the crystals rolled at 400°C recrystallized also with a very non-uniform grain size, with a tendency to large grains traversing the whole cross-section, this method was abandoned and replaced by hot swaging.

In order to end up with samples of a reasonable diameter after swaging, representative for bulk polycrystalline tungsten, it was found necessary to zone melt tungsten bars of 8 mm diameter. This required certain modifications in the electron-beam zone refiner such as the construction of a new gun which would resist the excessive heat developed. Fig. 4 shows such an 8 mm thick tungsten single crystal .

For hot swaging the zone-melted tungsten crystals were first rectified to a uniform diameter and then introduced into a tightly fitting stainless steel tube of ≈ 1 mm wall thickness closed at one end. The open end was then closed by electron beam welding under vacuum. Hot swaging at 1000°C was then possible

without any visible oxidation of the tungsten samples. That no contamination had in fact taken place by this procedure is proved by the data in table I. The reduction in cross-section by hot swaging was about 73%. The structure after hot swaging is shown in Fig. 5, which represents a transversal cut through the bar (surface slightly etched). It shows that some polygonization has taken place.

However, some difficulties as regards the grain size were encountered in this case too. It was observed that such swaged tungsten single crystals develop in general a large grain size (average grain size : $\sim 450\mu$ ; scatter : $190\mu$ - $790\mu$) and that the grain size, especially the lower limit, could not be reproduced under identical conditions of recrystallization. It was found that this depends on the orientation of the tungsten single crystals and especially that a smaller grain size can be obtained by using ⟨111⟩- oriented crystals and a recrystallization temperature of 1425°C for 30 minutes. The reason for this behaviour is to be found in the orientation dependence of the work hardening of tungsten single crystals as shown in section IV and especially in the fact that the ⟨111⟩-orientation has the steepest work hardening rate and therefore also the greatest nucleation probability. Although with this orientation a reproducible "small" grain size could be obtained, it was found impossible to decrease the grain size further. This tendency for large grains seems to be a general property of high-purity refractory metals and made it impossible to study problems related to the ductile-to-brittle transition behaviour such as the grain-size dependence.

After hot swaging tensile test specimens were prepared by grinding with a diamond wheel, followed by electropolishing in a 2% NaOH solution. Fig. 6 shows the form of the samples and the exact dimensions after grinding and electropolishing. The first, large shoulder is used to fit in the grips whereas the second, smaller shoulder prevents the samples breaking in the shoulders themselves.

The gripping device is shown in Fig. 7. It consists of a hemispherical collar inserted into a holder with a hemispherical housing. Self-alignment of the samples is thus possible. Tensile testing was performed on an Instron machine at a strain rate of $3.3 \times 10^{-5}$ $sec^{-1}$ in the temperature range -196°C to 200°C, using either an oil thermostat or constant temperature mixtures.

c)Purity of the tungsten samples.

All tungsten samples used were of Plansee origin. Due to their low gas content these samples produce very little "spitting" during the zone melting of 8 mm thick bars. The samples were zone melted four times with a velocity of 1.4 cm/min. in a vacuum of approximately $5 \times 10^{-6}$ Torr. The carbon content was measured by a combustion-conductometric technique, the hydrogen, oxygen and nitrogen contents by a vacuum fusion method *. Table I shows the results of these analyses ; for the sake of comparison values quoted by the makers for the "as-received" samples are also given.
The discrepancy in certain values shows clearly that such analyses cannot give absolute values, but can only indicate a trend. Even when bearing this in mind, the tendency for reducing the carbon content by zone melting is evident.

---

* The analysis was carried out by W.E. Chambers and his co-workers at the Union Carbide Corporation, Parma Research Center, Parma, Ohio, U.S.A.

It seems further that some take-up of oxygen has taken place during recrystallization.

Table I.

| Tungsten (Plansee) in the different phases of preparation | H p.p.m. | O p.p.m. | N p.p.m. | C p.p.m. |
|---|---|---|---|---|
| as received | 0.2 | 1.9 | <1 | 4.7 |
| mean values given by Plansee | | (10 - 20) | | (20 - 50) |
| after purification by four zone passes | 0.3 | 2.2 - 3.6 | <1 | 0.5 - 0.6 |
| after purification and hot swaging | <0.2 | 2.5 | <1 | 0.5 - 0.8 |
| after purification, hot swaging and recrystallization in a vacuum of $10^{-8}$ Torr. | <0.2 | 5.8 | <1 | 0.7 |

Experimental Results.

a) Mechanical properties.

A sample was regarded as brittle if there was no detectable plastic strain. With the Instron tensile tester used a deviation of 0.05% strain was still detectable and samples having this or a greater deviation from proportionality were regarded as ductile. Consequently in order to characterize fully the mechanical properties of the samples the yield stress and the total elongation (in the case of ductility) or the brittle fracture stress (in the case of brittleness) were measured as functions of temperature. Some samples which broke in the shoulders were eliminated from the measurements.

Fig. 8 shows the yield stress for recrystallized high-purity polycrystalline tungsten prepared from randomly oriented tungsten single crystals, Fig. 9 the total elongation and Fig. 10 representative stress-strain curves, all three as functions of temperature in the range -196°C to + 200°C. It can be seen that

i) all samples show some ductility in this temperature range, but the ductility rises to appreciable values only above + 100°C ;

ii) all samples have after yielding a considerable work hardening rate, which decreases with increasing temperature ;

iii) the yield stress increases with decreasing temperature.

It was very surprising that this behaviour changes strongly if one uses ⟨111⟩-oriented single crystals for the preparation of the polycrystalline tungsten. Fig. 11 and Fig. 12 show this. It can be seen that in this case

i) a ductile-to-brittle transition takes place at about -40°C.

ii) the yield stress increases also with decreasing temperature between + 200°C

and -40°C but this increase is steeper than in the previous case ;

iii) the ductility increases to appreciable values only from about + 150°C on.

As in both cases tungsten of the same origin was used, and further zone melting, hot swaging and recrystallization of the hot swaged tungsten single crystals were carried out under identical conditions, and also the difference in grain size is not too large, the only factor which can explain this change in the mechanical properties is the initial ⟨111⟩- orientation of the single crystals in contrast to the random orientation in the polycrystal. It is probable that in one of the two cases a preferential texture has been established after recrystallization. Some tests have been undertaken in this direction but no conclusive results have been obtained so far.

Whereas the first two test series have been recrystallized in an ultra-high vacuum, produced by a mercury diffusion pump, one test series was recrystallized in the vacuum produced by the cryogenic pumping unit. Nine samples have been so tested. In this case also ⟨111⟩-oriented tungsten crystals were used for the preparation of the polycrystalline material. Fig. 13 and Fig. 14 show the results obtained. In principle the same behaviour was obtained as before (Fig. 11 and Fig. 12) showing that high-purity polycrystalline tungsten prepared from ⟨111⟩-oriented crystals follows a special law.

Tensile tests at room temperature were also made with "as-received" tungsten, recrystallized in the ultra-high vacuum installation. The grain size obtained was much smaller. In no case was any ductility observed.

b) Deformation and fracture mode.

In order to find out what kind of deformation, as measured by the deviation of the stress-strain curve from the proportionality, has taken place, the sample surfaces were examined after testing by ordinary microscopic methods as well as by phase contrast and interference microscopy (Normansky system). The following results have been obtained :

i) In the whole range of temperatures investigated (+200°C to -196°C) deformation twins were observed. This is demonstrated by Fig. 15 (200°C), Fig. 17 (150°C), Fig. 19 (100°C), Fig. 20 (50°C) and Fig. 22 (-40°C). At higher temperatures, approximately from -40°C on, the twins were found more concentrated near the fracture surface, whereas at lower temperatures down to -196°C twins were also found some distance away. The amount of twinning decreases with increasing temperature.

ii) In the whole range of temperatures investigated (+200°C to -196°C) deformation by slip was found. This is demonstrated by Fig. 16 (200°C), Fig. 18 (150°C), Fig. 19 (100°C), Fig. 21 (50°C), Fig. 23 (-45°C), Fig. 24 (-80°C) and Fig. 25 (-196°C). As expected, the amount of slip decreases strongly with decreasing temperature.

iii) Characteristic surface denivelations were found near the grain boundaries. At higher temperatures the phenomenon known as "orange peel" was found, as shown in Fig. 16. At lower temperatures from approximately +50°C on a characteristic change takes place. As shown in Fig. 26 (20°C), the grain boundaries near the fracture surface appear in relief and it was proved by interference microscopy (Fig. 27), that a step is formed at these grain boundaries. Fig. 28, showing the same area after polishing, proves that a certain

correlation exists between these steps and microcracking. The small microcracks follow the grain grain boundaries exactly. However, as there are stretches along the grain boundaries where no cracking has taken place, but where a continuous step has been observed before polishing, one is led to the assumption that some "grain-boundary sliding" has taken place. It is not understood completely how this phenomenon, which is normally observed only at higher temperatures,can take place at low temperature (+50°C to -196°C) and further work will be necessary to clarify the situation.

The fracture surface was also examined by optical and electron microscopy using carbon replicas in the latter case. The following results have been obtained :

i) In the temperature range -196°C to + 200°C the fracture paths were both transgranular and intergranular. Fig. 29 shows an example of such a composite cleavage and intergranular fracture. In addition a fine structure line was observed on intergranular surfaces (see grain C of Fig. 29. For clarity this area is shown in Fig. 30 at higher magnification). These striations can be attributed to gas adsorption on small steps, as first demonstrated by Plateau et al (2).

ii) As a consequence of the formation of mechanical twins the fracture mode was also influenced and a number of samples have been found where the fracture path followed to some extent the twin boundaries. Fig. 31 a and 31b show such a fracture mode on non-parallel twin boundaries. The question therefore arises whether fracture has not been initiated in this case by the deformation twins. Examples of this kind have been described in the literature, e.g. that at the intersection of two deformation twins a crack is formed or that the

surface denivelation produced at the emergence of a deformation twin can act as a notch producing a crack in a notch- sensitive material. However, although these examples are mostly well consolidated, this is not applicable in our case, as none of our stress-strain curves showed a typical twin mark within the limit of detection. One is therefore led to assume that the deformation twins are not produced before fracture but during fracture by the shock during the breaking of the samples. It may be necessary to revise this view when better measurements in the ductile range of the stress-strain curve become available, but this will have to await further developments in commercial tensile testing machines.

Discussion.

These results prove clearly that some ductility at room temperature and even lower temperatures can be achieved in polycrystalline tungsten provided high-purity tungsten single crystals are used as starting material and recrystallization is carried out in an ultra-high vacuum of $10^{-8}$ Torr. On the other hand it must be admitted that this work has raised as many questions as it has solved.

First of all the relatively large grain size was a great drawback for the whole investigation and it will be necessary to find methods to reduce the grain size further. The most promising way is to introduce more deformation into the sample than in the present case (which was round 73% reduction in cross-section). However, in order to keep the dimensions of the tensile specimens to those shown in Fig. 6, which can be regarded as giving results representative for bulk material, it will be necessary to grow high-purity tungsten single crystals with greater diameter, e.g. 2 to 3 cm. For reasons connected with the stability of the molten zone it will probably not be possible to do this by electron beam zone

melting, but possibly drawing from the melt can solve the problem.

Furthermore, as shown in Fig. 8, the increase in yield stress with decreasing temperature is much less pronounced here than in the work reported in (3). Although there is an appreciable difference in grain size between the two series of measurements , see Fig. 8, this alone cannot explain the difference in the yield stresses. The tungsten used in Section V (3), was Union Carbide Linde single crystals prepared by Verneuil's technique in an argon atmosphere and although we have no valid analysis for this material it can be accepted safely that our single crystal material is much purer. Thus the yield stress versus temperature curve approaches more nearly ideal condition in our case which permits some conclusions on the frictional stress responsible for this effect.

It has been suggested (4) that this frictional stress is due to a large Peierls-Nabarro force. However, the lower rate of increase in our case (see Fig. 8) seems to rule out definitely a large Peierls-Nabarro force, especially in conjunction with the results obtained by Wronski and Fourdeux, a conclusion which has already been proposed by (3) (5) (6) (7) (8). Stein and Low (9) and Schadler (10) described therefore this behaviour as "due to an increase in the dynamic resistance to dislocation motions as the temperature is lowered".

The concept of dynamic resistance to dislocation motions would be consistent with the view of Schoeck (8) that this resistance is possibly due to a high jog concentration, which should be common to all b.c.c. metals, as the dislocations are not extended. Indications for such a behaviour have been found by (11) and (12) and can well explain the present results.

If as suggested the frictional force is due to a high jog concentration, orientation will play an essential rôle, as conservative motion of jogs can only proceed in the plan of the jog and will depend on the resolved shear stress on the jog plane. In Fig. 11 the yield and brittle fracture stress of high-purity polycrystalline tungsten prepared from ⟨111⟩- oriented single crystals is shown. There are two marked differences in comparison with Fig. 8. First, the yield stress increases more rapidly and second, the ductile-to-brittle transition, previously absent down to -196°C, is raised to approximately -40°C.* The more rapid increase of the yield stress with decreasing temperature can well be the result of a certain texture, bringing the orientation dependence of the frictional force, as explained above, into action. As mentioned before, no conclusive results on such a preferential texture were obtained so far and more work is required in this direction.

The investigation of the fracture mode showed clearly that even in this very pure form and probably in the absence of precipitates on the grain boundaries, the grain boundaries themselves still control the fracture process, since intergranular fracture has always been found.

However, as microcracks have been observed along grain boundaries and near the fracture surface (see Fig. 28), this implies that in the high - purity form of polycrystalline tungsten the propagation of a crack does not occur as easily as in unpurified tungsten.

---

* The results obtained with similar polycrystalline tungsten, which however was recrystallized in the vacuum produced by a cryogenic pump, show the same behavior and prove that polycrystalline tungsten prepared from ⟨111⟩-oriented single crystals follows a special law.

Summarizing it can therefore be said that purification improves in general the ductility of polycrystalline tungsten and that brittleness is not an inherent property of this material. However, one must also accept that to a great extent the fracture process is controlled by the grain boundaries.

Acknowledgements :

Experimental assistance of J. Dossin, J. Francou, E. Vanderschueren, J. Remy and E. Van Wemmel is appreciated. The electronmicroscopic replica studies of the fracture surface were made by Miss A. Fourdeux.

Legends to Figures :

Fig. 1 : The ultra-high vacuum electron beam annealing furnace :
(1) electrodes, (2) sample holder, (3) $Al_2O_3$ radiation screen,
(4) tantalum radiation shield, (5) tungsten cathode filament,
(6) samples, (7) tungsten radiation and focusing shields,
(8) $Al_2O_3$ support, (9) liquid nitrogen cooled stainless steel jacket.

Fig. 2 : The complete ultra-high vacuum installation with electron beam annealing furnace on the top of the S-tube and a liquid nitrogen baffled mercury diffusion pump at the bottom. On the right side of the installation the high-voltage power supply.

Fig. 3 : Same installation as in Fig. 2, but connected to a Union Carbide Linde cryogenic pumping equipment.

Fig. 4 : Tungsten single crystal, approximately 8 mm thick, after four electron-beam zone melting passes.

Fig. 5 : The structure of high-purity tungsten after hot swaging. The picture represents a transversal cut through the bar and the surface was slightly etched. Some polygonization has already taken place.

Fig. 6 : Tensile test specimen form for swaged and recrystallized tungsten. Dimensions in mm.

Fig. 7 : The system for gripping the tensile test specimens :
(1) holder with hemispherical housing , (2) hemispherical collar, (3) centering ring, (4) sample, (5) spring to hold the collar.

Fig. 8 : The yield stress as function of test temperature of high-purity polycrystalline tungsten prepared from randomly oriented single crystals. For comparison a similar curve from the work of A. Wronski and A. Fourdeux (3) is presented. The point at + 20°C includes samples of the whole range of grain sizes.

Fig. 9 : Elongation in % as function of test temperature of high-purity polycrystalline tungsten prepared from randomly oriented single crystals. Same test series as in Fig. 8.

Fig. 10 : Representative stress-strain curves of the same test series as in Fig. 8 and 9. Yield stress indicated.

Fig. 11 : Yield or brittle fracture stress as function of test temperature of high-purity polycrystalline tungsten, prepared from ⟨111⟩-oriented single crystals.

Fig. 12 : Elongation in % as function of temperature for the same test series as in Fig. 11.

Fig. 13 : Yield or brittle fracture stress as function of temperature of high-purity polycrystalline tungsten prepared from⟨111⟩-oriented single crystals and recrystallized in the vacuum of a cryogenic pump. Between + 20°C and -196°C the curve is not certain because of lack of measurements.

Fig. 14 : Elongation in % as function of test temperature for the same test series as in Fig. 13.

Fig. 15 : Twinning and slip in high-purity polycrystalline tungsten tested at + 200°C.

Fig. 16 : Slip and orange peel in high-purity polycrystalline tungsten tested at + 200°C.

Fig. 17 : Twinning in high-purity polycrystalline tungsten tested at + 150°C.

Fig. 18 : Slip in high-purity polycrystalline tungsten tested at + 150°C.

Fig. 19 : Slip and twinning in high-purity polycrystalline tungsten tested at + 100°C.

Fig. 20: Twinning and cracking in high-purity polycrystalline tungsten tested at + 50°C.

Fig. 21 : Slip in high-purity polycrystalline tungsten tested at + 50°C.

Fig. 22 : Twinning in high-purity polycrystalline tungsten tested at -45°C. Interference microscopy (Normansky system, which produces double image).

Fig. 23 : Slip in high-purity polycrystalline tungsten tested at -45°C.

Fig. 24 : Slip concentration in high-purity polycrystalline tungsten tested at -80°C.

Fig. 25 : Slip concentration in high-purity polycrystalline tungsten tested at -196°C.

Fig. 26 : Denivelation of grain boundaries near fracture surface. Tested at + 20°C.

Fig. 27 : Same area as in Fig. 26, but interference microscopy (Normansky system, which produces double image). Proves the production of a step at the grain boundaries.

Fig. 28 : Same area as in Fig. 26 but polished electrolytically. Cracks along the grain boundaries become evident.

Fig. 29 : Electron microscopic replica of the fracture surface of high-purity polycrystalline tungsten tested at + 20°C. Note intergranular fracture of grains A, B and C and cleavage fracture of grains D and E.

Fig. 30 : Same area as in Fig. 29, higher magnification. Note striations in grain C due to intergranular gas adsorption on small steps.

Fig. 31a and 31b : Example of a fracture along non-parallel twin boundaries. Sample tested at -40°C. Photographs taken at different levels.

REFERENCES

(1) B.S. Chandrasekhar and P.A. Flinn : Rev. of Sci. Inst. 33, 1247 (1962).

(2) J. Plateau, G. Henry and C. Crussard : Iron Steel Inst. (London), Rept. N° 64, p. 57 (1959).

(3) A. Wronski and A. Fourdeux : present report, Section V.

(4) J. Heslop and N.J. Petch : Phil. Mag. 1, 866 (1956).

(5) D.F. Stein, J.R. Low and A.U. Seybolt : Acta Met. 11, 1253 (1963).

(6) N. Brown and R.A. Ekvall : Acta Met. 10 1101 (1962).

(7) A. Fourdeux and A. Wronski : J. Less-Common Metals, 6, 11 (1964).

(8) G. Schoeck : Acta Met. 9, 382 (1961).

(9) D.F. Stein and J.R. Low : J. Appl. Phys. 31, 362 (1960).

(10) H.W. Schadler : Acta Met. 12, 861 (1964).

(11) R.M. Rose, D.P. Ferris and J. Wulff : Trans. Metall. Soc. 224, 982 (1962).

(12) E. Votava : Phys. stat. sol. 5, 421 (1964) ; present report, Section II.

## Appendix I.

## Rolling of Tungsten Single Crystals at Room Temperature.

by

E. Votava, J.M. Dossin, E. Vanderschueren

High-purity tungsten single crystals prepared by electron-beam zone refining are ductile in uniaxial tension (see section IV). Experiments have now been conducted to evaluate the ductility of such crystals in a swaging or rolling operation at room temperature and the following results were obtained :

a) Such crystals are brittle on swaging with conventional speed (312 RPM).

b) On rolling (rolling speed 320 mm/sec.) such crystals have some ductility of the order of 6% reduction in thickness, but break later always in a dramatic way on cleavage planes. However, complete ductility for rolling could be achieved by heating these crystals between 300 to 400°C.

During the experiments mentioned under b) it was observed that quite a great reduction in thickness could be achieved if the cylinders of the rolling machine were statically pressed together with the single crystal between. The reduction in thickness, however, which can be obtained in such a way before brittle fracture occurs depends on the orientation of the single crystal. Compression on a {100} plane of a crystal with the axis in the ⟨110⟩ direction was found as the best orientation.

This observation stimulated the idea of compressing properly oriented crystals completely between two flat plates. Crystals treated in such a way broke, however, easily and it was thought therefore that repeated static compression along the crystal can be best achieved by considerably reducing the rolling speed. Tests with a rolling speed of 1 mm/sec. proved to be successful. Tungsten single crystals of 2 mm diameter could be reduced 80%, those of 5 mm thickness at least 50% in thickness at room temperature.

It must, however, be stated that the rolling operation has to be performed with the greatest care. From a certain degree of deformation on the rolled single crystals are very sensitive to cleavage cracks. The development of one crack anywhere along the single crystal is sufficient to produce a sort of shock wave of cleavage cracks along the whole crystal.

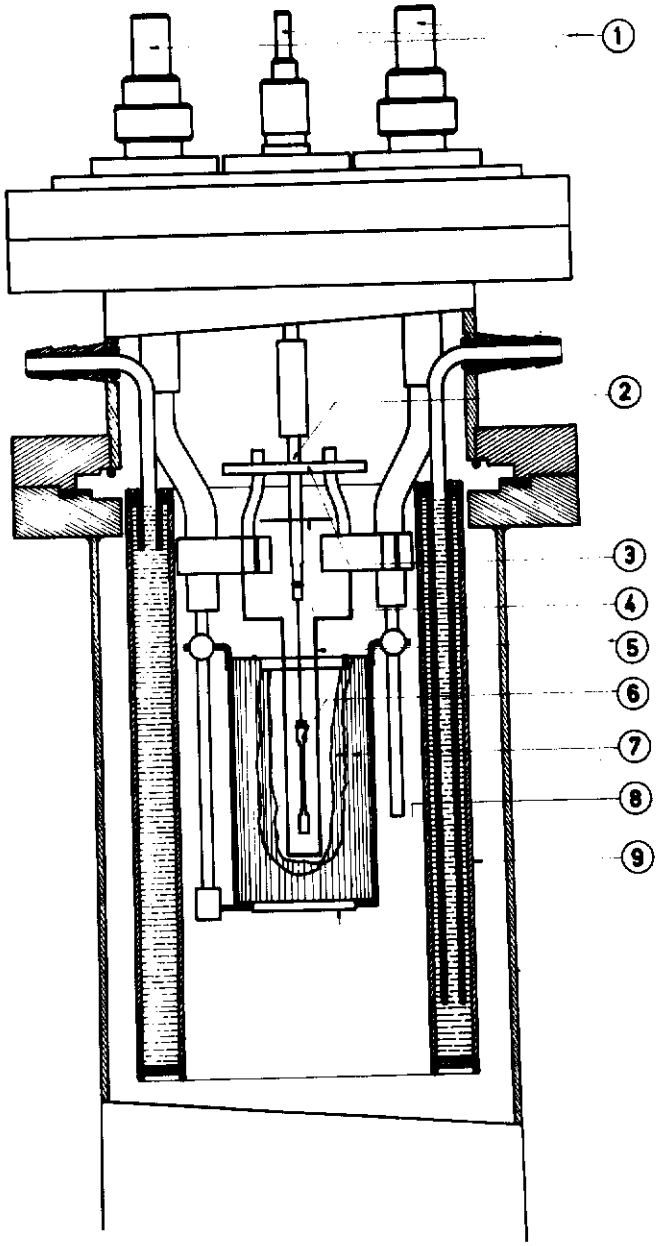


Fig.1

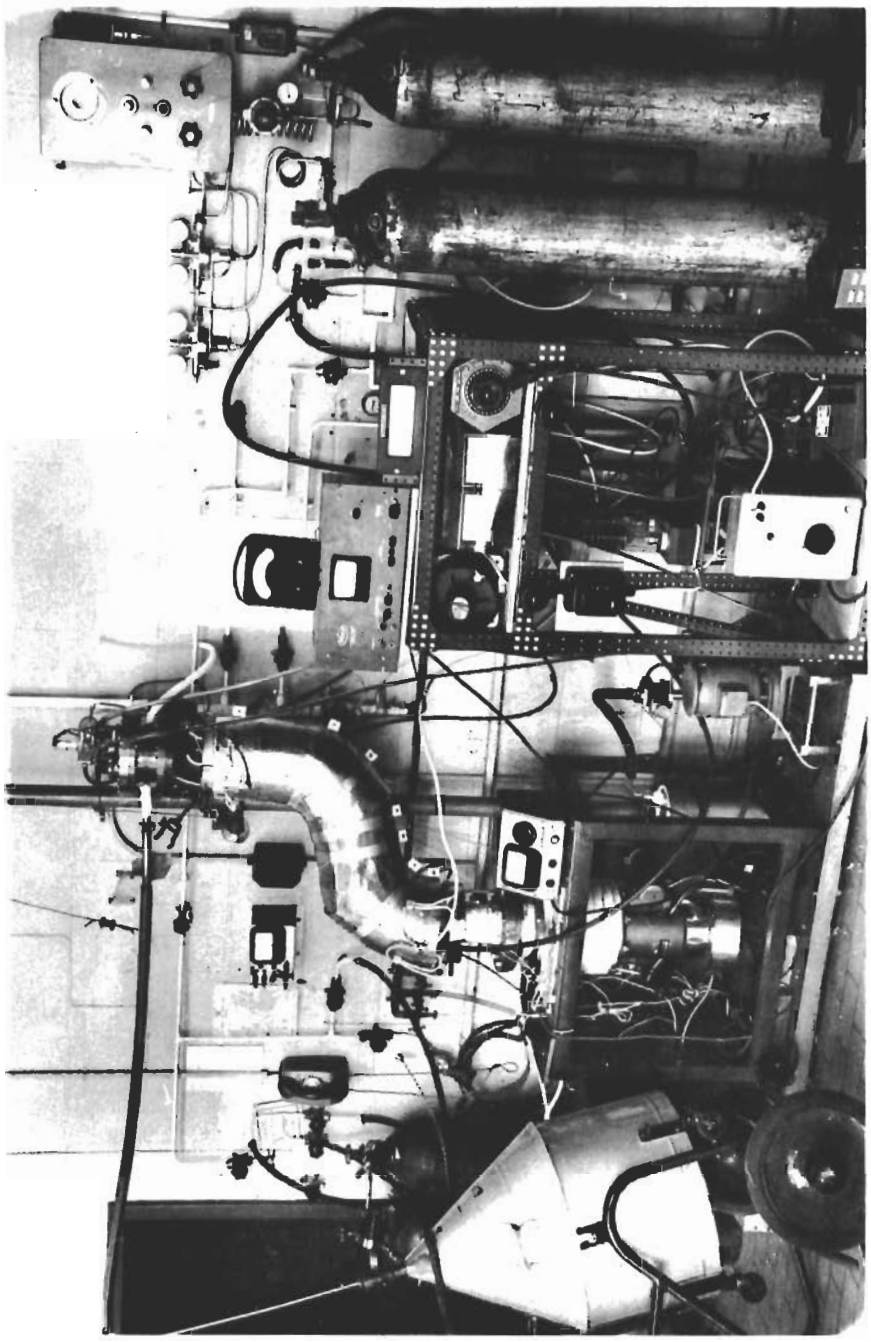

Fig.2

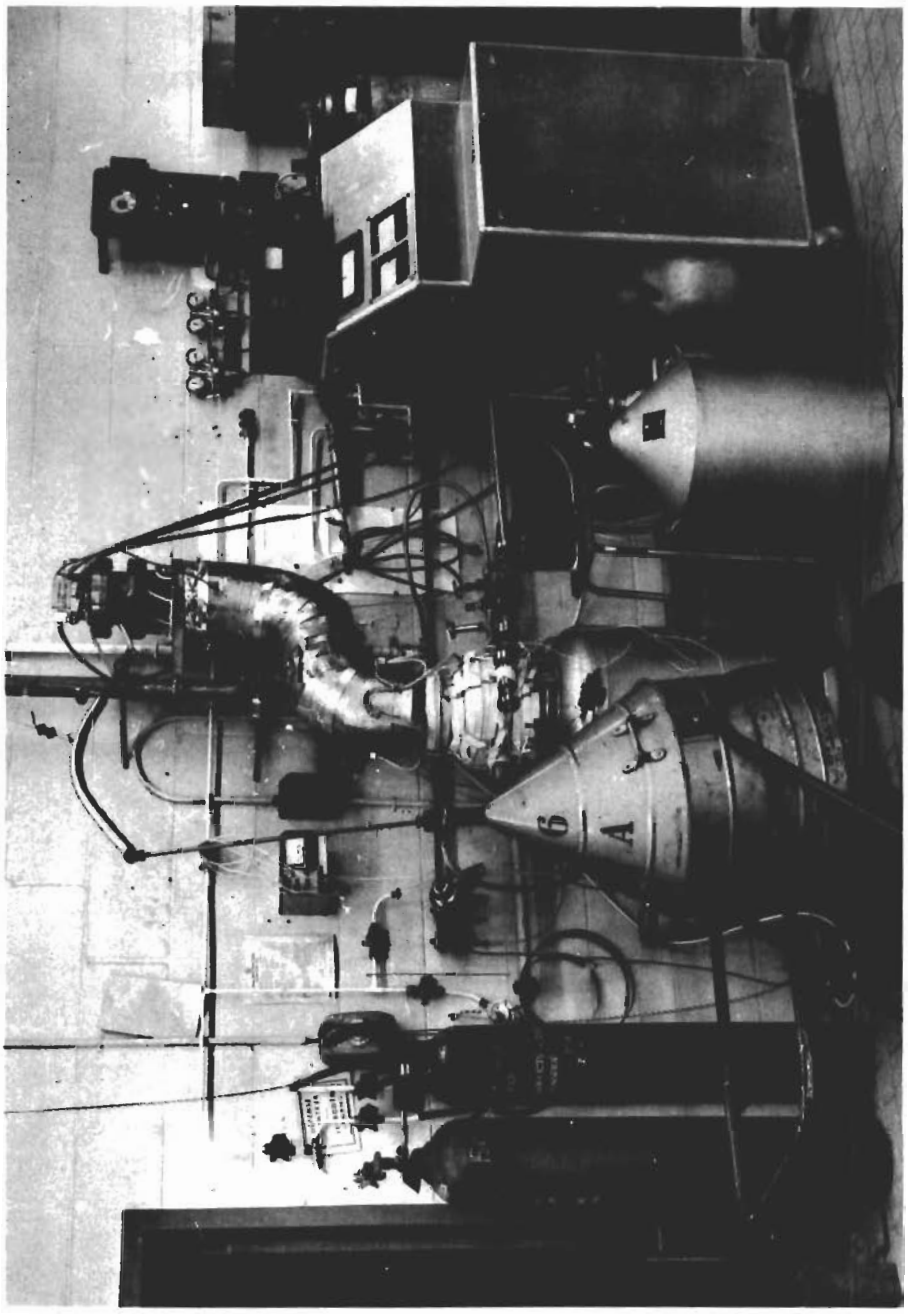

Fig.3

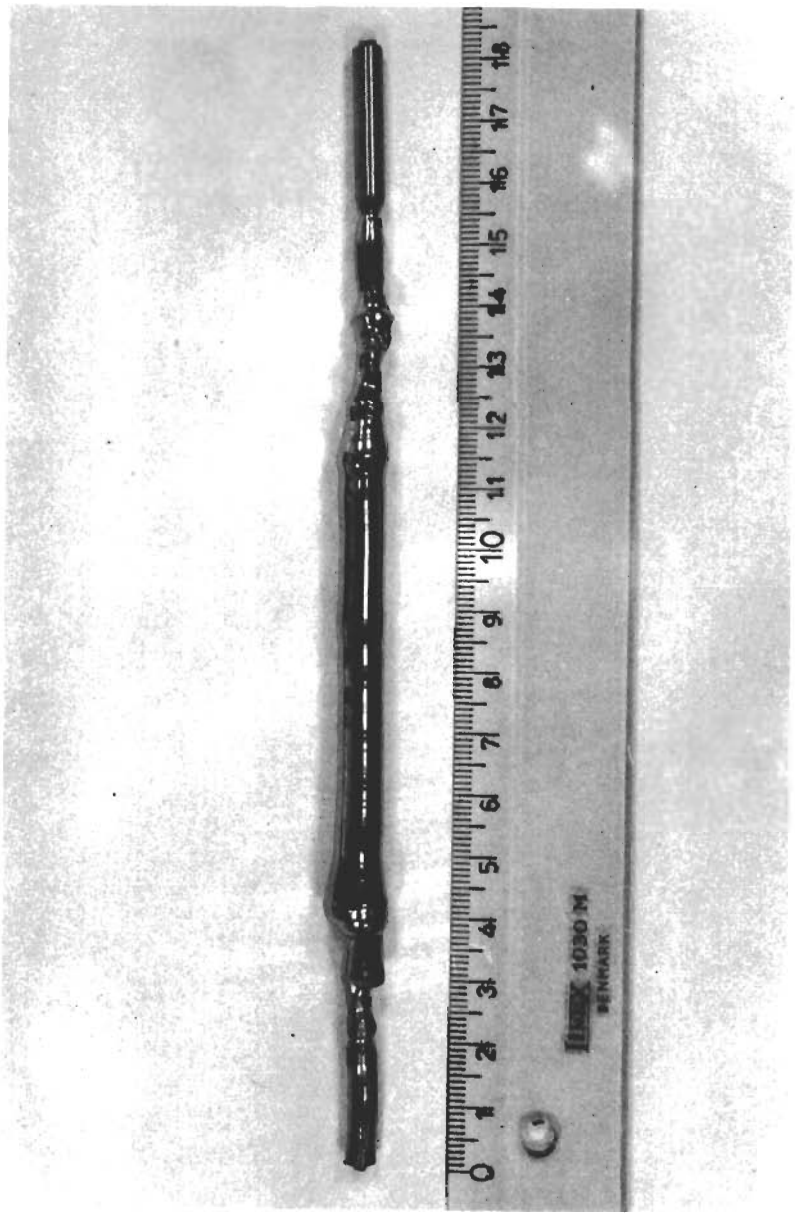


Fig.4

Fig.5

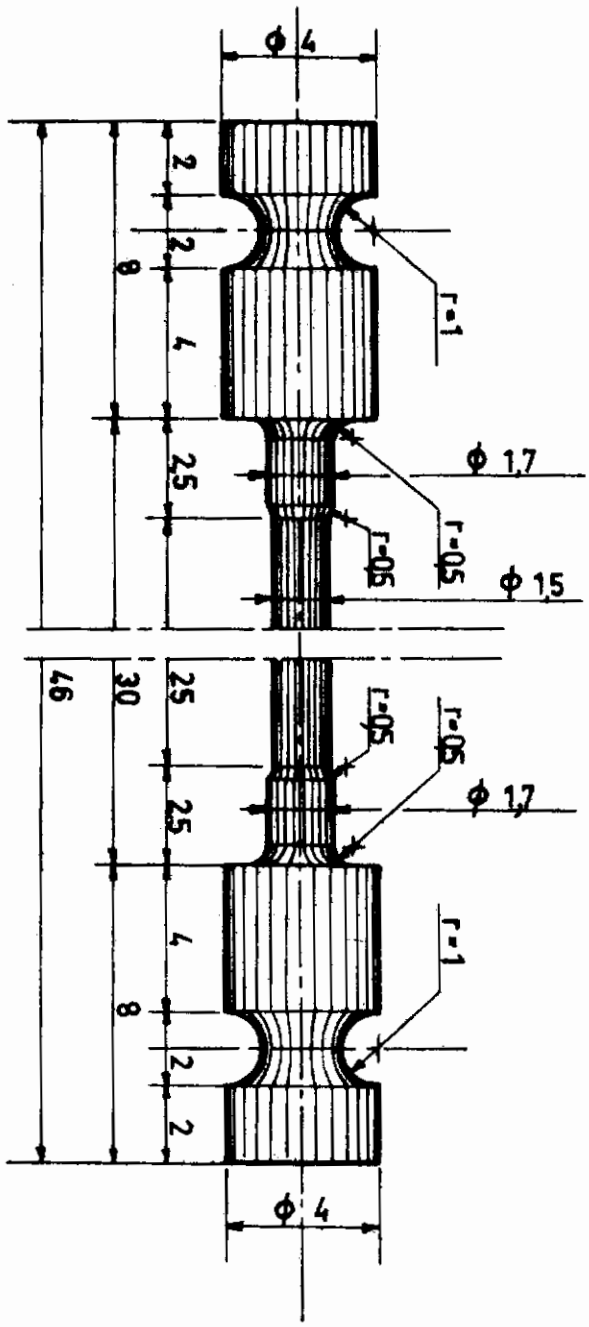


Fig. 6

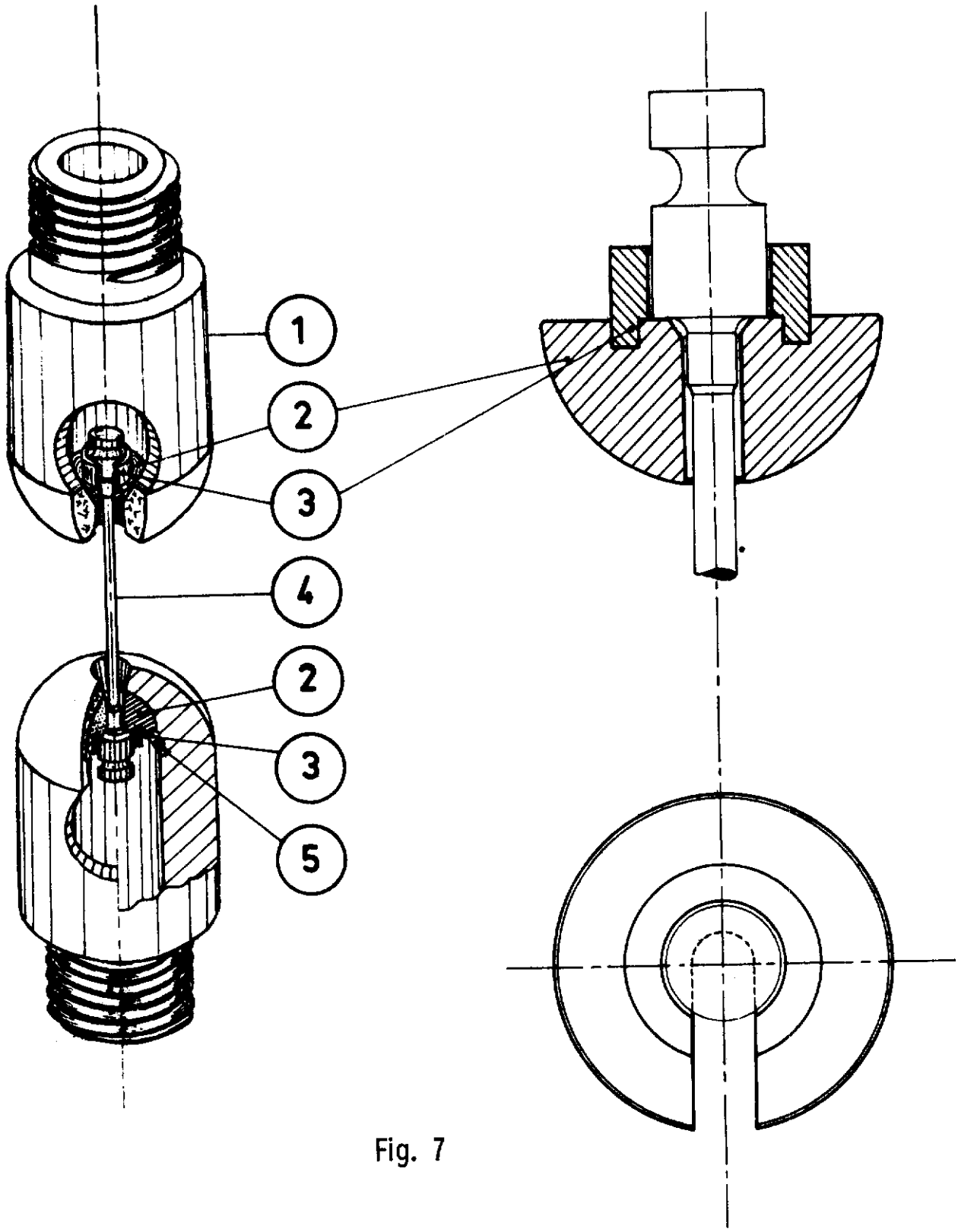


Fig. 7

Fig. 8

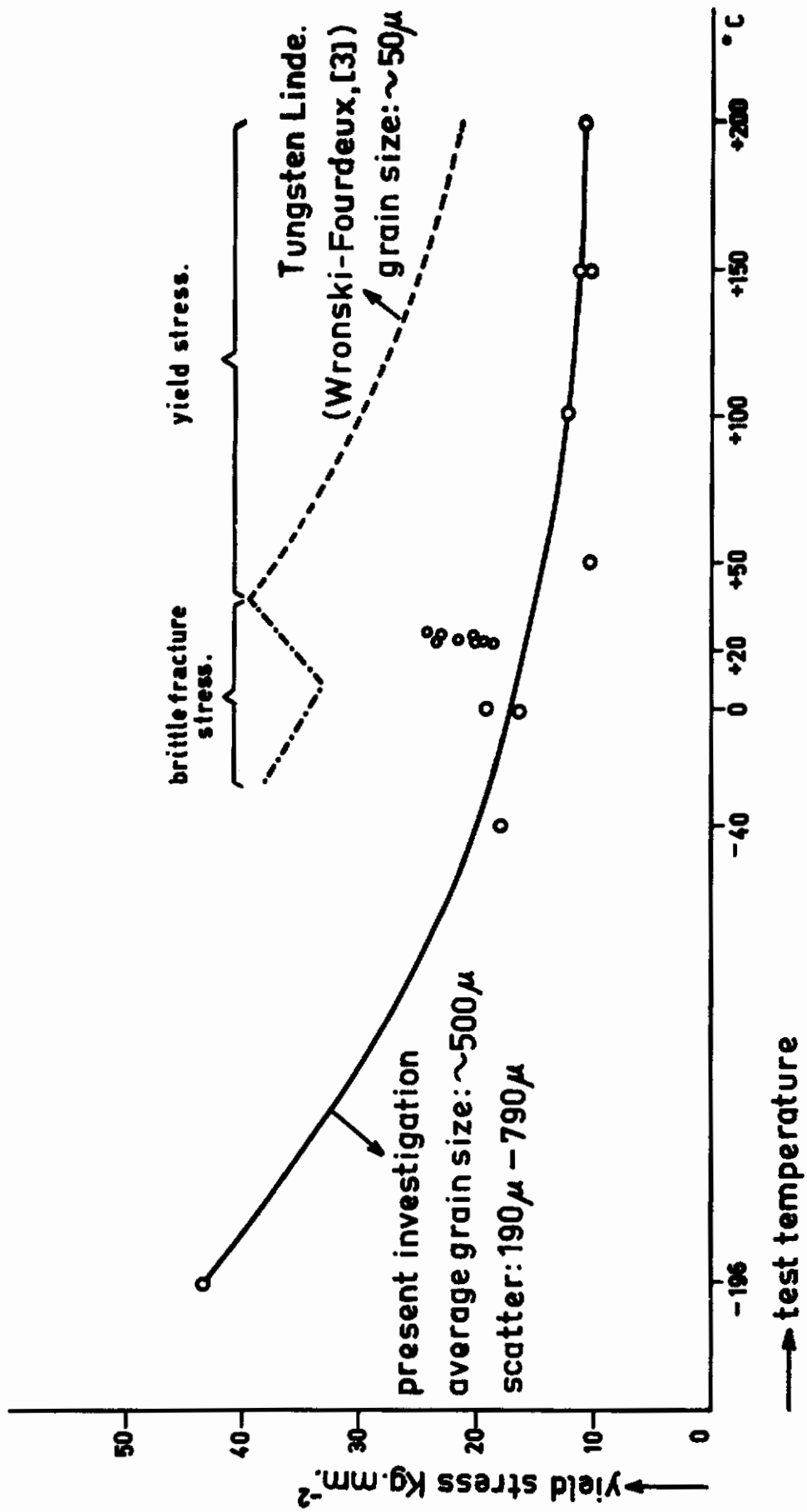

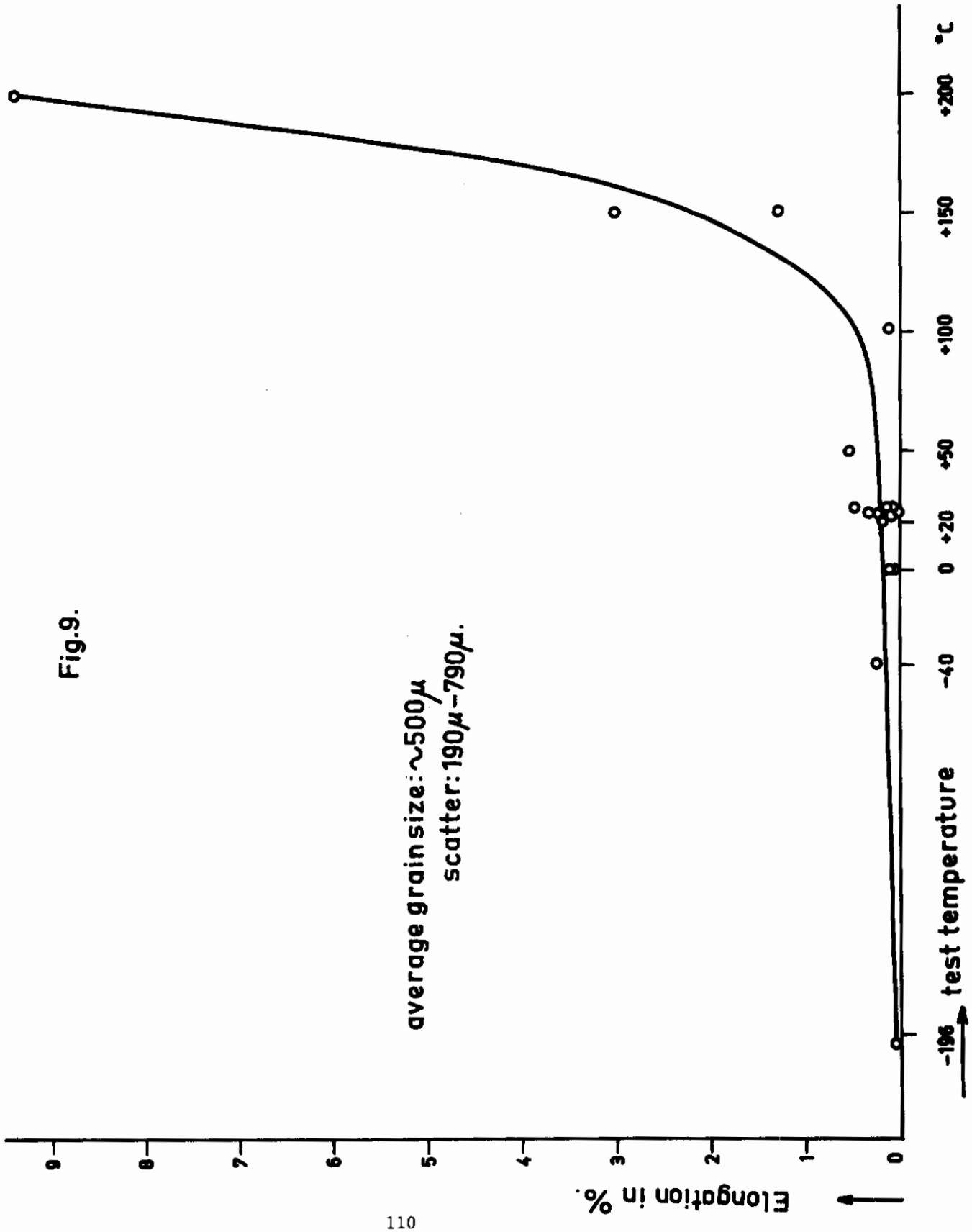


Fig.9.

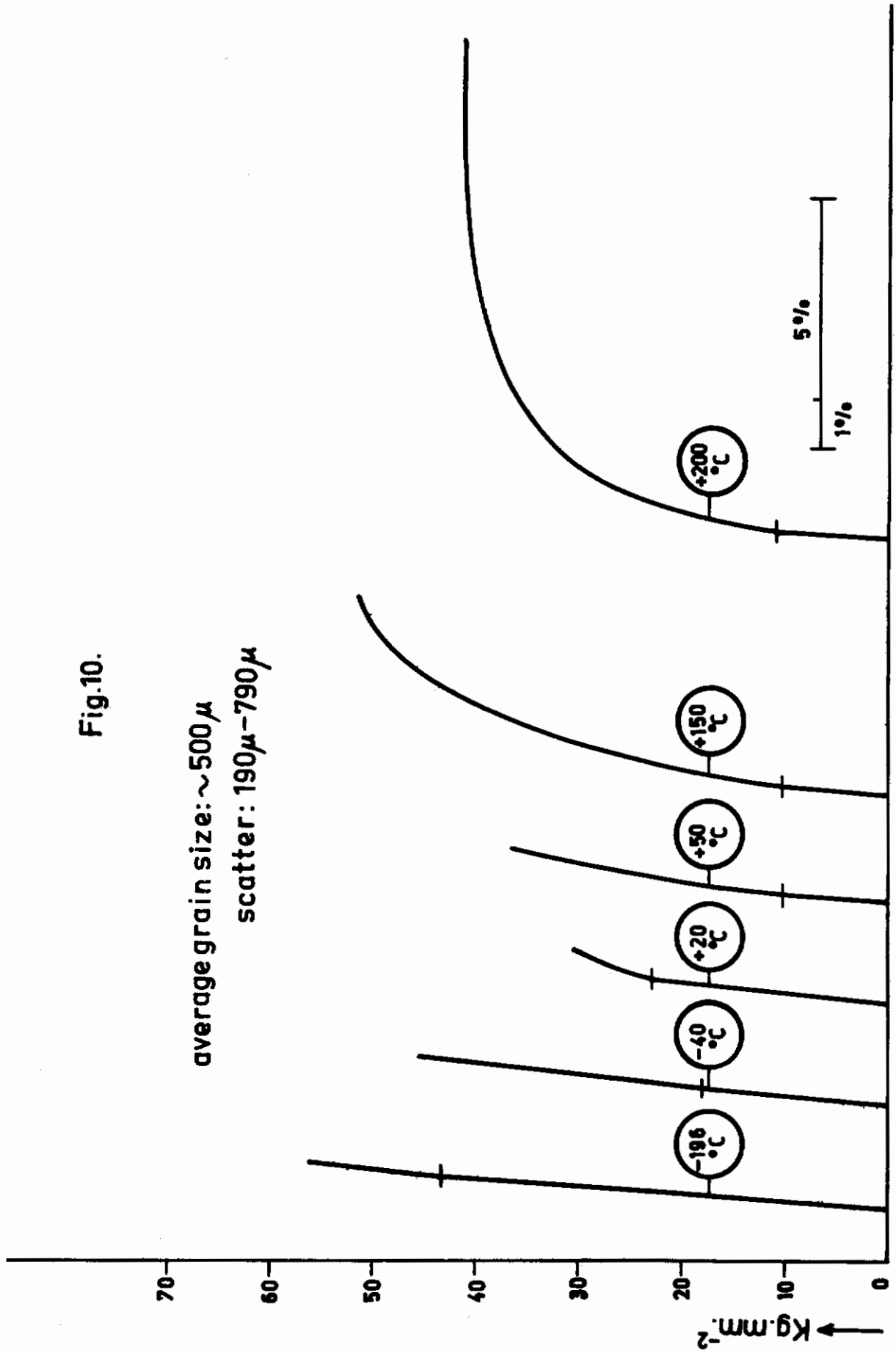


Fig.10.

average grain size: ~500 μ

scatter: 190 μ – 790 μ

Fig.11.

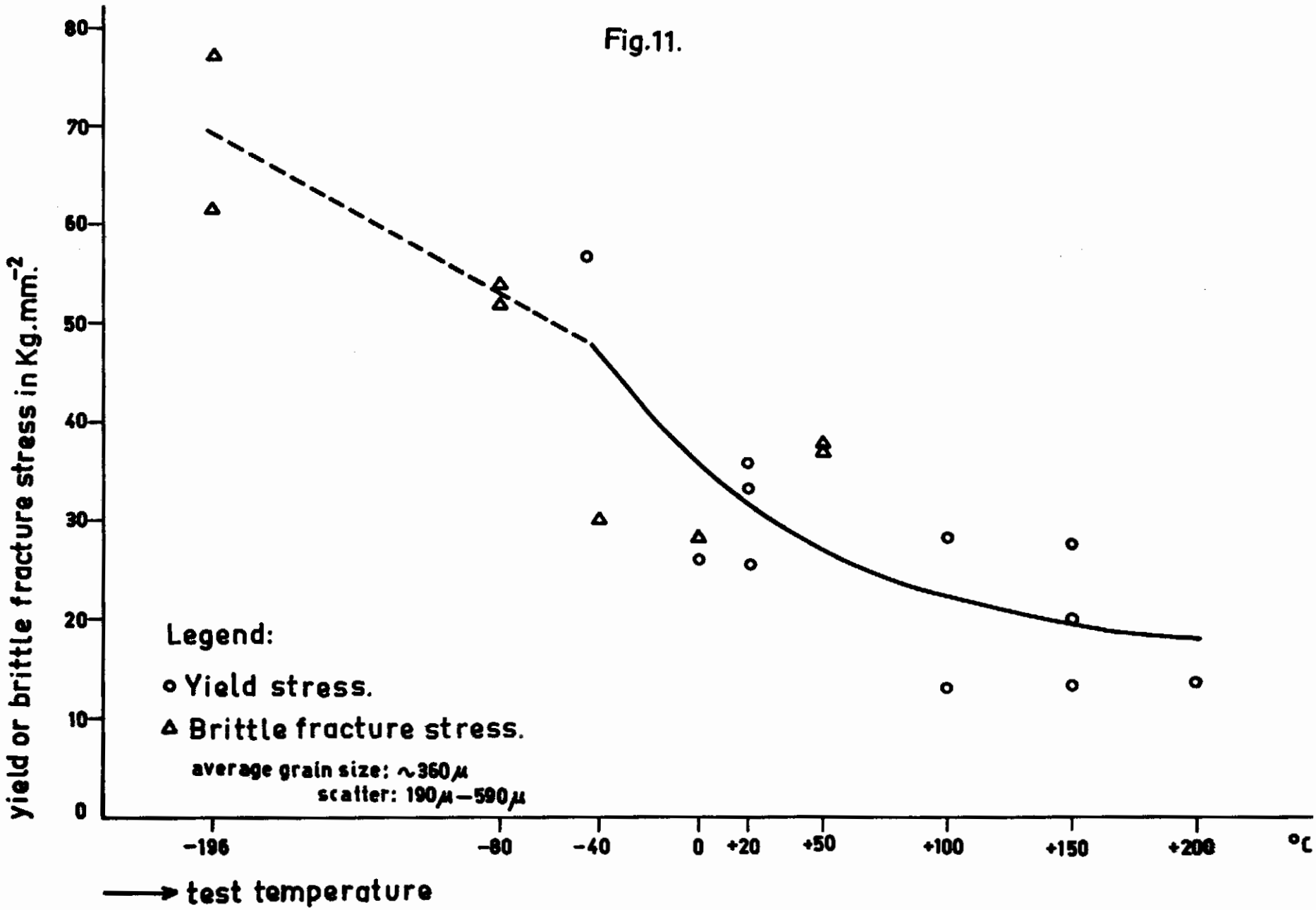

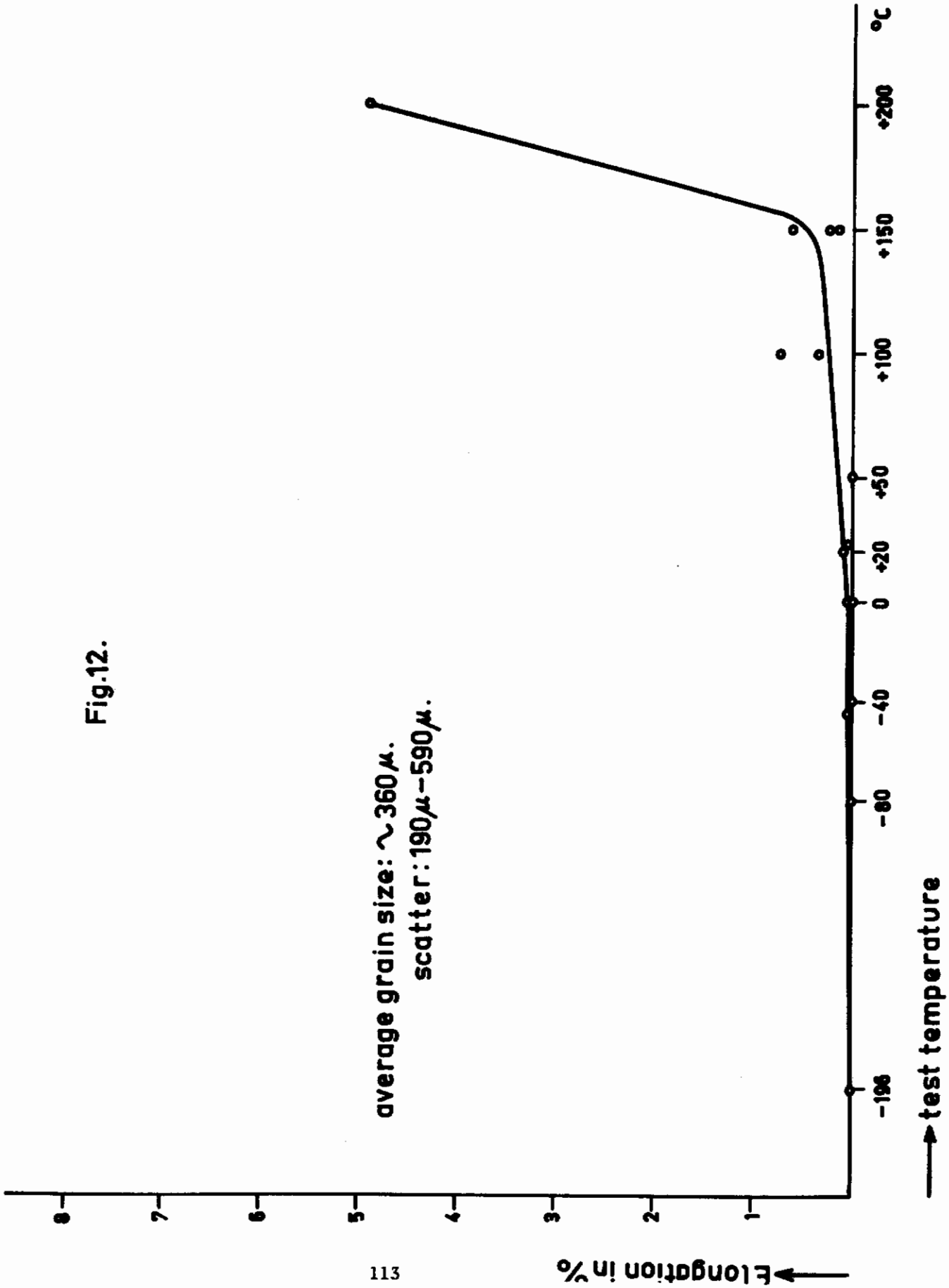


Fig.12.

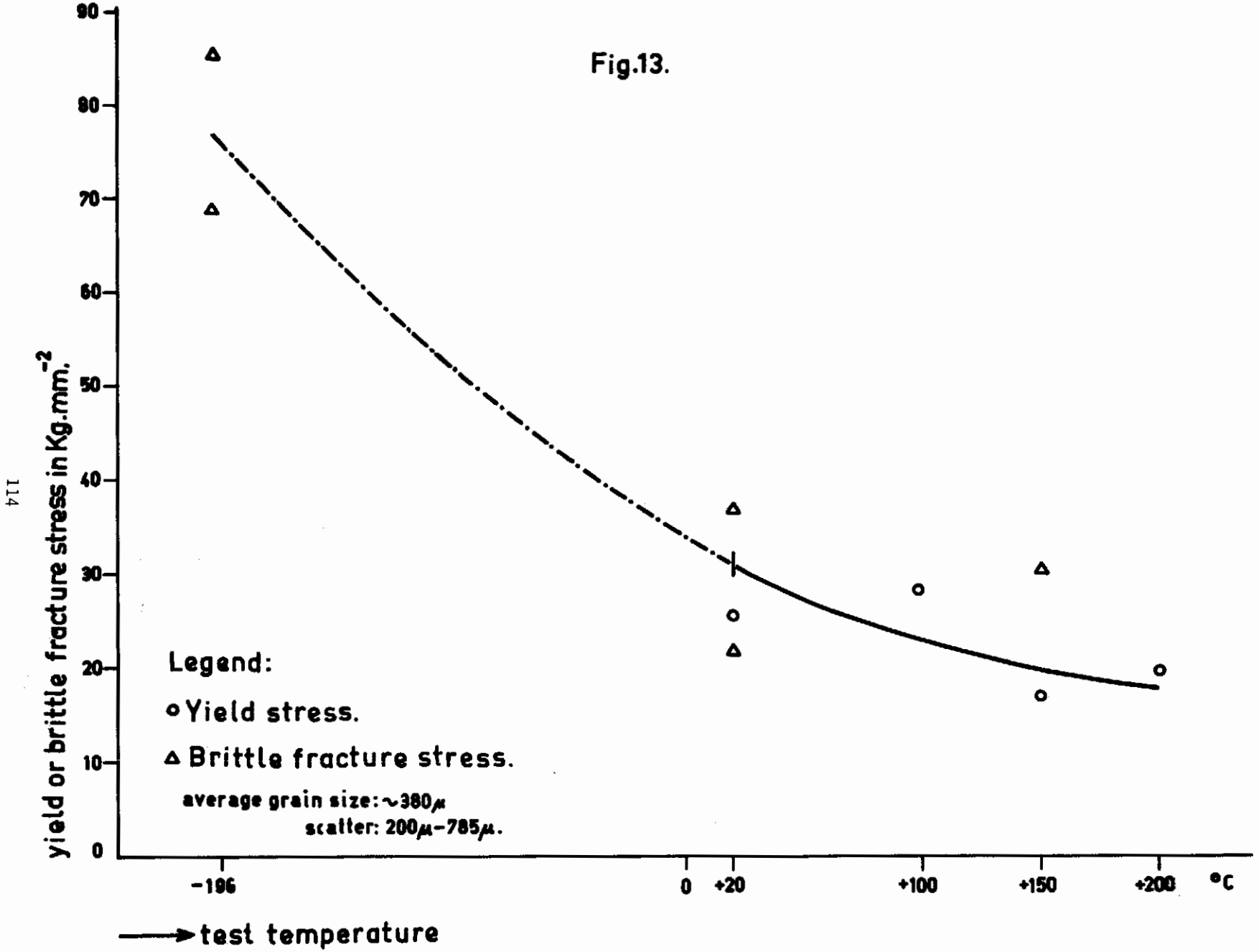

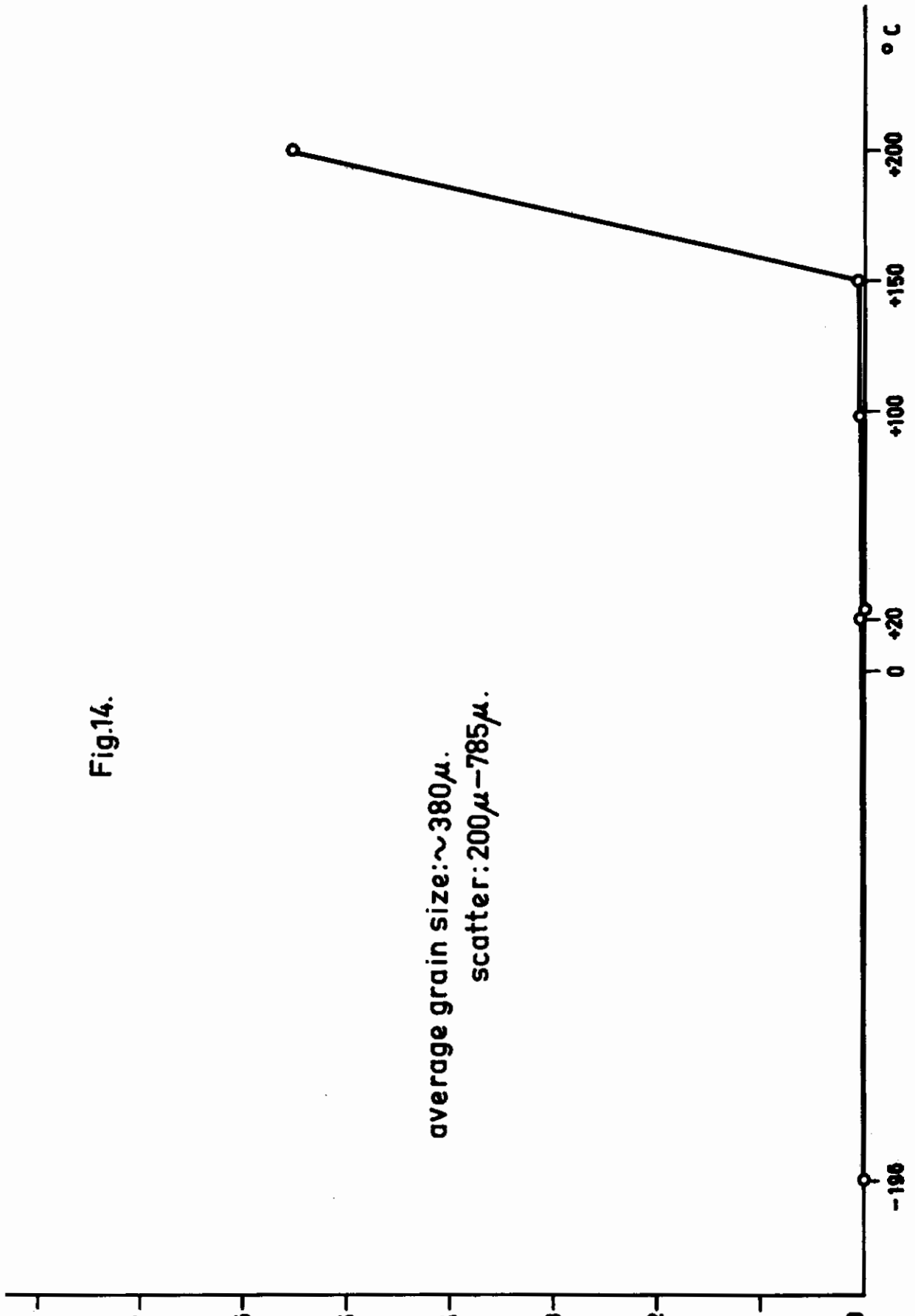


Fig.14.

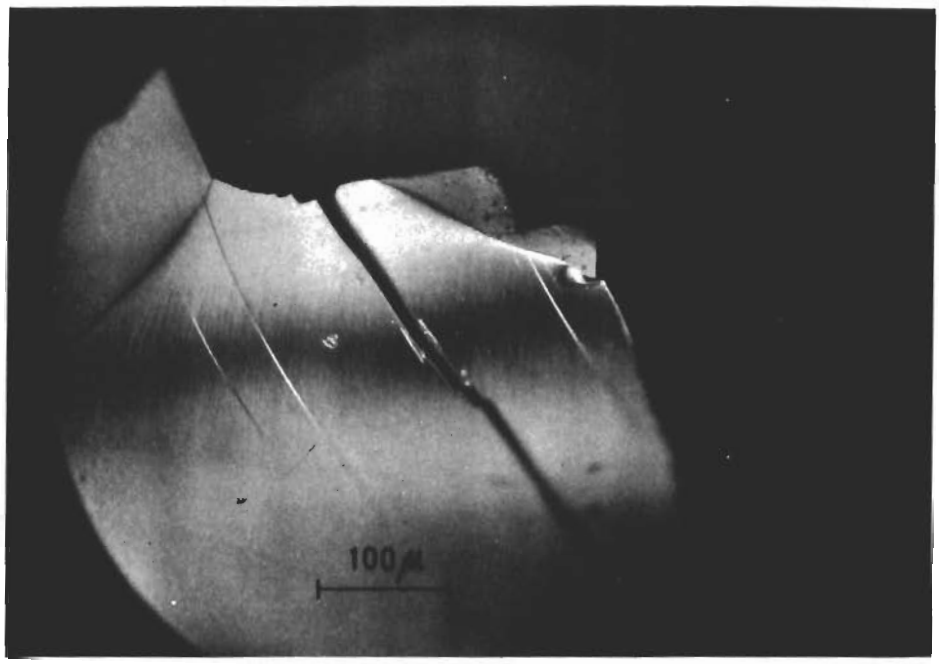


Fig.15.

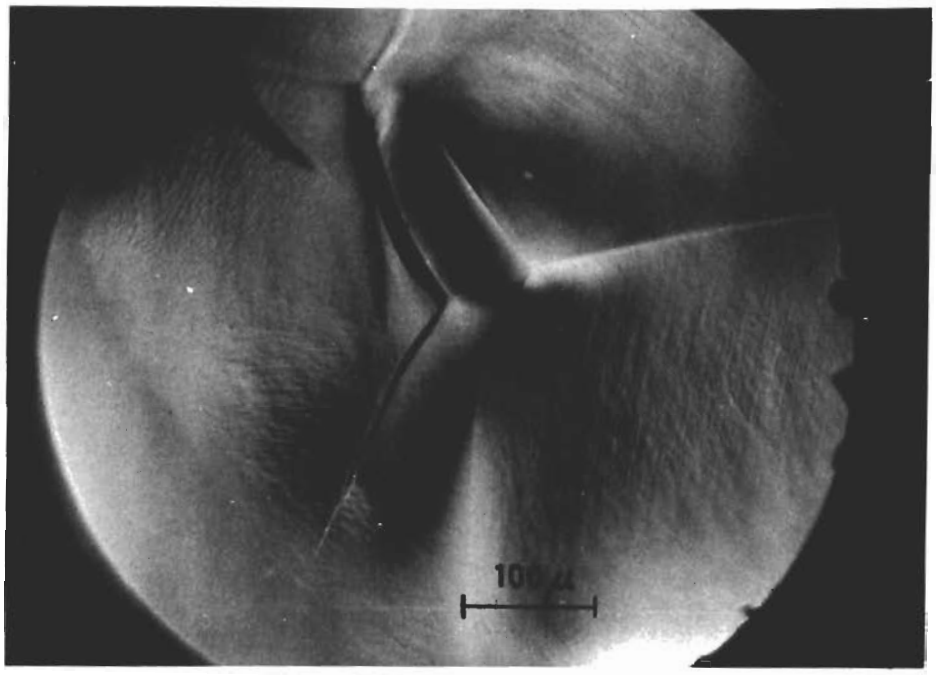


Fig.16.

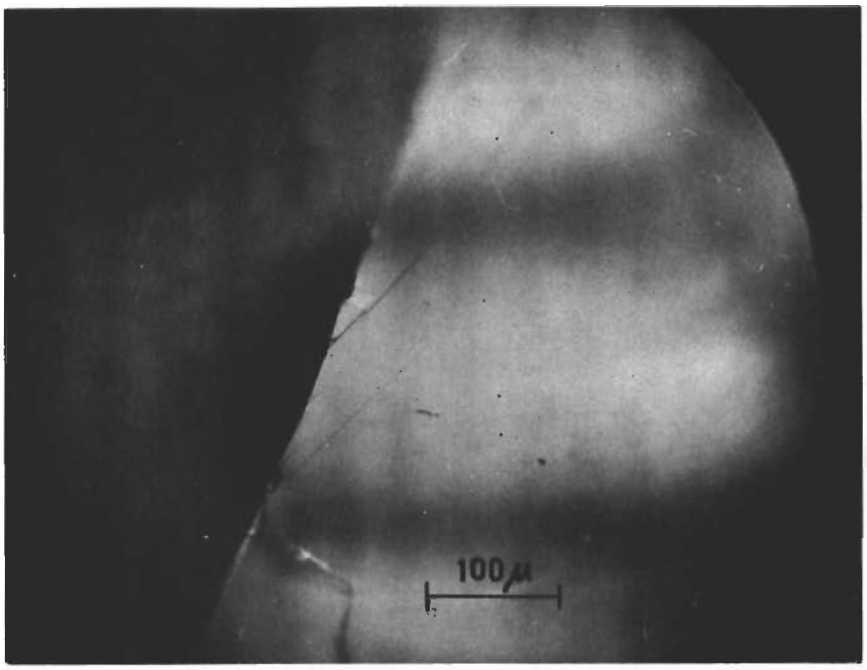


Fig.17.

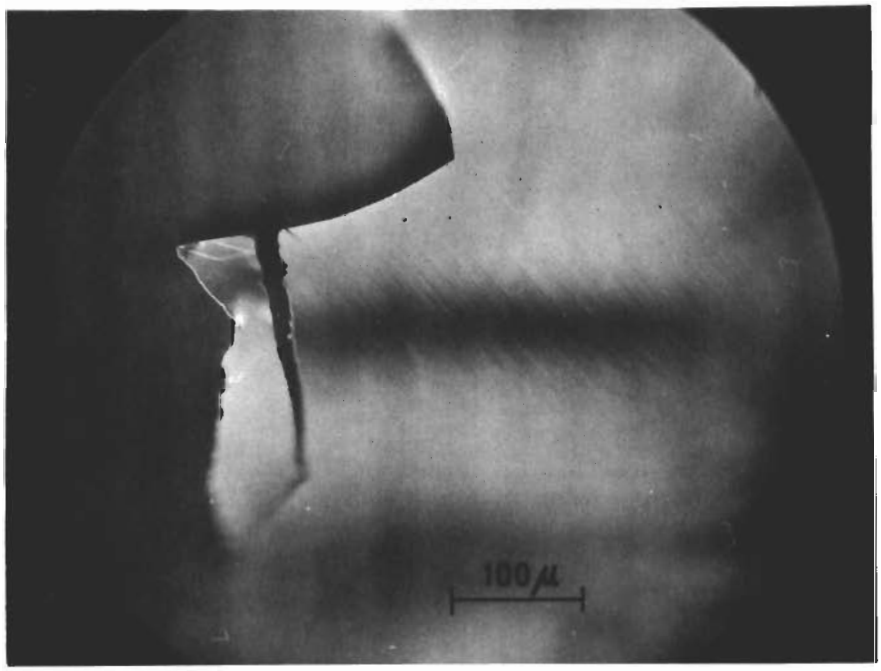


Fig.18.

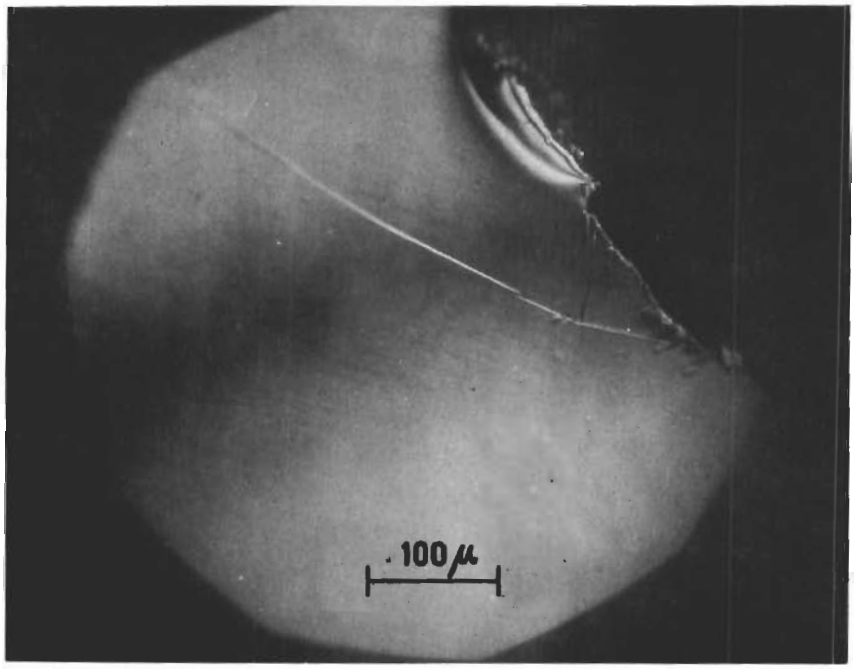


Fig.19.

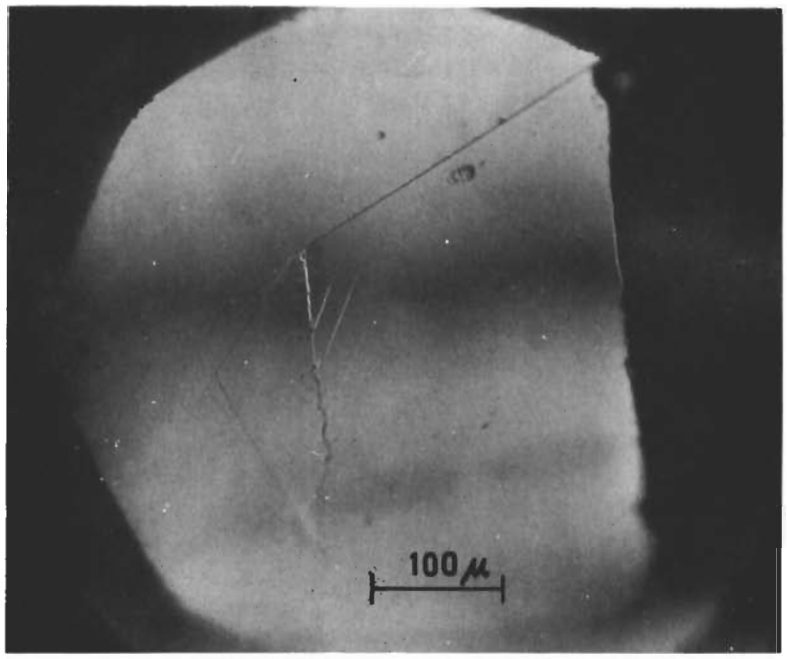


Fig.20.

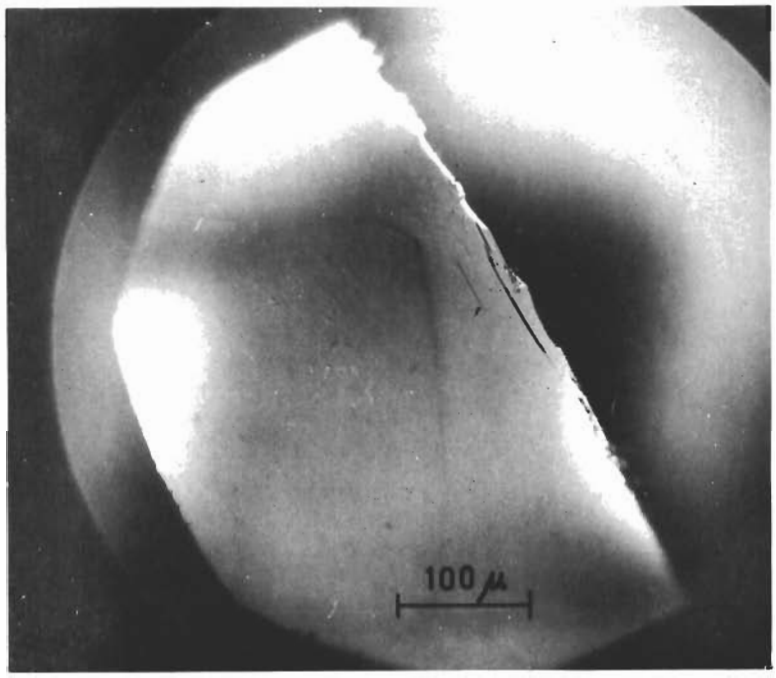


Fig.21.

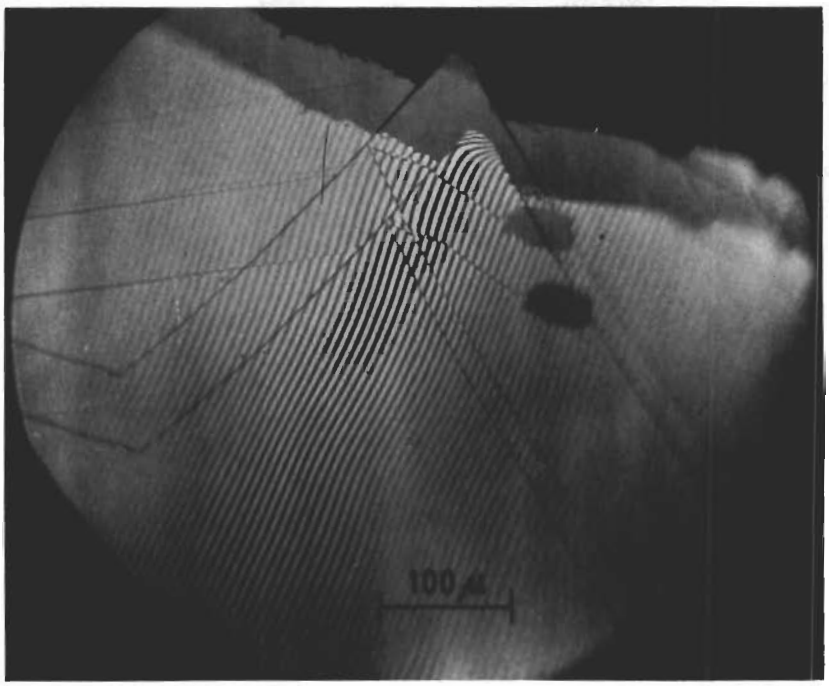


Fig.22.

Fig.23.

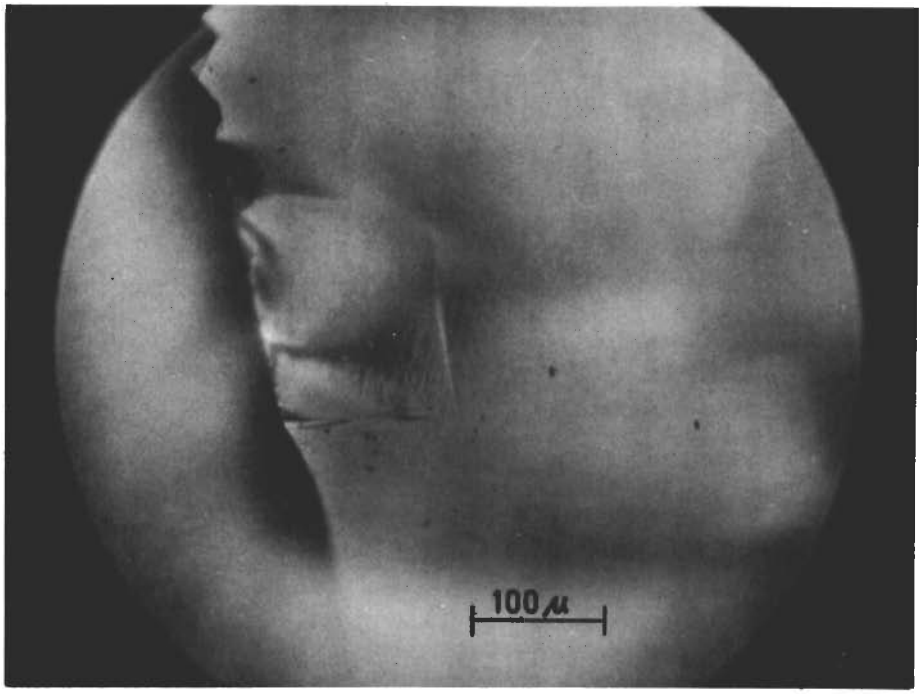


Fig.24.

Fig.25.

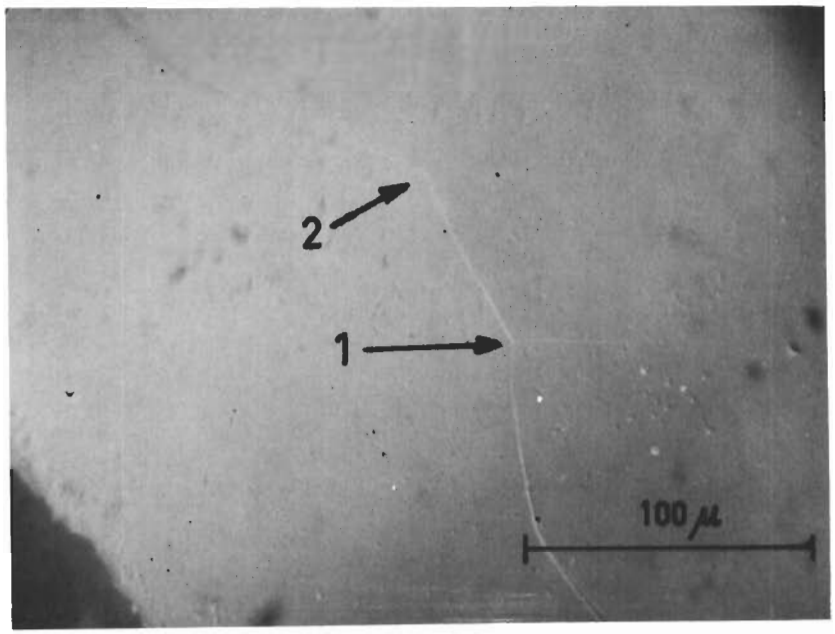


Fig.26.

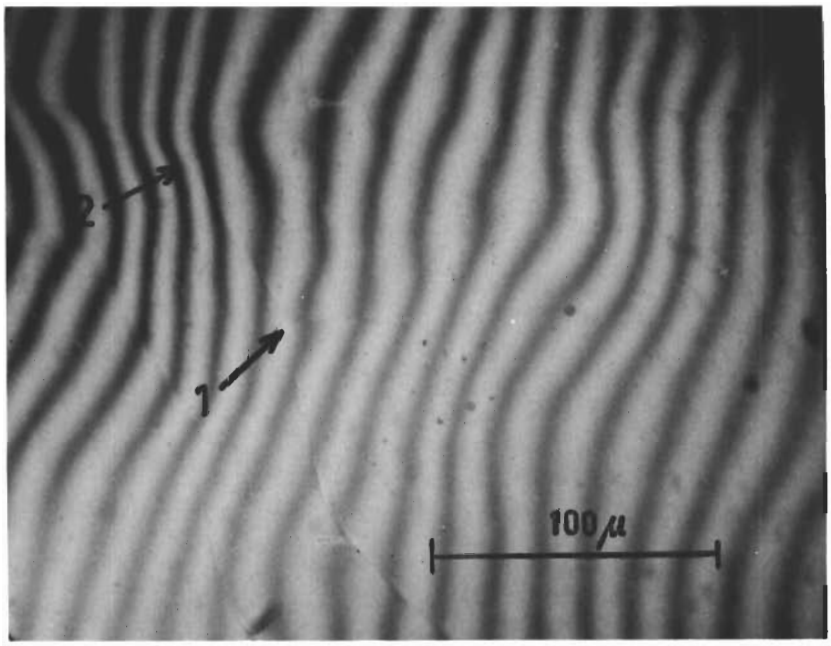


Fig.27.

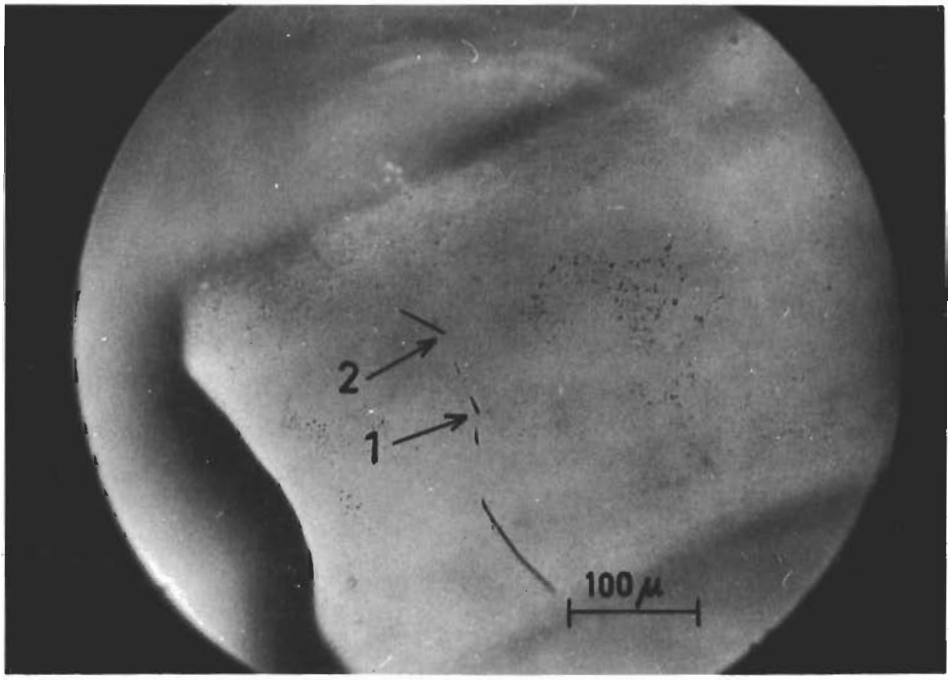


Fig.28.

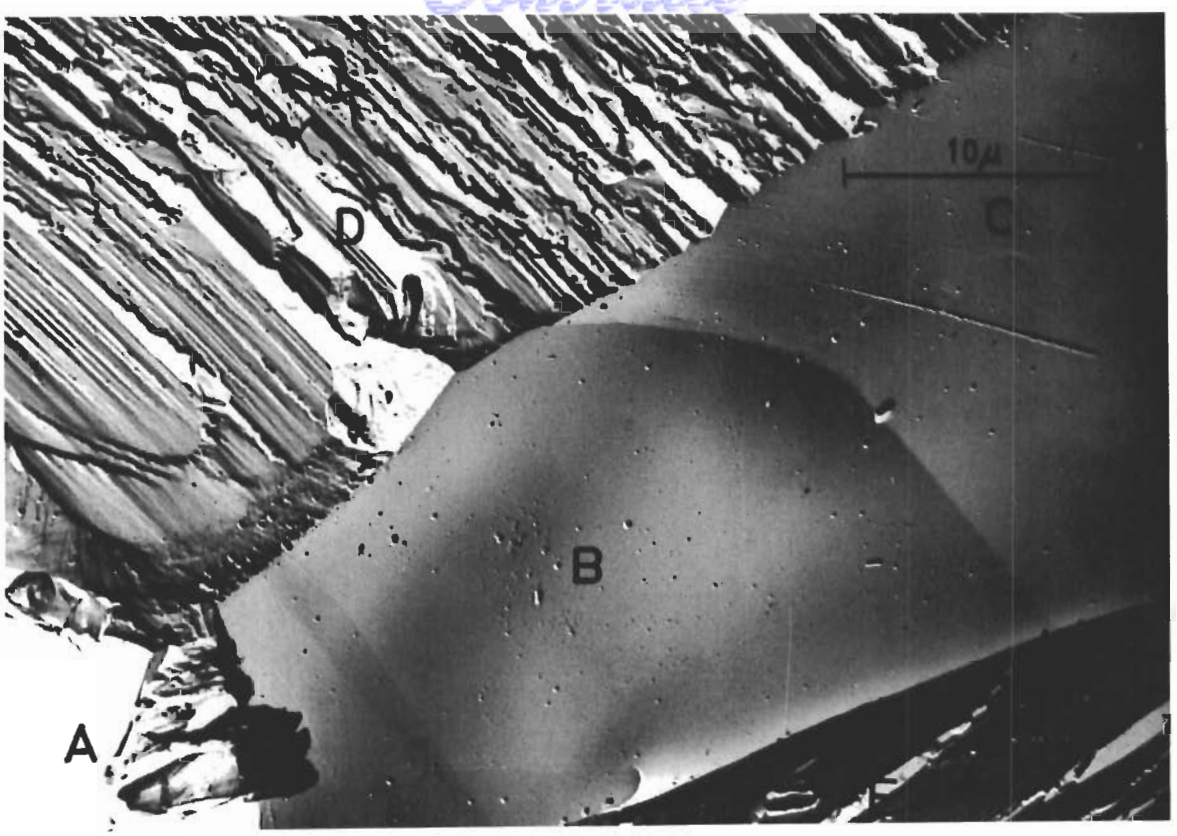


Fig.29.

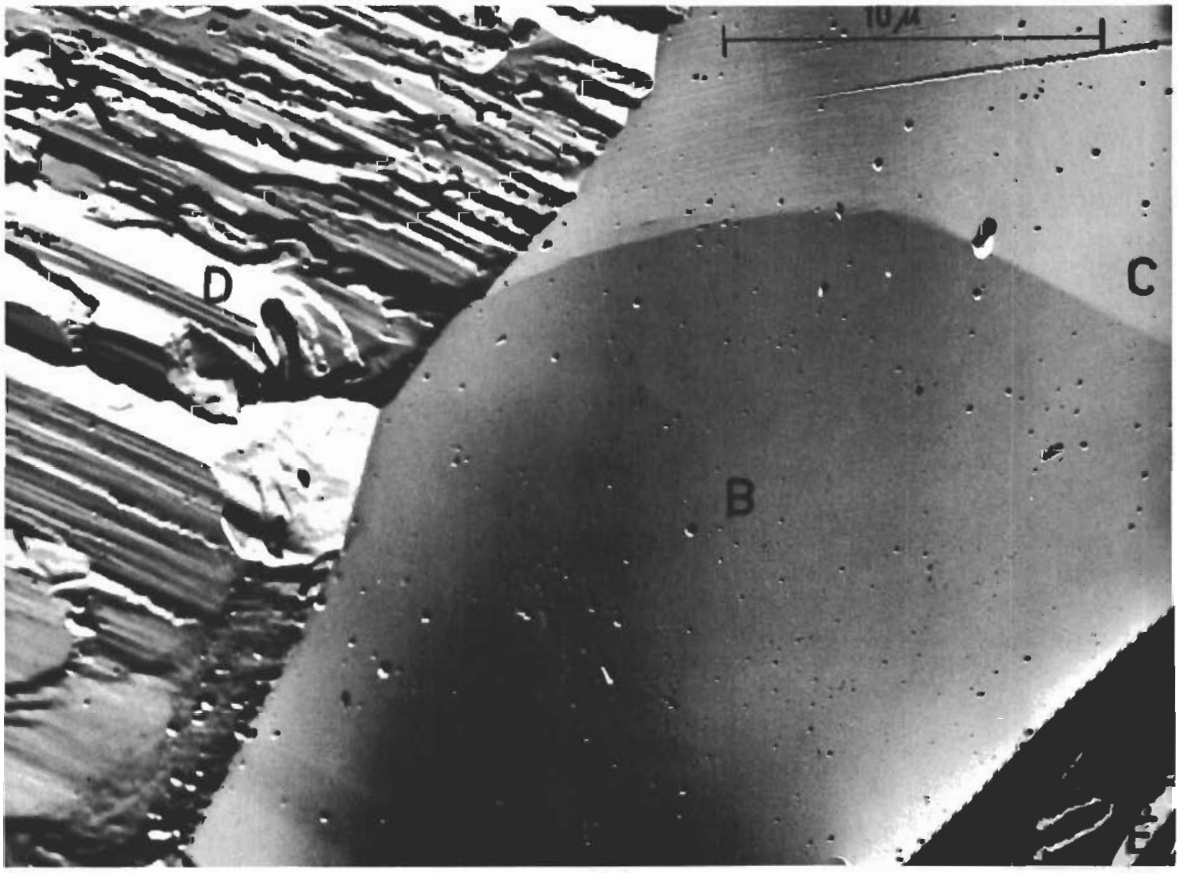


Fig.30.

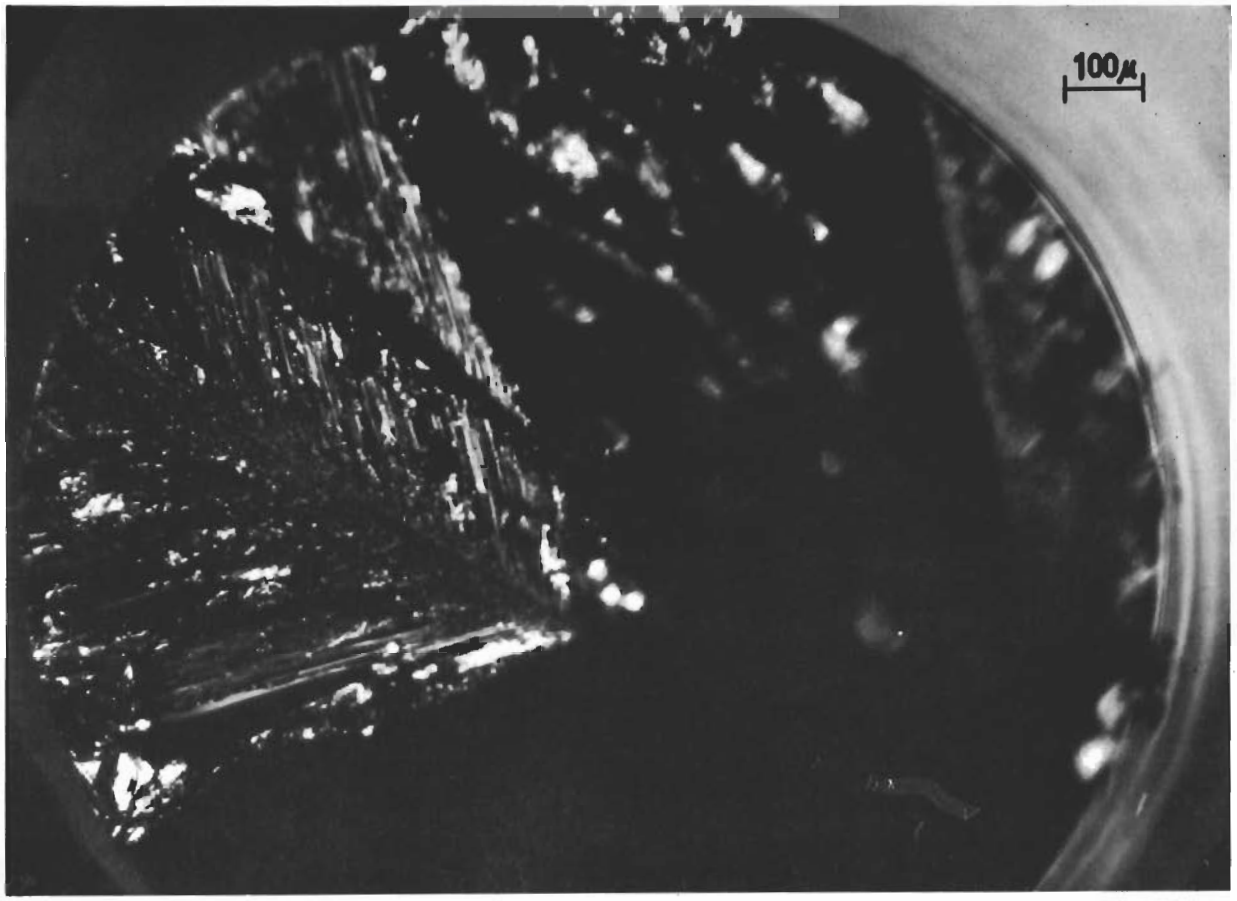


Fig.31a.

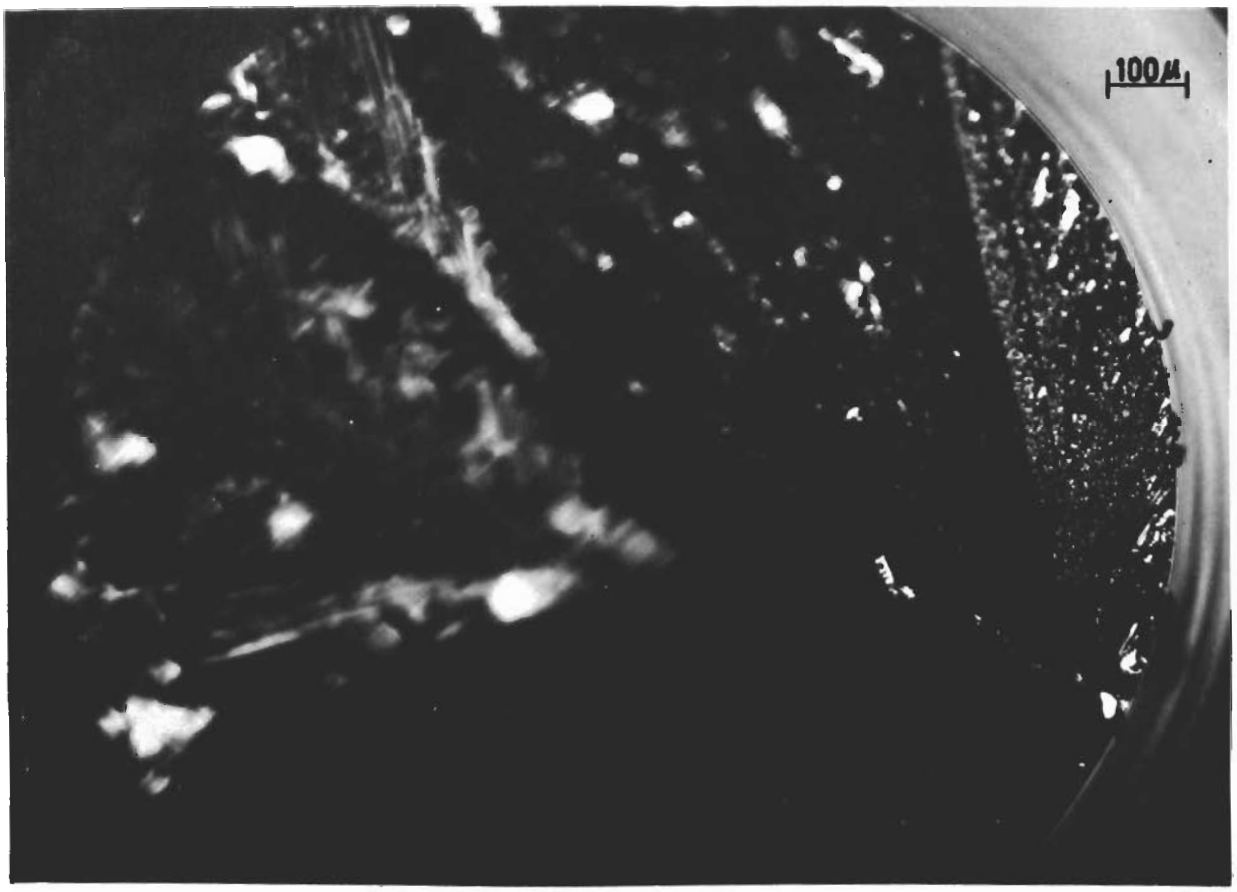


Fig.31b.

## SECTION VII.

# Transmission Electron-Microscopic Investigations of High-Purity Niobium and Tungsten.

by

A. Fourdeux, F. Rueda, and E. Votava.

## Introduction

The present investigation has been initiated with the aim of underpinning the results of sections II to VI and of obtaining a better understanding of the distribution and behavior of dislocations in niobium and tungsten of high purity. The selective results obtained in the time available are reported below.

## Experimental Technique.

### a) Preparation of Thin Foils from 5 mm Thick Single Crystals.

A method described first by (1) and utilized also by (2) was used for the strain-free preparation of flat plates out of 5 mm thick single crystals. The apparatus is shown schematically in Fig. 1. It consists of a rotating stainless steel wheel (6 rpm) for use with tungsten or a bakelite wheel for use with niobium, about 2 cm wide and 7,5 cm in diameter ; the cylindrical surface is covered by a strip of cloth. Chemical polishing is used for niobium, the cloth used is Buehler 1576 AB micro-cloth, and the wheel dips into a 1.1 mixture of a 40% aqueous solution of HF and of $HNO_3$ of d = 1,41. Electrolytic polishing is used for tungsten, the cloth used is Buehler 1576-S AB Seloyt, and the wheel dips into a 9% aqueous solution of NaOH. The single crystal is contacted carefully with the liquid transported by the cloth and after a sufficiently deep cut is produced the crystal is turned 180° and the same process repeated. Flat plates of 0·1 mm thickness can be produced in this way with a precision of $\pm$ 0·01 mm.

Further deformation-free thinning proceeds as follows :

i) Tungsten : The single crystal plate is covered with Lacomit (manufactured by Canning, Birmingham, England) and dried. A 2 mm x 1 mm grid is then traced carefully into the Lacomit film with a thin pointed stick wetted with solvent

(see Fig. 2) and the small rectangles are separated electrolytically in a 2% aqueous solution of NaOH.

The individual rectangles are fixed on a tungsten framework with Wood's metal and the whole covered with a film of Lacomit except for an area of about 0·75 x 1·5 mm in the middle of the sample (see Fig. 3). Thinning is then continued electrolytically in a 0·5% aqueous solution of NaOH at a tension of 10 Volt until holes begin to appear in the foil. The Lacomit is then dissolved and after careful repeated cleaning in alcohol the sample is ready for observation.

ii) Niobium :

The method is the same as for tungsten except that paraffin wax is used instead of Lacomit. This is necessary because the separation of the different rectangles is effected chemically in a mixture of 30% HF and 70% $HNO_3$, which attacks Lacomit.

Subsequent thinning, using the same mounting as for tungsten (but with a niobium framework and a paraffin wax coating), can be carried out either chemically or electrolytically (85% $H_2SO_4$ of d = 1.84 and 15% HF at 30°C under a tension of 8.5 Volt).

b) Preparation of Micro-Tensile Specimens.

For the observation of the deformation process inside the electron microscope a specially designed micro-strain equipment described by (3) was used. The specimens used were first thinned by standard electrolytic methods down to a thickness of about 0·001 mm. A 10 mm x 2 mm strip was then cut out by painting a strip of Lacomit or paraffin wax on both sides and further polishing. After cleaning both ends were bent several times so that the sample could be

fixed in the grips. The middle part was then thinned further until the necessary thickness was obtained.

Experimental Results.

a) High-Purity Niobium Single Crystals.

The density of random dislocations found in these crystals was quite low and no sub-boundaries have been observed. On the one hand, this demonstrates clearly the great perfection of these crystals ; on the other hand, it has been verified by a technique of etch pits that the sub-grains in these crystals are fairly large (mean diameter ~ 5 mm) and because of their size are not observed in the electron microscope.

In some rare cases striking fringe patterns have been observed ; an example is shown in Fig. 4. The fringe patterns are distinctly different from those due to stacking faults : it can be seen clearly in Fig. 4 that they are not symmetrical, but that the first fringe and the last fringe are opposite in nature. Fringe patterns of the same kind have already been observed by Van Landuyt and Amelinckx (4) and have been attributed to domain walls due to the presence of interstitial impurities, e. g. oxygen.

However, in addition to these domain walls other structures have been observed, which have all the characteristic features of stacking faults. This is shown in Figs. 5, 6, 7 and 8. In this case the fringe patterns are symmetrical ; the first fringe and the last fringe are of the same nature, both dark. On observation, in the dark field (see Figs. 9a and 9b) the fringe patterns change their nature : the first fringe is bright, the last dark. According to (5) and (6) this is characteristic for a stacking fault.

It is difficult to understand the development of stacking faults in high-purity niobium, because investigations of the slip mechanism (see Section II) as well as transmission electron-microscopic studies (7) showed that cross-slip occurs frequently in niobium, which means that the dislocations should not be dissociated. The observation of domain boundaries indicates as mentioned before that some local contamination has taken place. It is therefore possible that the stacking-fault-like structures are also due to local contamination, but further diffraction work will be necessary to arrive to a definite conclusion. Three possible sources of local contamination can be envisaged :

i) Impurities are introduced into the samples during the observation inside the electron microscope. This, however, is not very probable as in this case domain boundaries and stacking-fault-like structures should have been observed more frequently.

ii) A chemical bath containing $HNO_3$ was used for thinning and accidental contamination by oxidation is therefore possible.

iii) The zone melting process leaves behind some minor inhomogeneities or impurities are taken up during cooling after zone melting.

b) High-Purity Tungsten Single Crystals.

A very low dislocation density was found in this case, too, (see Fig. 10) and no subgrain boundaries could be observed although their presence could be proved by an etch pit technique.

No fringe patterns were observed at all in the tungsten crystals. As both the niobium and the tungsten crystals were prepared under identical conditions, except that niobium was thinned chemically and tungsten electrolytically, this indicates that if the stacking-fault-like structures observed in niobium (see Figs. 5 to 9) are due to oxygen contamination, the probable

cause is that given under (ii) above. In fact attempts have been made to thin the niobium single crystals electrolytically and no fringe patterns were observed then any more. However, since a sufficient number of observations could not be made no definitive conclusion can be drawn ; further work is required in this direction.

Deformation Structure in High-Purity Polycrystalline Tungsten.

High-purity polycrystalline tungsten prepared from single crystals was deformed outside the electron microscope at room temperature and at 250°C and the resulting dislocation structure observed. Fig. 11 shows the state before deformation. No precipitates are observed at the grain boundaries and only a few dislocations are visible within the grains. Deformation at room temperature produces some accumulation of dislocations at the grain boundaries, as can be seen in Fig. 12, but not many dislocations were observed within the grains.

This situation is drastically changed on deformation at +250°C. In this case, a considerable number of dislocations are accumulated at the grain boundaries (see Fig. 13) and a band-like structure is formed within the grains, as demonstrated by Figs. 14 and 15. The dislocation bands, seen at higher magnification in Fig. 16 are mostly parallel to a ⟨100⟩ or ⟨110⟩ direction and the dislocations of which they consist are of a very irregular form. Furthermore, as can be seen on Fig. 15, there is a difference in contrast between the different bands, indicating a strong orientation difference as a consequence of the dislocation bands.

The development of these bands has certainly something to do with the development of work hardening, but more detailed investigations on single crystals are necessary for an interpretation.

The Deformation Behavior of Polycrystalline Niobium and Tungsten Inside the Electron Microscope.

Thin foils of high-purity polycrystalline niobium and tungsten were also deformed inside the electron microscope, using a specially designed micro-strain equipment described by (3). The following results were obtained : a) In niobium the dislocations do not move in straight lines but with repeated cross-slip as can be seen in Fig. 17. Similar observations have been made by (7). b) On the other hand, in tungsten the dislocations move in straight lines and no cross-slip is apparently observed. This is seen on Figs. 18 and 19. Further, if the deformation is stopped, the dislocations remain essentially in the slip planes. Such a state is seen on Fig. 20.

These observations show clearly the marked difference in the deformation behavior between a Va and a VIa metal and explain also the difference in the mechanical properties of niobium single crystals on one hand (8) (9) and tungsten single crystals on the other (10), which is characterized in the first place by a much greater ductility (as expressed by uniform elongation) for niobium. Cross-slip is a means for transmitting slip easily over the entire length of the crystal even in the absence of a sufficient number of dislocation sources and all possible slip planes can therefore be really exhausted, especially in the easy-glide range. On the other hand, due to the absence of cross-slip only slip planes which contain a dislocation source can be activated in tungsten and

not all possible slip planes can therefore participate. From this it becomes clear that less ductility should be found in tungsten single crystals than in niobium single crystals and this corresponds with the experimental facts. In addition in a metal in which dislocations cross-slip there can be no dislocation pile-ups near obstacles such as precipitates, voids, or grain boundaries and the ductility is therefore not influenced drastically. This, however, will no longer be the case if there is no cross-slip so that precipitates, voids, and grain boundaries will become dominant features. The behavior of impure polycrystalline tungsten corresponds with this view.

## Conclusion.

This investigation has shown that in high-purity niobium and tungsten single crystals the dislocation density is low. In niobium crystals domain boundaries and stacking-fault-like structures have occasionally been found. It is thought that both are due to local oxygen contamination, but for the stacking-fault-like structures more diffraction work is necessary to verify this.

Deformation experiments inside the electron microscope proved that in tungsten the dislocations move in straight lines, whereas in niobium repeated cross-slip is observed. This observation explains well the differences in the mechanical properties of the two metals.

## Acknowledgement :

Experimental assistance of Mrs. G. Heckmus, Mrs. M. Jonesco, Mr. J. Francou and Mr. E. Vanderschueren is appreciated.

Description of Figures :

Fig. 1 : Schematic view of the equipment for the strain-free electrolytic or chemical thinning of tungsten and niobium single crystals.

Fig. 2 : Single crystal plate covered with Lacomit or paraffin on which a grid has been traced. Separation of the different rectangles is done either electrolytically or chemically.

Fig. 3 : Principle of the final thinning of the single crystal plates.

Fig. 4 : Domain boundaries in a niobium single crystal. Note that the first and the last fringes are opposite in nature.

Figs. 5, 6, 7 and 8 : Examples of stacking-fault-like structures in niobium. Note the symmetry of the fringes.

Fig. 9a : Stacking-fault-like structure in bright field.

Fig. 9b : Same area as in Fig. 9a, but dark field.

Fig. 10 : Dislocations in high-purity tungsten single crystals.

Fig. 11 : An electron-micrograph of polycrystalline high-purity tungsten.

Fig. 12 : Polycrystalline high-purity tungsten after uniaxial deformation to rupture at room temperature outside the electron microscope.

Figs. 13, 14, 15 and 16 : High-purity polycrystalline tungsten, deformed in uniaxial tension at + 250°C outside the electron microscope.

Fig. 17 : Niobium, deformed inside the electron microscope. Note the repeated cross-slip of the moving dislocations.

Fig. 18 and 19 : Tungsten deformed inside the electron microscope. Note the straight movement of the dislocations.

Fig. 20 : Tungsten deformed inside the electron microscope. Tension released.
Note that the dislocations remain in the slip plane.

## REFERENCES


(1) P. R. Strutt : Rev. Scient. Instr. 32, 411 (1961).

(2) A. Lawley and H. L. Gaigher : Phil. Mag. 10, 15 (1964).

(3) A. Berghezan and A. Fourdeux : Proceedings of the 4th International Conference on Electron Microscopy, p. 567 (1958) : Berlin (Springer Verlag).

(4) J. Van Landuyt and S. Amelinckx : Appl. Phys. Letters, 4, 15 (1964).

(5) A. Howie and V. Valdré : Phil. Mag. 8, 1981 (1963).

(6) A. Art, R. Gevers and S. Amelinckx : Phys. stat. sol. 3, 697 (1963).

(7) A. Fourdeux and A. Berghezan : 6e colloque de métallurgie, Saclay, 91 (1962).

(8) T. A. Mitchel, R. A. Foxall and P. B. Hirsch : Phil. Mag. 8, 1895 (1963).

(9) E. Votava : Phys. stat. sol. 5, 421 (1964).

(10) R. M. Rose, D. P. Ferris and J. Walff : Trans. Met. Soc. AIME, 224, 982 (1962) ; also present contract-section IV.

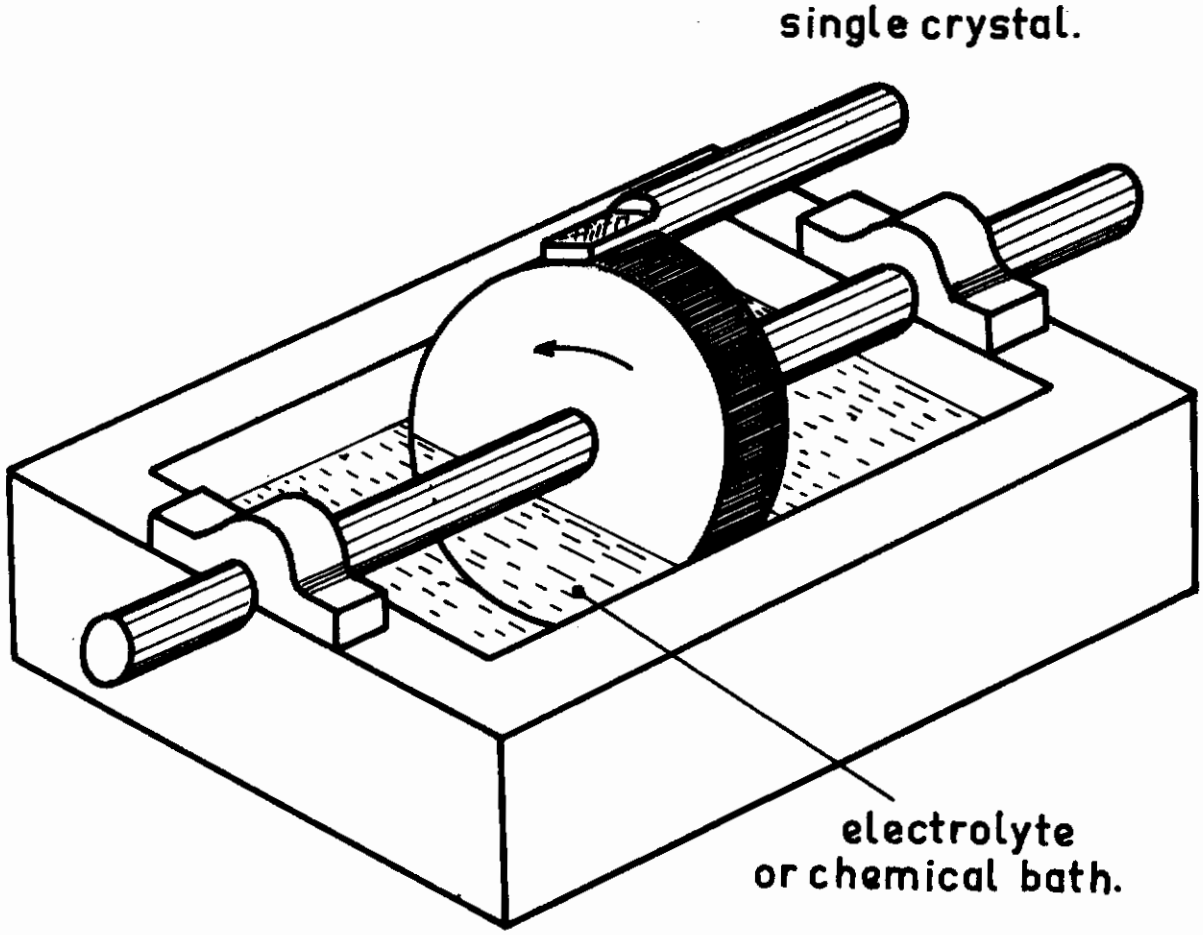


Fig.1.

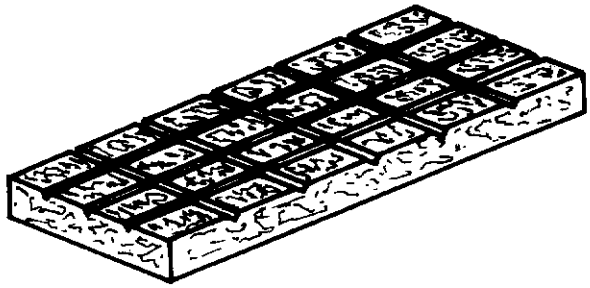

Fig. 2.

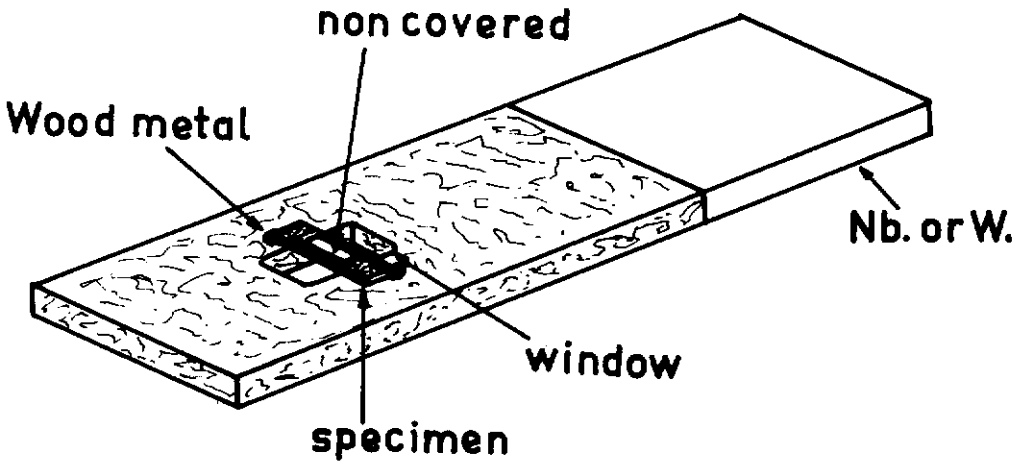


Fig. 3.

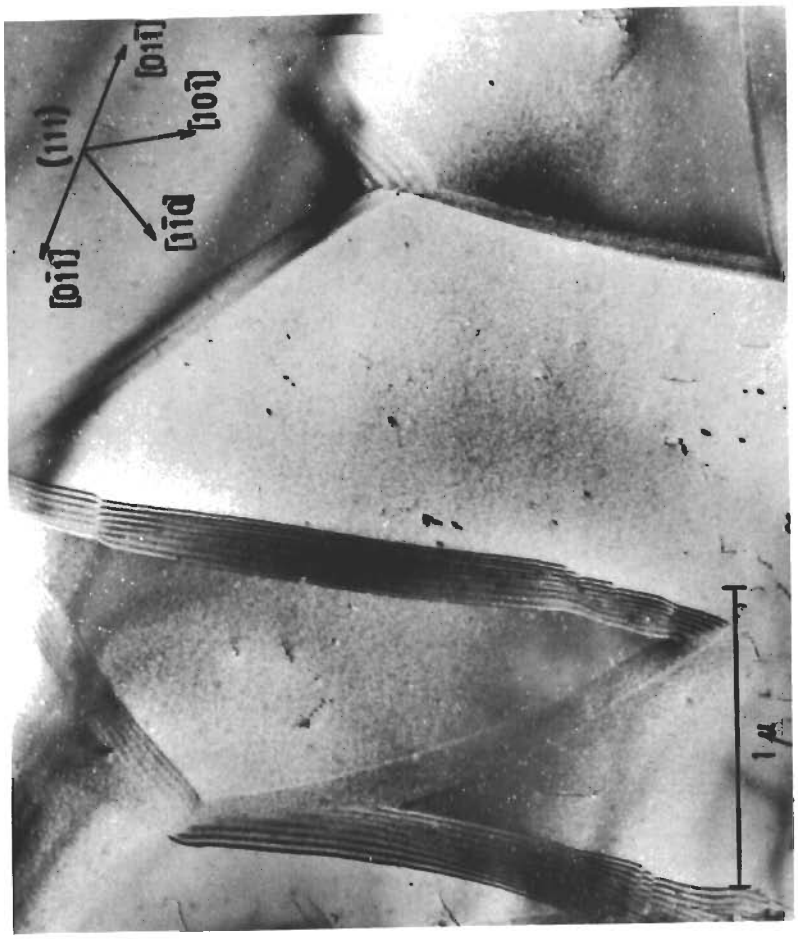


Fig.4.

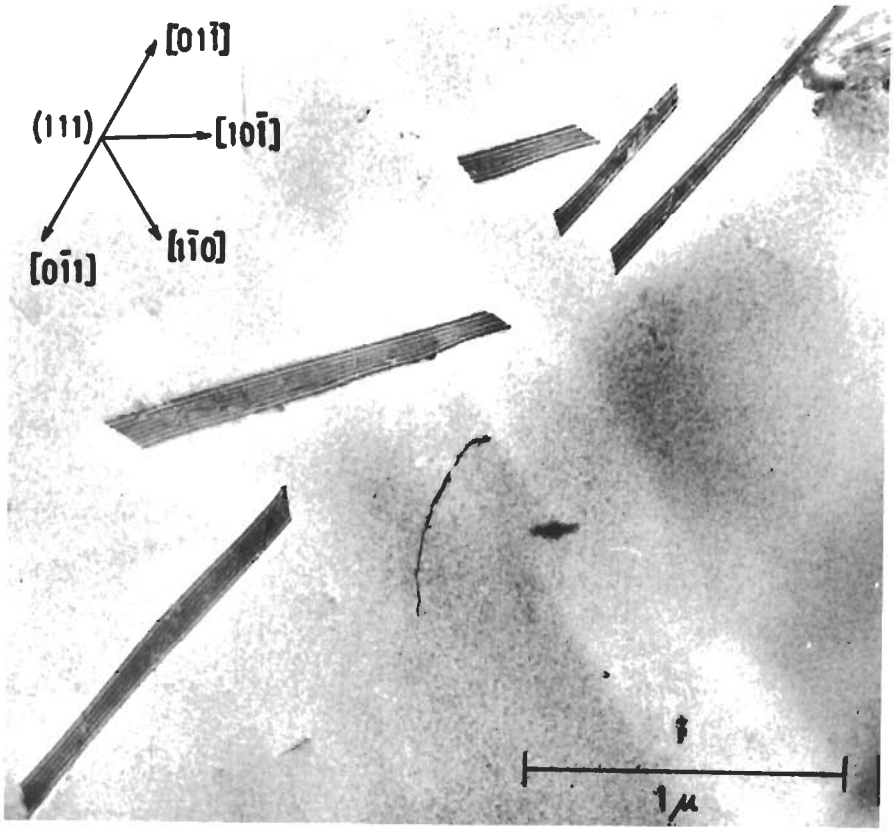


Fig.5.

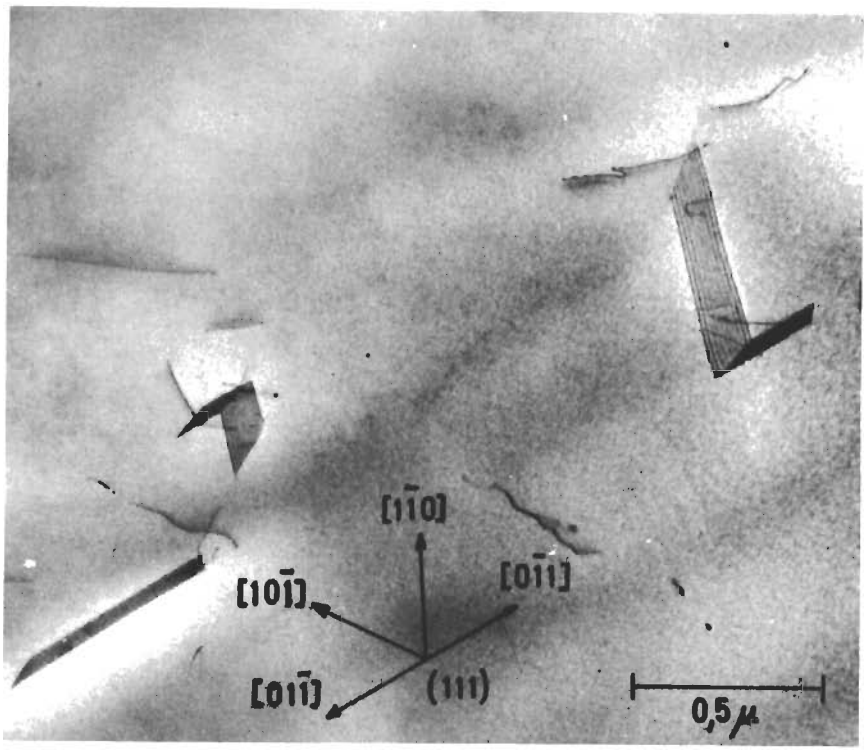


Fig.6.

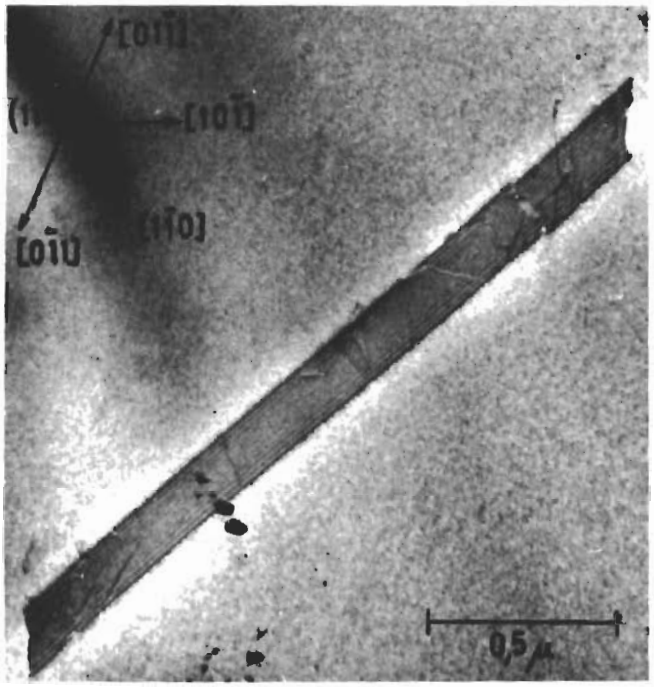


Fig.7.

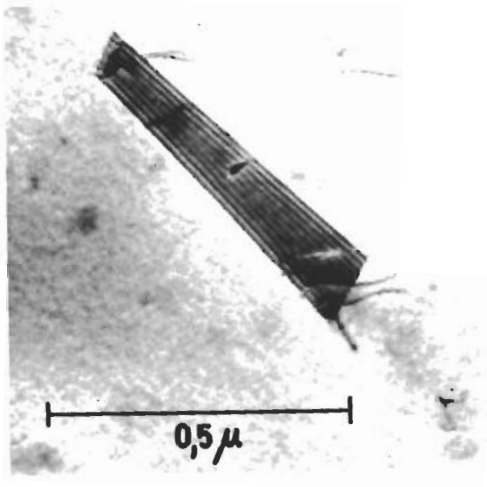


Fig.8.

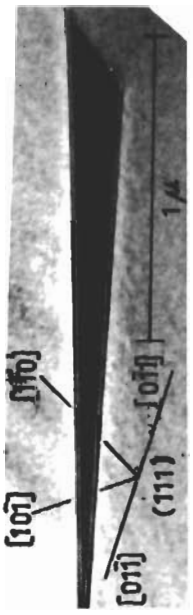


Fig.9a.

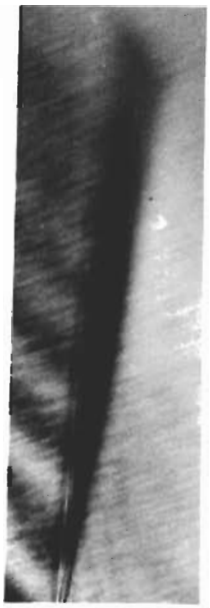

Fig.9b.

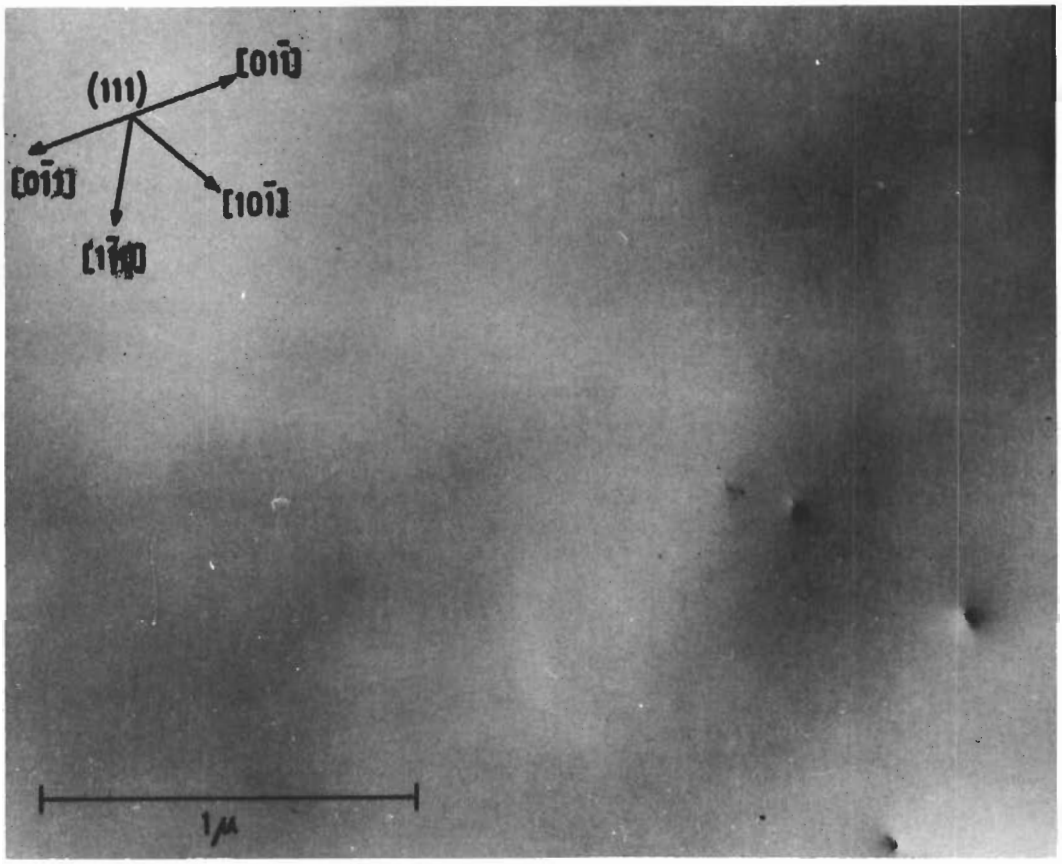


Fig.10.

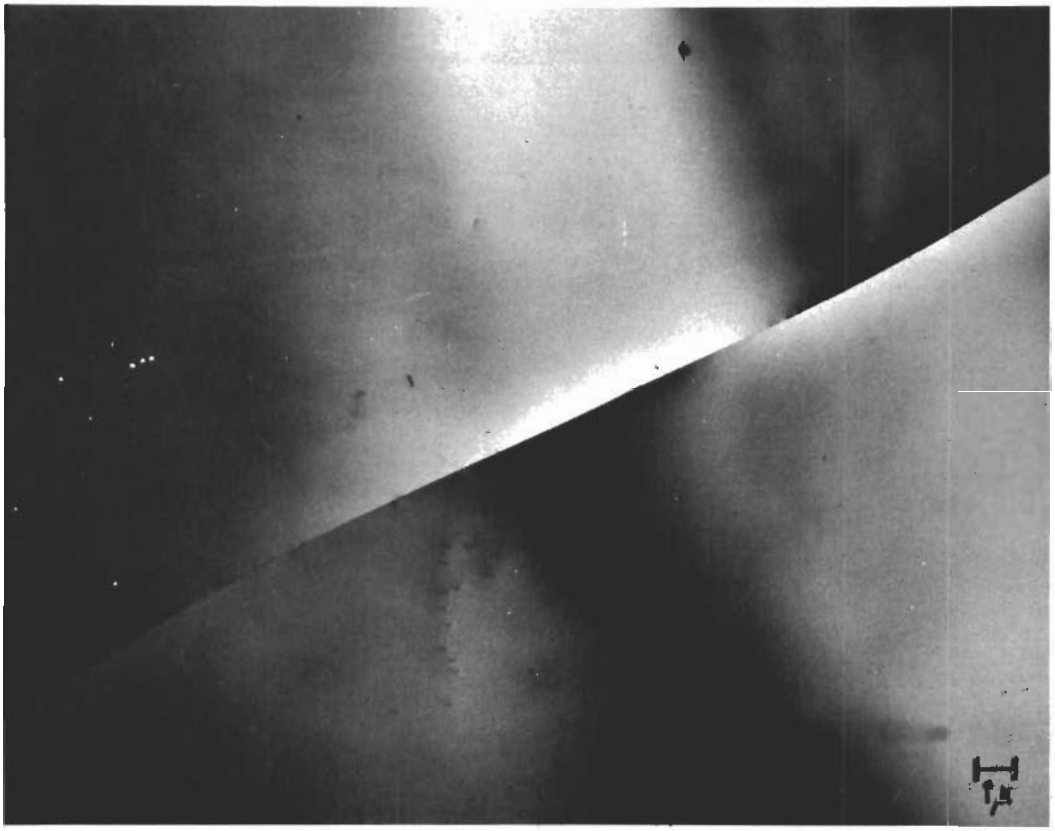


Fig.11.

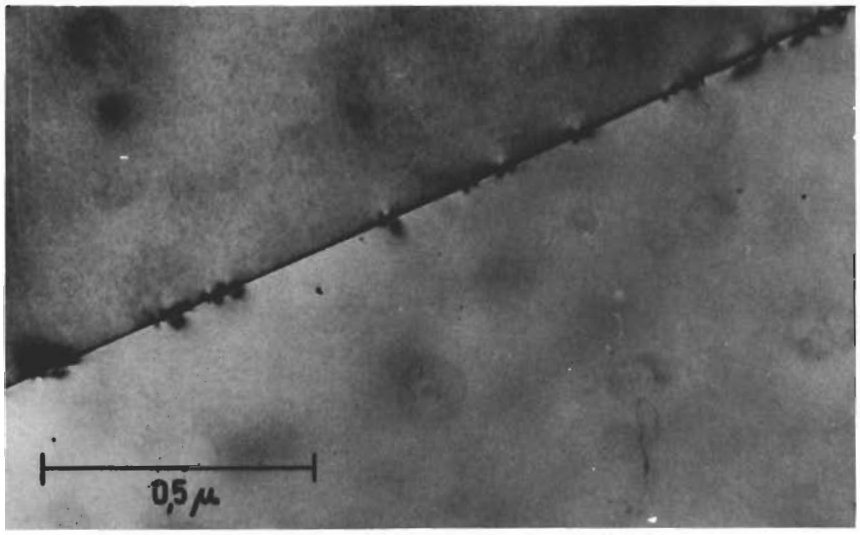


Fig.12.

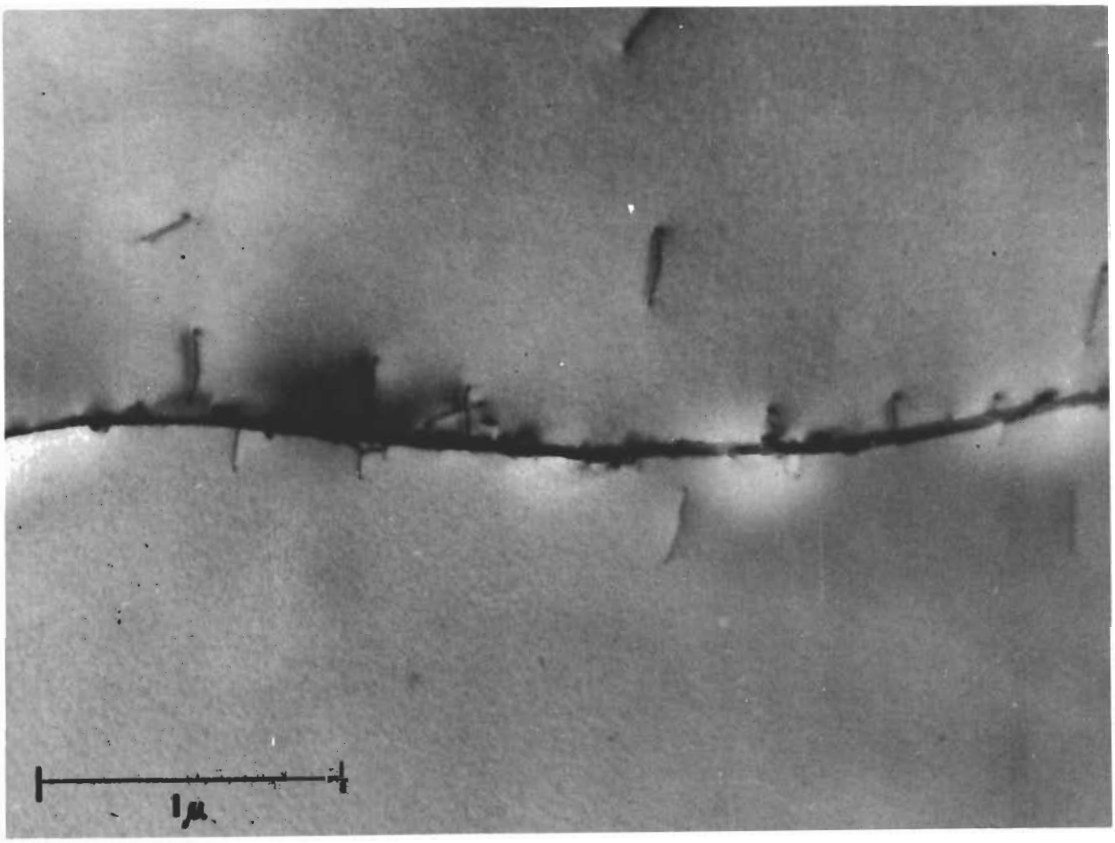


Fig.13.

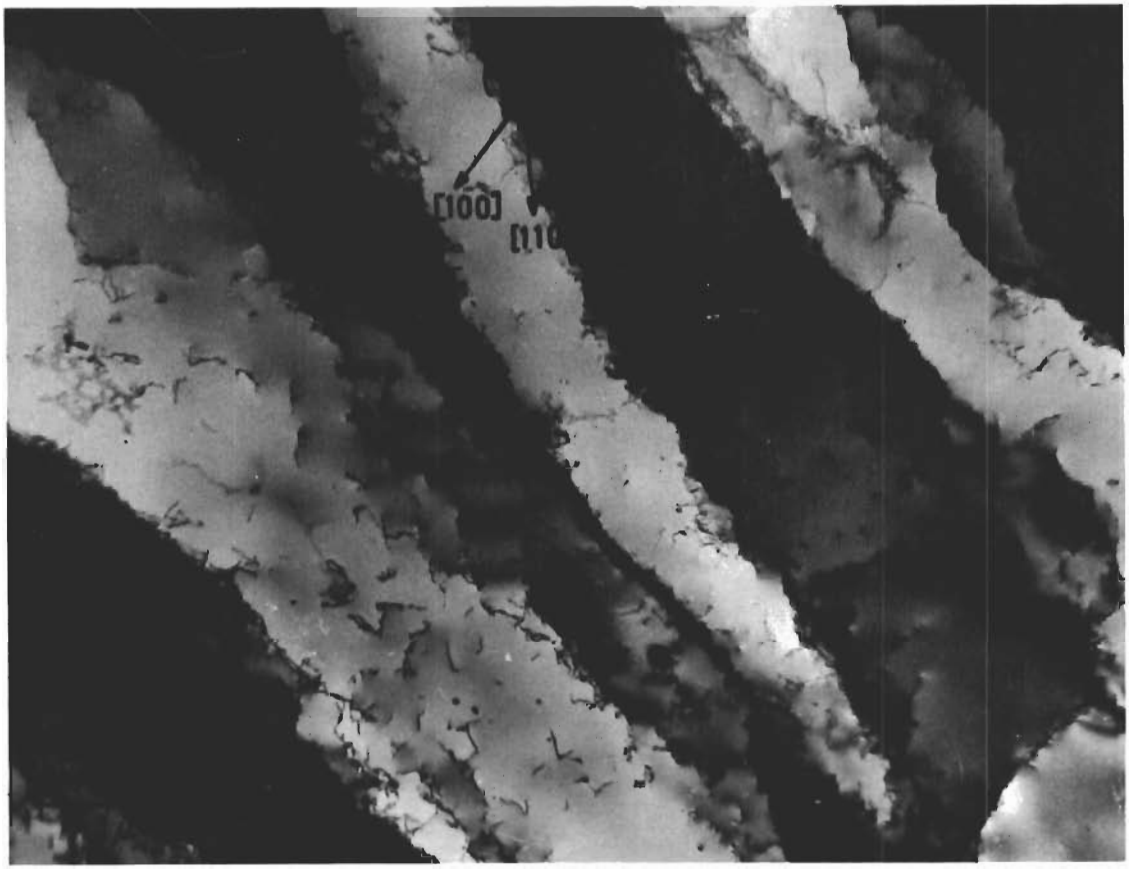


Fig.14.

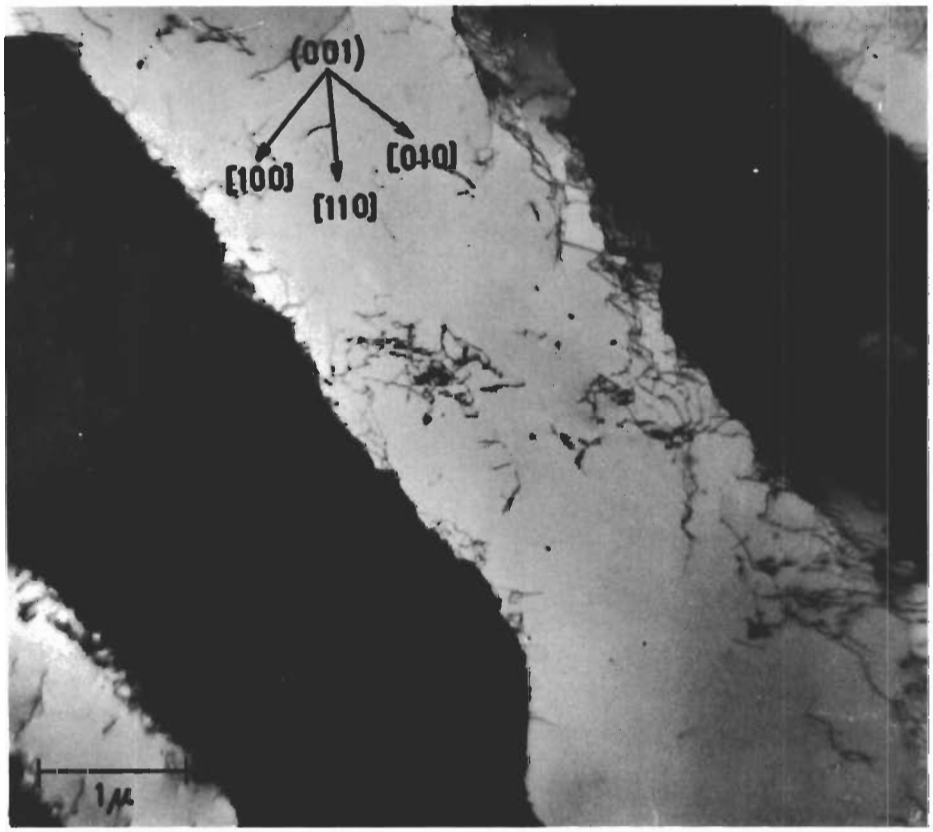


Fig.15.

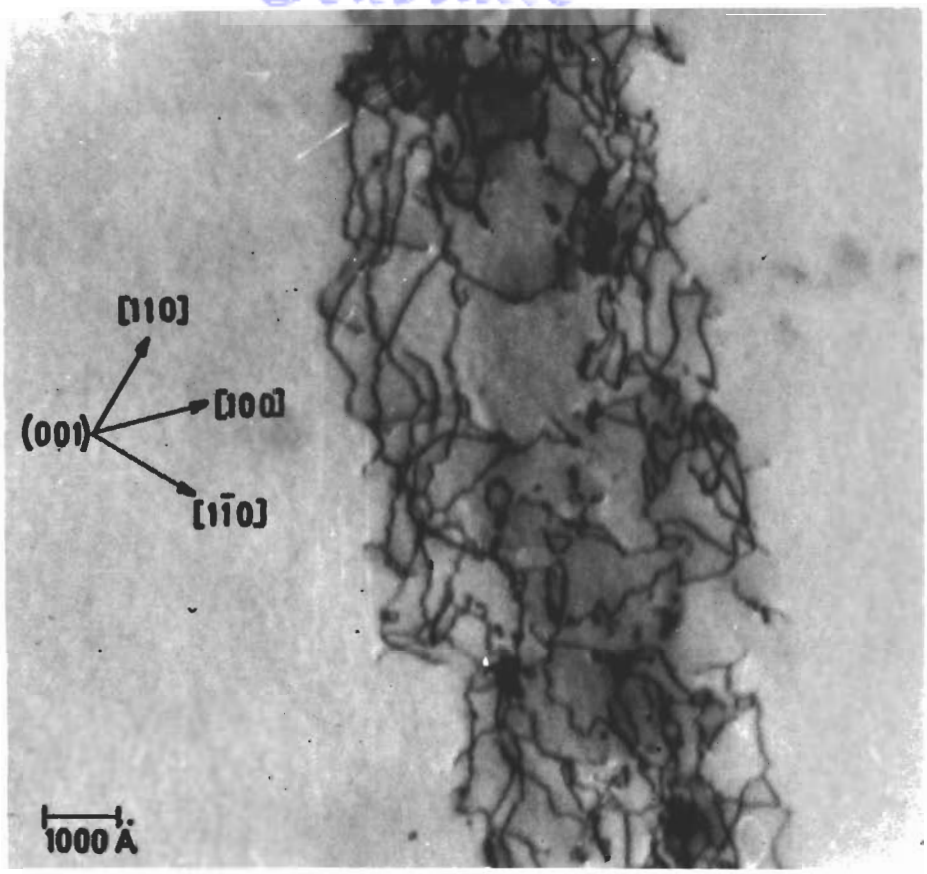


Fig.16.

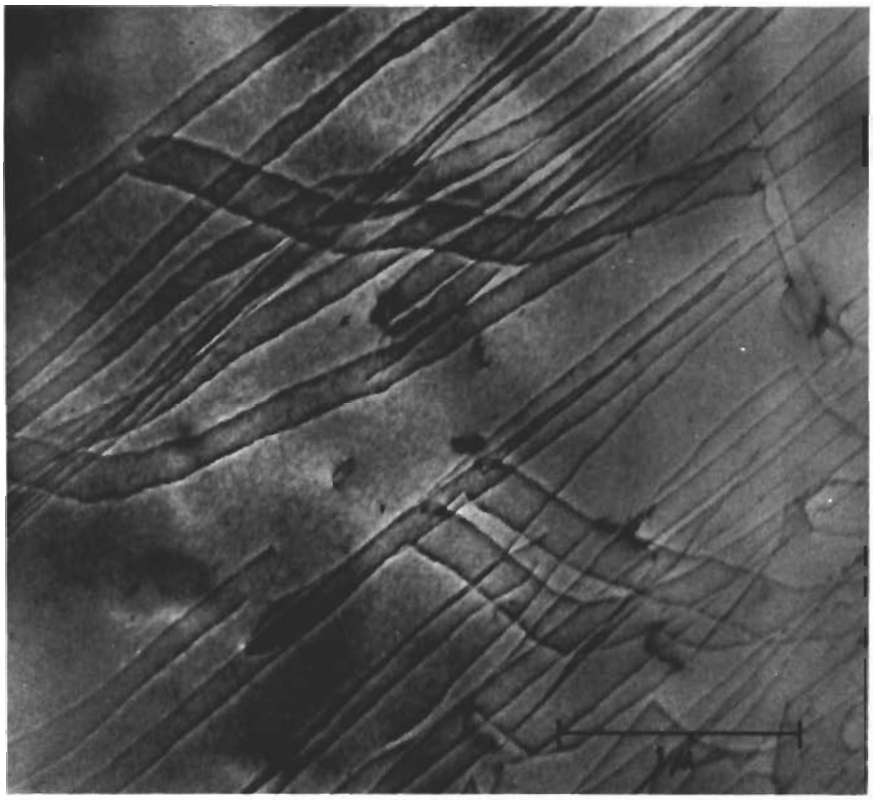

Fig.17.

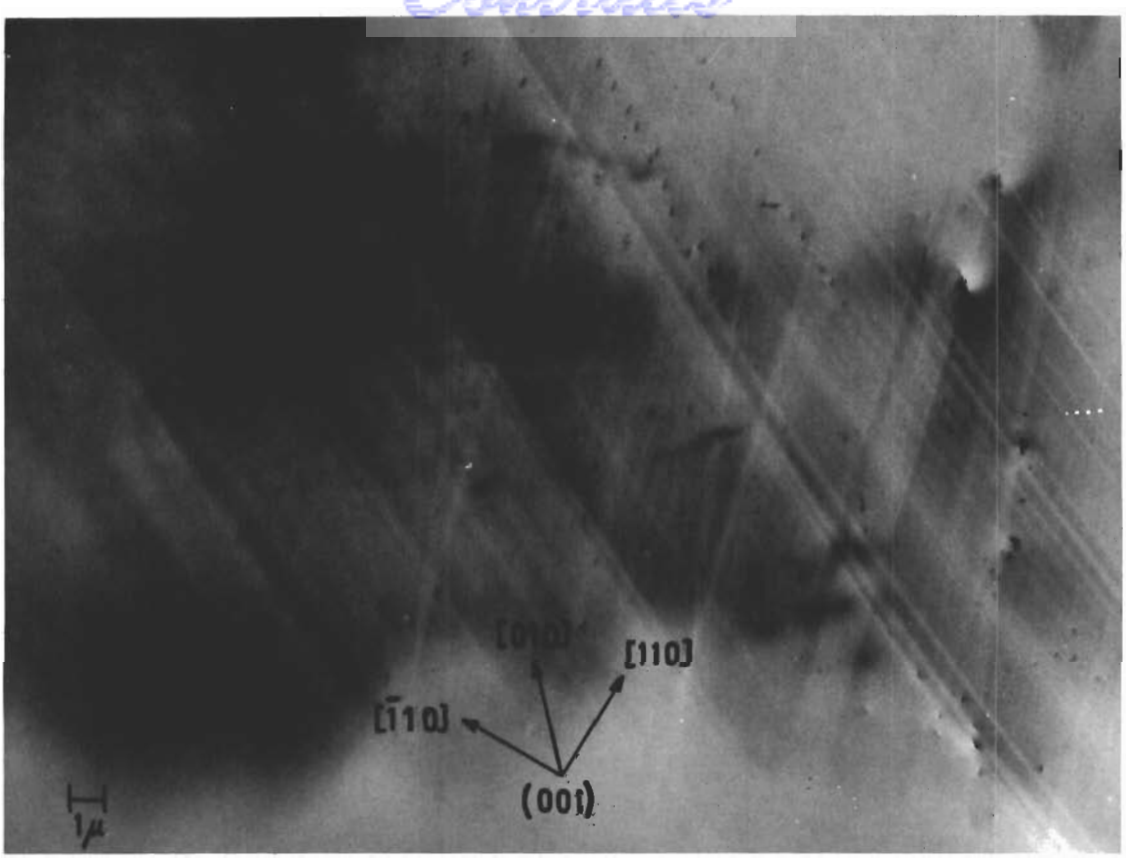


Fig.18.

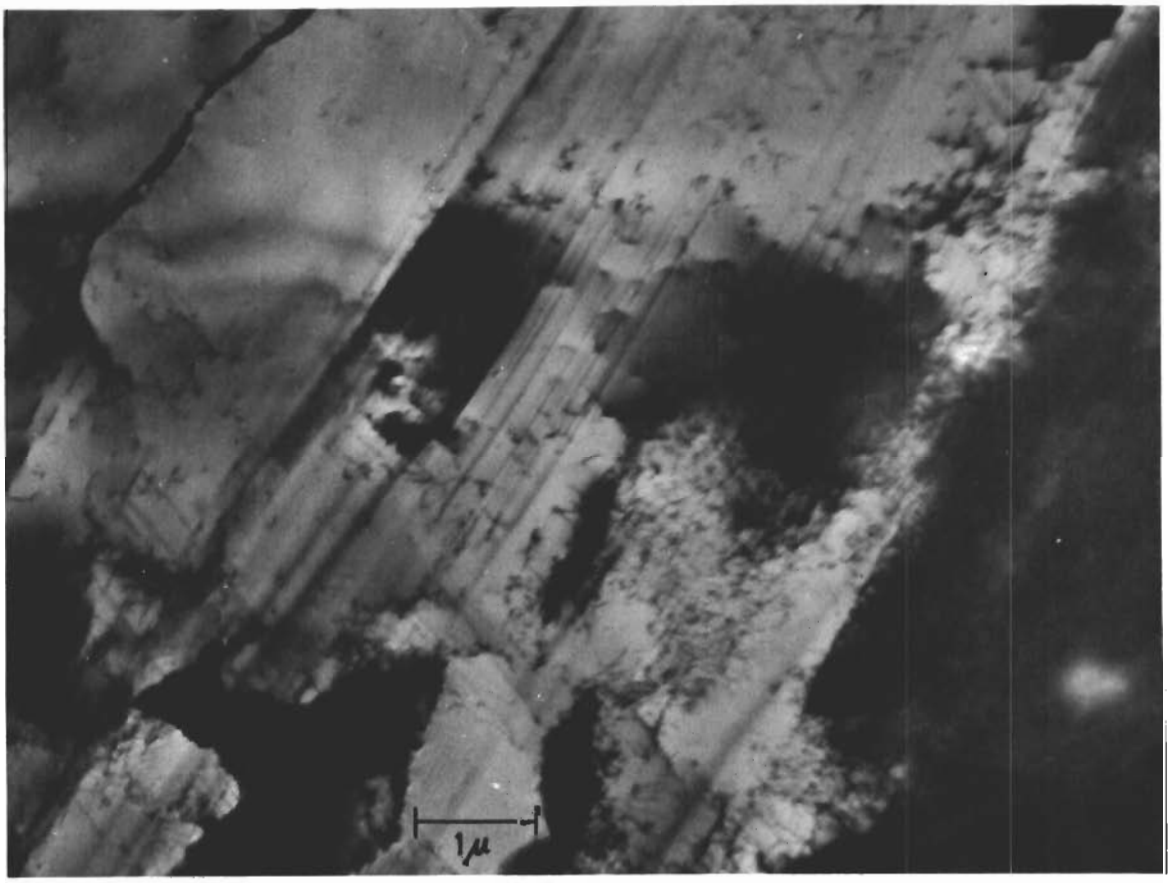


Fig.19.

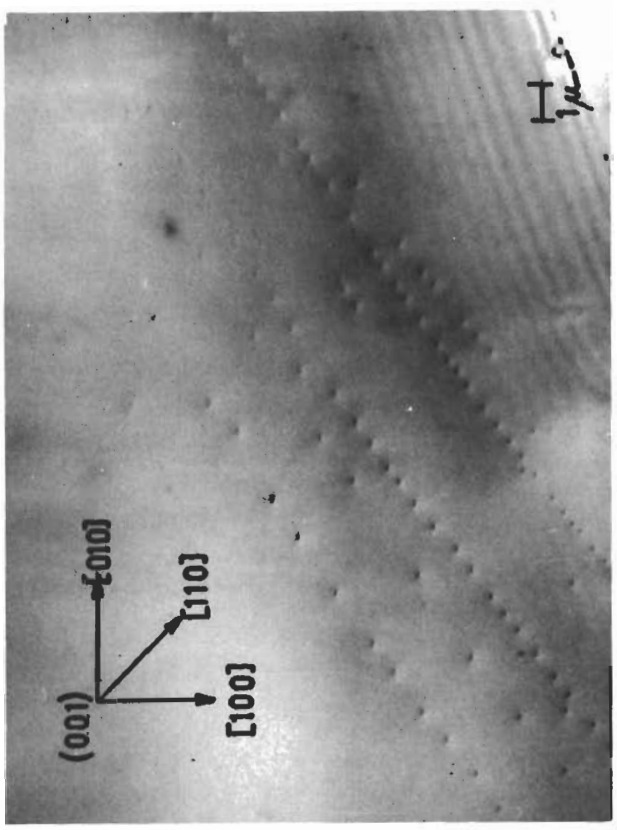


Fig.20.

Acknowledgement :

The authors would like to thank Drs. Roger H. Gillette and A. Berghezan for encouragement and Dr. Hans Tompa for stimulating discussions and help in preparing this report.

Unclassified
Security Classification

## DOCUMENT CONTROL DATA - R&D

*(Security classification of title, body of abstract and indexing annotation must be entered when the overall report is classified)*

| 1. ORIGINATING ACTIVITY (Corporate author) | 2a. REPORT SECURITY CLASSIFICATION |
|---|---|
| Union Carbide European Research Associates, s.a.<br>Brussels, Belgium | Unclassified |
| | 2b. GROUP<br>None |

3. REPORT TITLE

(U) Surface and Interfacial Effects in Relation to Brittleness in Refractory Metals

4. DESCRIPTIVE NOTES (Type of report and inclusive dates)

Summary Technical Report

5. AUTHOR(S) (Last name, first name, initial)

Fourdeux, A. Wronski, A.
Rueda, F.
Votava, E.

| 6. REPORT DATE | 7a. TOTAL NO. OF PAGES | 7b. NO. OF REFS |
|---|---|---|
| April 1966 | 148 | 124 |

| 8a. CONTRACT OR GRANT NO. | 9a. ORIGINATOR'S REPORT NUMBER(S) |
|---|---|
| AF 61(052)-774 | AFML-TR-65-226 |
| b. PROJECT NO.<br>7351 | |
| c. Task No.<br>735101 | 9b. OTHER REPORT NO(S) (Any other numbers that may be assigned this report) |
| d. | |

10. AVAILABILITY/LIMITATION NOTICES

This document is subject to special export controls and each transmittal to foreign governments or foreign nations may be made only with prior approval of the Metals and Ceramics Division (MAM), Air Force Materials Laboratory, Wright-Patterson AFB, Ohio.

| 11. SUPPLEMENTARY NOTES | 12. SPONSORING MILITARY ACTIVITY |
|---|---|
| | AFML (MAMP)<br>Wright-Patterson AFB, Ohio 45433 |

13. ABSTRACT

An experimental program was conducted to compare the mechanical properties of high purity and impure niobium and the mechanical properties of high purity tungsten, both in polycrystalline and single crystal forms.

Slip in high purity niobium takes place on the {110} planes in the <111> directions and yielding is governed by the conservative motion of jogs in screw dislocations, rather than by the unlocking of dislocations from the interstitial impurity cloud. Between the upper and lower yield points there is a sudden generation of a large number of dislocations by double cross-slip mechanism. High purity niobium has greater ductility, higher uniform elongation, increased work hardening, but lower strength than impure Columbium. Further, it has a yield point in the temperature range 20°C to 800°C.

Appreciable ductility can be achieved at room temperature in commercially pure tungsten, but the mechanical properties are strongly orientation dependent. The ductile-to-brittle transition temperature is about 100°C higher sintered material than in melted material which is of coarser gran size and probably higher purity. Very high purity polycrystalline tungsten was found to show some ductility down to -196°C in the recrystallized condition. However, the fracture process is controlled to a considerable extent by grain boundaries in the temperature range +200°C to -196°C.

DD FORM 1 JAN 64 1473

Unclassified
Security Classification

Security Classification

| 14. KEY WORDS | LINK A | | LINK B | | LINK C | |
|---|---|---|---|---|---|---|
| | ROLE | WT | ROLE | WT | ROLE | WT |
| | | | | | | |

## INSTRUCTIONS

1. ORIGINATING ACTIVITY: Enter the name and address of the contractor, subcontractor, grantee, Department of Defense activity or other organization *(corporate author)* issuing the report.

2*a*. REPORT SECURITY CLASSIFICATION: Enter the overall security classification of the report. Indicate whether "Restricted Data" is included. Marking is to be in accordance with appropriate security regulations.

2*b*. GROUP: Automatic downgrading is specified in DoD Directive 5200.10 and Armed Forces Industrial Manual. Enter the group number. Also, when applicable, show that optional markings have been used for Group 3 and Group 4 as authorized.

3. REPORT TITLE: Enter the complete report title in all capital letters. Titles in all cases should be unclassified. If a meaningful title cannot be selected without classification, show title classification in all capitals in parenthesis immediately following the title.

4. DESCRIPTIVE NOTES: If appropriate, enter the type of report, e.g., interim, progress, summary, annual, or final. Give the inclusive dates when a specific reporting period is covered.

5. AUTHOR(S): Enter the name(s) of author(s) as shown on or in the report. Enter last name, first name, middle initial. If military, show rank and branch of service. The name of the principal author is an absolute minimum requirement.

6. REPORT DATE: Enter the date of the report as day, month, year; or month, year. If more than one date appears on the report, use date of publication.

7*a*. TOTAL NUMBER OF PAGES: The total page count should follow normal pagination procedures, i.e., enter the number of pages containing information.

7*b*. NUMBER OF REFERENCES: Enter the total number of references cited in the report.

8*a*. CONTRACT OR GRANT NUMBER: If appropriate, enter the applicable number of the contract or grant under which the report was written.

8*b*, 8*c*, & 8*d*. PROJECT NUMBER: Enter the appropriate military department identification, such as project number, subproject number, system numbers, task number, etc.

9*a*. ORIGINATOR'S REPORT NUMBER(S): Enter the official report number by which the document will be identified and controlled by the originating activity. This number must be unique to this report.

9*b*. OTHER REPORT NUMBER(S): If the report has been assigned any other report numbers *(either by the originator or by the sponsor)*, also enter this number(s).

10. AVAILABILITY/LIMITATION NOTICES: Enter any limitations on further dissemination of the report, other than those imposed by security classification, using standard statements such as:

(1) "Qualified requesters may obtain copies of this report from DDC."

(2) "Foreign announcement and dissemination of this report by DDC is not authorized."

(3) "U. S. Government agencies may obtain copies of this report directly from DDC. Other qualified DDC users shall request through _____."

(4) "U. S. military agencies may obtain copies of this report directly from DDC. Other qualified users shall request through _____."

(5) "All distribution of this report is controlled. Qualified DDC users shall request through _____."

If the report has been furnished to the Office of Technical Services, Department of Commerce, for sale to the public, indicate this fact and enter the price, if known.

11. SUPPLEMENTARY NOTES: Use for additional explanatory notes.

12. SPONSORING MILITARY ACTIVITY: Enter the name of the departmental project office or laboratory sponsoring *(paying for)* the research and development. Include address.

13. ABSTRACT: Enter an abstract giving a brief and factual summary of the document indicative of the report, even though it may also appear elsewhere in the body of the technical report. If additional space is required, a continuation sheet shall be attached.

It is highly desirable that the abstract of classified reports be unclassified. Each paragraph of the abstract shall end with an indication of the military security classification of the information in the paragraph, represented as *(TS)*, *(S)*, *(C)*, or *(U)*.

There is no limitation on the length of the abstract. However, the suggested length is from 150 to 225 words.

14. KEY WORDS: Key words are technically meaningful terms or short phrases that characterize a report and may be used as index entries for cataloging the report. Key words must be selected so that no security classification is required. Identifiers, such as equipment model designation, trade name, military project code name, geographic location, may be used as key words but will be followed by an indication of technical context. The assignment of links, rules, and weights is optional.

Security Classification